Transcriptional targets of Eph receptor and ephrin signalling in the zebrafish hindbrain

Hannah Amy Stanforth

University College London

and

The Francis Crick Institute

PhD Supervisor: Dr David Wilkinson

A thesis submitted for the degree of

Doctor of Philosophy

University College London

February 2018

Declaration

I Hannah Amy Stanforth confirm that the work presented in this thesis is my own. Where information has been derived from other sources, I confirm that this has been indicated in the thesis.

Abstract

In vertebrates, there is a large family of Eph receptor tyrosine kinases and their ephrin ligands, which have complex and varied roles during development and in adult homeostasis. The most researched role of Eph receptors and ephrins is in control of cell migration through the regulation of the actin cytoskeleton and cell adhesion. More recently, it has been found that in some tissues Eph-ephrin signalling also leads to changes in gene transcription, for example to control cell differentiation. In the zebrafish hindbrain, Eph receptors and ephrins are expressed segmentally in the rhombomeres in a complementary pattern with respect to their binding partner. Signalling via this pathway induces a unique cell population to arise at rhombomere borders, known as the boundary cells.

In order to understand more about Eph receptor and ephrin function in the hindbrain, RNA-sequencing was carried out on dissected hindbrains of zebrafish with endogenous Eph-ephrin signalling and fish that lack Eph-ephrin signalling. The transcriptional profiles were then compared to identify potential downstream targets, which were verified using RT-qPCR and *in situ* hybridisation. This identified four genes regulated downstream of Eph-ephrin signalling that are markers of progenitor cells and neural differentiation. When Eph-ephrin signalling is disrupted the expression of these genes alters, and the expression pattern of one gene, *mdka*, was consistent with loss of hindbrain boundary cells.

To investigate this observation further, the expression of progenitor and neurogenic markers was determined when Eph-ephrin signalling was disrupted. This supported previous studies which found that Eph-ephrin signalling is required for formation of boundary cells and that boundary cell loss results in ectopic neurogenesis. In addition, it was found that ectopic neurogenesis was accompanied by the depletion of *nestin*-expressing neural progenitor cells at later stages of development. Together these findings support previous work showing that hindbrain boundary cells are essential for restricting neurogenesis to neurogenic zones adjacent to the boundaries.

Impact Statement

Eph-ephrin signalling is important for normal development as it is active in many tissues and regulates a variety of cellular processes. It has been well characterised that signalling results in regulation of the actin cytoskeleton and cell adhesion leading to cell responses such as cell migration. This ensures that cell populations are organised at the correct location as well as forming boundaries between different cell populations. In addition, Eph-ephrin signalling has also been shown to regulate transcription in many tissues. In the hindbrain Eph-ephrin signalling prevents intermingling between segments as well as being responsible for the induction of a distinct cell population that arise at the borders of segments. As little is known about the genes that are regulated by Eph-ephrin signalling, identifying these will help to contribute to understanding hindbrain development. Understanding Eph-ephrin signalling is also important as when signalling is mis-regulated this can have detrimental consequences. During early development, this can result in the incorrect formation of head structures as signalling is responsible for guiding the neural crest cells to the correct location. Regulation of Eph-ephrin signalling is also important later in life and a mouse model for Alzheimer's disease shows that Eph receptors are expressed at the incorrect levels. Finally, Eph-ephrin signalling is mis-regulated in many types of cancers, and leads to changes in cell migration.

In this project, the role of Eph-ephrin signalling in regulating gene expression was investigated in the context of hindbrain development. This has unveiled novel genes that are regulated downstream of Eph-ephrin signalling, and based on their function imply that signalling is regulating the progression of neurogenesis. Further investigation has shown that Eph-ephrin signalling is important for patterning of neurogenesis via the induction of boundary cells. These findings will contribute to understanding hindbrain development and the role that Eph-ephrin signalling plays in regulating hindbrain neurogenesis.

During this PhD, I have generated gene expression data by RNA-sequencing to identify transcriptional targets of Eph-ephrin signalling. Whilst I was able to validate several of these target genes, this list still holds many possibilities for avenues of further research. One approach could be to investigate the significance of altered

expression of other genes found by RNA-sequencing analysis. In addition, the quality control method designed for selecting hindbrains with low contamination from tissues surrounding the hindbrain continues to be used in the lab for future RNA-sequencing experiments. Finally, during this PhD I have communicated my research by presenting posters at several meetings, including the 18th International Congress of Developmental Biology, the Young Embryologist Meeting and student symposia at the Francis Crick Institute.

Acknowledgements

Firstly, I would like to thank David for giving me the opportunity to carry out this project in his lab and for his continued support and guidance throughout the course of my PhD. I would like to thank the rest of the members of the Wilkinson Lab, past and present, for making the last four and a half years enjoyable, for celebrating the successes, and sharing the frustrations, of science. In particular, I would like to thank Jordi for his advice, suggestions, as well as the use of his fish lines, one of which was invaluable to the success of this project. I would also like to thank Qiling for sharing her wealth of knowledge about zebrafish alongside being a caring lab-mate and an excellent cook. I must thank Probir, who not only analysed the RNA-sequencing data collected during this project, and was also patient in dealing with the many questions that came with this task. Thank you to the High Throughout Sequencing facility, who sequenced all the samples in this project and the Crick Aquatics staff for looking after the fish that I have used. I would also like to thank my thesis committee: Vassilis Pachnis, Francois Guillemot and Mike Gilchrist for their advice and useful discussions.

I would like to thank my family and friends for their support over the course of my PhD. Thank you to my parents for continually paying an interest, their belief in my capabilities and for their consistent encouragement throughout. Laurence, my husband-to-be, for having more faith in me than I do in myself, for celebrating all the small victories along the way and for looking after me during this process, therefore, I cannot thank you enough. Thank you to Ben and Jade for their support, understanding and checking in on how things are going. I would also like to thank my grandparents, for always asking irrespective of not knowing exactly what I was doing. Thank you to my friends, scientist and non-scientists, for their motivation and ever-increasing interest in fish, especially Katie for her supporting audio notes. Thank you to the Forman's for sending snacks in the post.

Finally, thank you to a few groups of people. Firstly, I would like to thank my fellow Crick students who have attended 'Breakfast Club' over the past four years to provide a wonderful support network over a few hash browns. Thank you to the Crick Running Club, who have made Thursday lunchtimes fun and kept my mind clear during my writing up. Finally, thank you to London Heathside AC who have kept me moving and lowered my stress levels in the final phases.

Table of Contents

Table of figures

List of tables

Abbreviations

A-P – anterior-posterior

Dvl - Dishevelled

Eph – erythropoietin-producing human hepatocellular receptors

FAK – Focal adhesion kinase

FGF – fibroblast growth factor

FN – fibronectin

GAP - GTPase-activating protein

GDP - guanosine diphosphate

GEF - guanine exchange factor

GTP - guanosine triphosphate

hpf – hours post fertilisation

Jak-Stat - Janus kinase-signal transducer and activator of transcription

GPI – glycosylphosphatidylinositol

LB - L Broth

LBD – ligand binding domain

MAPK - mitogen activated protein kinase

MHB - midbrain-hindbrain boundary

MO – morpholino oligonucleotide

N-WASP - Neural Wiskott-Aldrich syndrome

neurog1 – neurogenin1

r1-r7 – rhombomere 1 – rhombomere 7

RA – retinoic acid

rfng – radical fringe

RNA – ribonucleic acid

SAM – sterile alpha motif

SB – splice blocking

ss – somite stage

STAR - Spliced Transcripts Alignment to a Reference

TB – translation blocking

TM – transmembrane

vHnf1 - variant hepatocyte nuclear factor 1

Chapter 1. Introduction

The aim of this PhD project has been to identify and investigate the role of transcriptional targets of Eph receptor and ephrin signalling during zebrafish hindbrain development. In this chapter, the background of the project will be discussed, including an overview of Eph-ephrin signalling and zebrafish hindbrain development, as well as the studies that demonstrate the role of Eph-ephrin signalling in regulating transcription.

1.1 Eph receptor and ephrin signalling

Since the first Eph receptor was cloned from human carcinomas (Hirai et al., 1987), there has been an increasing understanding of the roles in which Eph-ephrin signalling plays, as well as the downstream pathways that are activated. Eph receptors are a type of receptor tyrosine kinase and comprise the largest subfamily of this group. Receptor tyrosine kinases are typically receptors for growth factors, cytokines or hormones and have many roles during development and adult homeostasis (Robinson et al., 2000). Eph receptors are activated by their ephrin ligands and through downstream signalling pathways lead to cellular responses, for example through regulation of the actin cytoskeleton and cell adhesion (Meima et al., 1997; Xu and Henkemeyer, 2009; Park and Lee, 2015). This drives changes in cell behaviour such as cell migration, axon path finding, and angiogenesis (Pandey et al., 1995; Wang and Anderson, 1997; Smith et al., 1997).

1.1.1 Classes and domain structure of Eph receptors and ephrins

Eph receptor and ephrin proteins are comprised of several domains (Figure 1), and are classified into A and B subclasses (Gale et al., 1996). Both ephrinAs and ephrinBs are comprised of an extracellular receptor binding domain, but ephrinAs are membrane bound via a glycosylphosphatidylinositol (GPI) anchor whereas ephrinBs have a transmembrane domain (TM) and cytoplasmic domain. The cytoplasmic domain of ephrinBs includes conserved tyrosine residues and a c-terminal motif that can be bound by PDZ domain proteins. Eph receptors all contain

a ligand binding domain, a Sushi and EGF domain which together make the cysteine-rich domain, two fibronectin domains (FN), a TM, a tyrosine kinase domain, a sterile alpha motif (SAM) and a PDZ protein binding motif. Eph receptors are categorised into A and B subclasses based on which subclass of ephrins they preferentially bind and on their sequence similarity. Eph receptors and ephrins bind multiple partners within the same subclass, but at different affinities (Noberini et al., 2012). Binding also occurs between specific protein in different subclasses, for example EphB2 and ephrinA5, and EphA4 and ephrinB ligands (Gale et al., 1996; Himanen et al., 2004; Noberini et al., 2012).

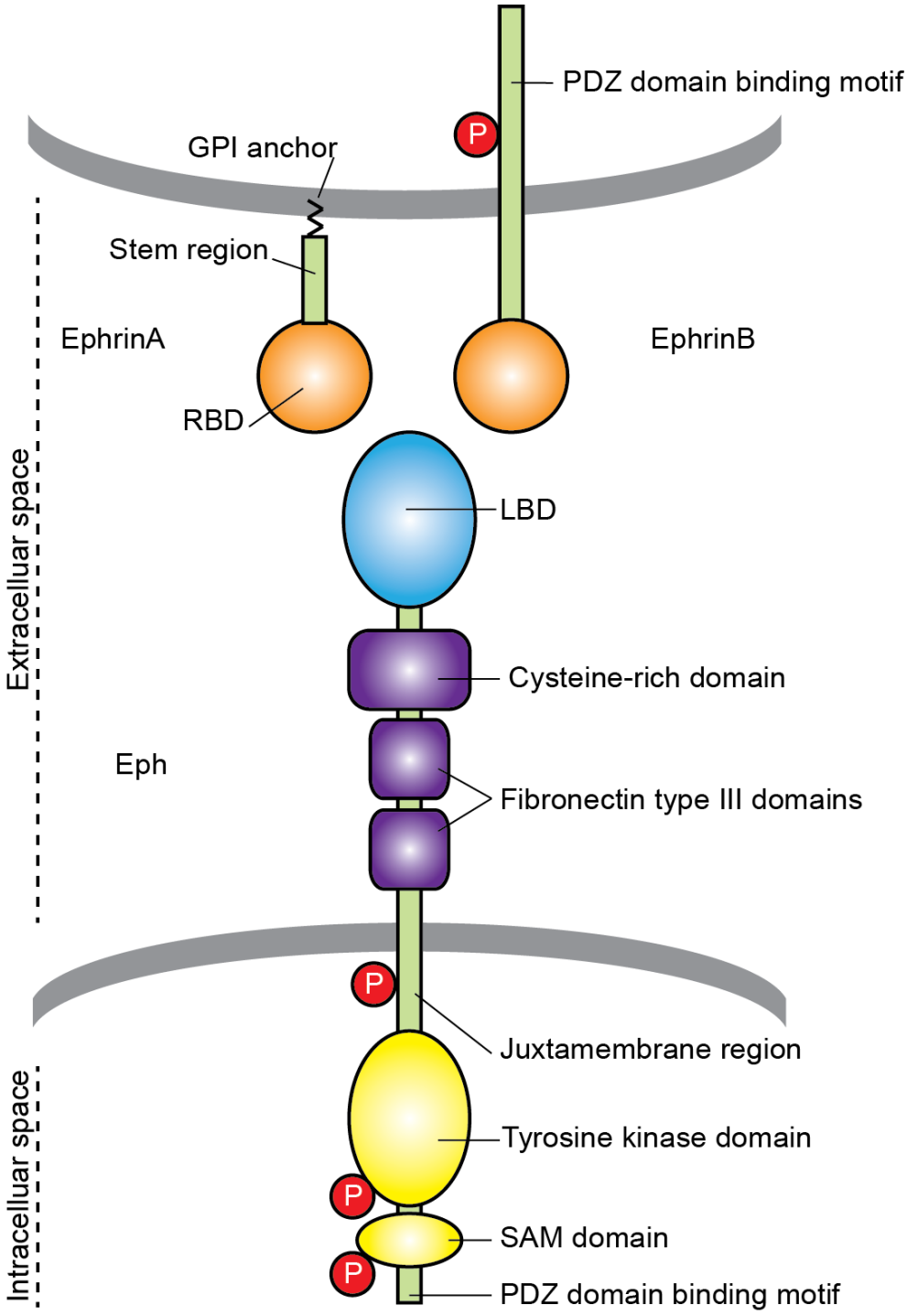

Figure 1 Eph receptor and ephrin protein domains

Schematic of ephrinA and ephrinB interacting with an Eph receptor. Extracellular receptor binding domain (RBD), glycosylphosphatidylinositol (GPI) anchor, ligand binding domain (LBD), sterile alpha motif (SAM). Figure based on Egea and Klein (2007).

Eph receptors and ephrins are conserved across vertebrates and invertebrates. There are 13 members of the human Eph receptor tyrosine kinase family, nine EphA receptors (EphA1-8 and 10) and five EphB receptors (EphB1-4 and 6), and there are

five ephrinA ligands (ephrinA1-5) and three ephrinBs (ephrinB1-3) (Kullander and Klein, 2002; Zerbino et al., 2018). Rodents have nine EphA receptors (A1-8 and 10) and five EphB receptors (EphB1-4 and 6), and five ephrinAs (ephrinA1-5) and three ephrinBs (ephrinB1-3) (Zerbino et al., 2018). In zebrafish, there are six EphA receptors (EphA3-8) and five EphB receptors (EphB1-4 and 6), and four ephrinAs (ephrinA1-3, 5) and three ephrinBs (ephrinB1-3) (Zerbino et al., 2018). In C. *elegans*, there is one Eph receptor and four ephrin ligands (George et al., 1998; Wang et al., 1999; Chin-Sang et al., 1999), and in Drosophila there is only one Eph receptor and one ephrin (Scully et al., 1999; Bossing and Brand, 2002).

1.1.2 Eph-ephrin signalling activation

Due to the membrane bound nature of Eph receptors and ephrins, signalling is limited to cells that are in contact with one another. Eph-ephrin binding can occur in *cis* and *trans* (Dudanova and Klein, 2011). When an Eph receptor and ephrin bind from the same cell signalling is inhibited, which is termed *cis* inhibition (Yin et al., 2004; Falivelli et al., 2013) (Figure 2). When signalling occurs between neighbouring cells where one cell expresses an Eph receptor and the adjacent cell expresses an ephrin ligand of a binding pair, this results in *trans* activation (Marquardt et al., 2005) (Figure 2). Upon binding, both Eph and ephrins become clustered leading to activation (Lisabeth et al., 2013), unlike other receptor tyrosine kinases that form dimers, Eph receptors and ephrins form of higher order clusters, and the amount of clustering may influence the cell response (Schaupp et al., 2014).

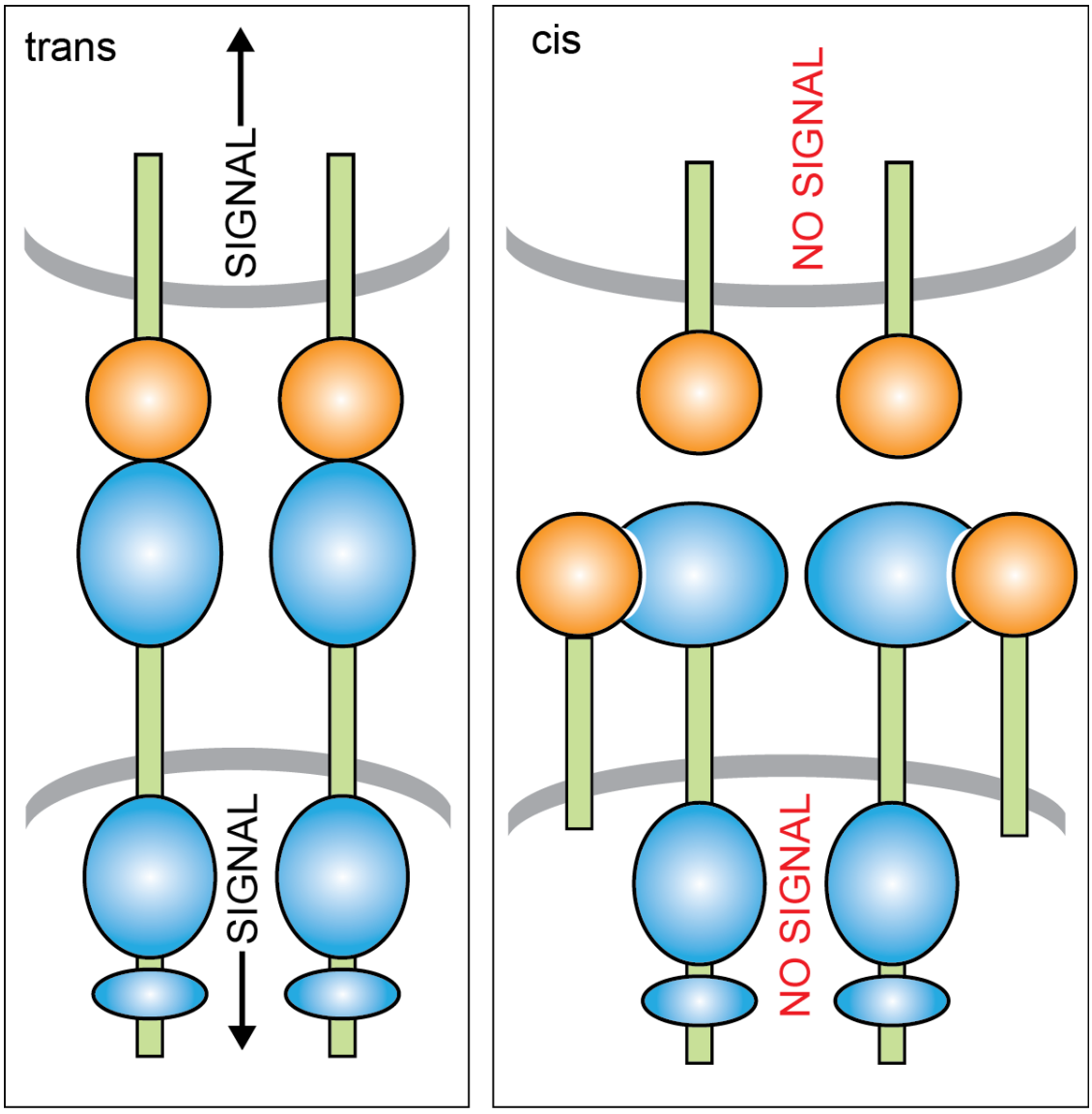

Figure 2 Cis and trans interaction of Eph receptors and ephrins

(A) Trans interaction of Eph receptor (blue) and ephrin (orange) from adjacent cells resulting in the activation of Eph-ephrin signalling. (B) *Cis* interaction of Eph receptor and ephrin within the same cell resulting in the inhibition of Eph-ephrin signalling. Figure based on Arvanitis and Davy (2008).

The first crystal structure of Eph-ephrin binding showed that Eph receptors and ephrins bind in a 2:2 stoichiometry. Upon binding of an ephrin to an Eph receptor, dimerization occurs at the plasma membrane, which then forms a tetramer comprised of two Eph receptors and two ephrins (Himanen et al., 2001). The way in which this structure forms is important for higher order clustering, which is essential for signalling to occur (Davis et al., 1994).

1.1.3 Downstream signalling from Eph receptors and ephrins

Eph-ephrin signalling is bidirectional, allowing messages to be relayed into the ephrin-expressing cell as well as the Eph-expressing cell. Reverse signalling was first discovered when five conserved tyrosine residues situated in the cytoplasmic domain of ephrinBs were identified and further investigation revealed that three of these can be phosphorylated and transmit downstream signalling (Holland et al., 1996; Bruckner et al., 1997; Kalo and Pasquale, 1999). A study identifying phosphorylated proteins downstream of EphB2 and ephirnB1 signalling showed that over 300 proteins had altered phosphorylation upon activation and that just under a third of these were shared between forward and reverse signalling (Jorgensen et al., 2009). The most understood pathways downstream of Eph-ephrin signalling regulate the actin cytoskeleton and adhesion, which are summarised in Figure 3 for EphB-ephrinB signalling and are discussed in more detail below.

Forward signalling through the Eph receptor is in part dependent on the tyrosine kinase domain, which leads to autophosphorylation of the activated Eph receptor (Egea and Klein, 2007). The phosphorylated tyrosine residues are then able to recruit adaptor proteins to the receptor which then become phosphorylated and are able to transmit signals. This includes SH2 domain proteins which lead to activation of phosphorylation cascades, for example via Nck which then results in c-Jun kinase activation (Stein et al., 1998) (Figure 3). Other adaptor proteins include Intersectin, which forms a complex with EphB2 and Neural Wiskott-Aldrich syndrome (N-WASP), and regulates the actin cytoskeleton for dendritic spine formation (Irie and Yamaguchi, 2002; Mohamed et al., 2012) (Figure 3). In addition, focal adhesion kinase (FAK) is kinase-dependent and binds to the SH2 domain of Eph receptors and also leads to changes in the actin cytoskeleton to regulate the morphology of dendritic spines (Moeller et al., 2006; Shi et al., 2009).

Ephexin is another protein that interacts with Eph receptors and is a guanine exchange factor (GEF) (Shamah et al., 2001), which then activates Rho family GTPases, including Rho, Rac and cdc42. These are active when bound to GTP and inactive when bound to GDP (Figure 3). This family of GTPases then regulate the actin cytoskeleton and are important for processes such a filopodia and lamelipodia

extension and retraction, as well as growth cone collapse (Kozma et al., 1997; Moeller et al., 2006; Tolias et al., 2007). In addition, another GEF, TIAM1, is activated by binding to Eph receptors, which results in increased Rac1 activity as well as facilitating Eph receptor and ephrin endocytosis and neurite outgrowth (Tanaka et al., 2004; Boissier et al., 2013) (Figure 3).

Eph downstream signalling can also regulate the mitogen activated protein kinase (MAPK) pathway by either activating or inhibiting this pathway. The GTPase-activating protein (GAP) RasGAP activates Ras, which then activates MAPK signalling. Active Eph receptors have been shown to block MAPK signalling by binding to RasGAP, resulting in cell differentiation (Haupaix et al., 2013). Another study has reported an inhibition of MAPK signalling resulting in growth cone collapse (Elowe et al., 2001). As well as repressing MAPK signalling, there are some experiments showing that MAPK signalling can be activated downstream of Eph receptors, which induces cellular processes such as cell proliferation, cell differentiation and cell survival (Zisch et al., 2000; Poliakov et al., 2008; Bush and Soriano, 2010).

Signalling via Eph receptors can also occur independently of the kinase domain. Kinase dependent and kinase independent signalling can induce different responses (Kullander et al., 2001), or contribute to the same response, resulting in blocking of kinase dependent and independent signalling having a more dramatic phenotype (Grossman et al., 2013). One pathway that is kinase independent and is shared between Eph receptor and ephrin signalling is via Dishevelled (Dvl), which interacts with the PDZ domain binding motif of Eph receptors or ephrins. This then activates RhoA and causes cell responses such as cell segregation and cell migration (Tanaka et al., 2003; Lee et al., 2006) (Figure 3).

Reverse signalling through the two ephrin subclasses differs because of how the ephrins are bound to the membrane: via a GPI anchor or transmembrane spanning domain, for ephrinAs and ephrinBs, respectively. EphrinBs do not have a kinase domain and are phosphorylated by Src family kinases that recruit SH2 domain proteins (Palmer et al., 2002; Daar, 2012) (Figure 3). One adaptor protein that binds phosphorylated ephrinBs is Grb4, which binds to ephrinB1 when activated upon

binding the EphB2 receptor. Downstream signalling regulates spine morphogenesis, synapse formation and focal adhesion disassembly altering cell shape (Cowan and Henkemeyer, 2001; Segura et al., 2007; Xu and Henkemeyer, 2009).

Signalling via ephrinBs can also be mediated via the PDZ domain binding motif which can interact with PDZ containing proteins. It has been suggested that it is constitutively activated and some of the proteins involved have been identified, however, this has not been resolved. One mediator is Rgs3 which binds to the PDZ domain binding motif of ephrinB1 causing inhibition of G-protein coupled receptor signalling. This is important for the cell response to neuronal guidance cues such as SDF-1 (Lu et al., 2001; Bush and Soriano, 2009; Yu et al., 2016). An additional signalling pathway downstream of ephrinBs is the Par polarity complex, which regulates cell-cell junctions and is important for cell adhesion and migration (McCaffrey and Macara, 2012). Studies have revealed that ephrinB1 can interact with Par6 which prevents cdc42-Par6 binding and results in aPKC inhibition of tight junctions (Yamanaka et al., 2001). When ephrinB1 is phosphorylated and becomes activated, it is no longer able to bind Par6 enabling the cdc42-Par6 complex to form and activate aPKC (Lee et al., 2008).

For ephrinAs, reverse signalling is yet to be deciphered, but it has been suggested that signalling occurs through transmembrane proteins that associate with ephrinAs (Pasquale, 2008). Reverse signalling by ephrinAs has also been shown to activate Src family kinases, as discussed for ephrinBs (Holen et al 2008). In addition, some of the proteins that interact with ephrinAs have been identified. This includes p75 neurotrophin receptor ($p75^{NTR}$), TrkB and Ret to mediate signalling that is involved in cell responses such as axon guidance (Lim et al. 2008; Marler et al. 2008; Bonanomi et al. 2012). When EphAs are activated by their ephrinA ligands, this causes ephrinA and $p75^{NTR}$ to colocalise, which results in the phosphorylation of the Src family kinase, Fyn, which causes cell repulsion (Lim et al., 2008). In retinal ganglion cell neurons, Trk has been shown to interact with ephrinA5, which increases the activity of Akt and results in increased axonal branching (Marler et al., 2008). Finally, Ret and ephrin-As have been shown to colocalise leading to increased phosphorylation of Ret and the cell to respond to chemoattractive cues (Bonanomi et al., 2012).

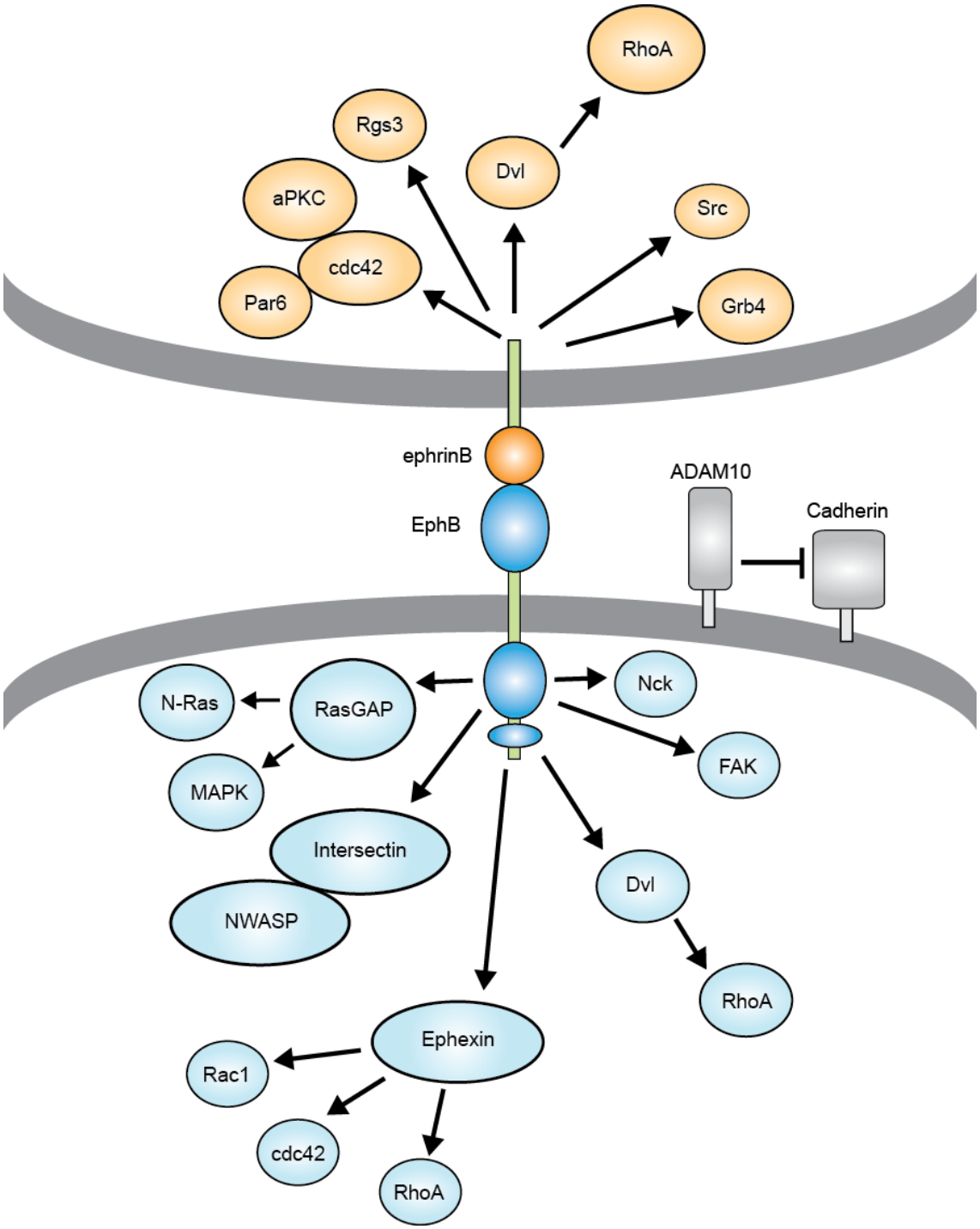

Figure 3 Downstream pathways of EphB-ephrinB signalling

Pathways that are regulated downstream of EphB and ephrinB signal activation, with the focus on pathways that regulate the actin cytoskeleton and cell adhesion. Forward signalling is relayed into the EphB-expressing cell (pathways shown in blue) and reverse signalling is relayed into the ephrinB expressing cell (pathways shown in orange).

1.1.4 Eph-ephrin internalisation and cleavage

It was shown that ephrinA2 is cleaved by the metalloprotease ADAM10, which terminates EphA signalling (Hattori et al., 2000) (Figure 3). Later studies showed that after Eph receptor and ephrinB binding and signal activation, the receptor-ligand complex can be internalised into either the Eph-expressing or ephrin-expressing cell (Marston et al., 2003; Zimmer et al., 2003). Endocytosis of the EphB2-ephrinB1 signalling complex is needed to overcome the strong binding of cells as a result of Eph-ephrin interaction, to enable cells to move apart (Zimmer et al., 2003). A similar mechanism was also shown in venous endothelial cells with EphB4 and ephrinB2, in which Rac is needed to mediate actin polymerization for endocytosis to occur (Marston et al., 2003). Upon internalisation, Eph receptors are either recycled back to the plasma membrane to receive further signals or are inactivated by degradation in lysosomes (Boissier et al., 2013). One mechanism of Eph receptor degradation is by ubiquitination, mediated by the ubiquitin ligase Cbl (Walker-Daniels et al., 2002; Fasen et al., 2008).

1.1.5 Roles of Eph-ephrin signalling

There are an increasing number of examples of how Eph-ephrin signalling is able to induce a range of responses. To demonstrate the diversity of responses and that signalling operates in a variety of cell types, some examples are discussed below.

A major role of Eph-ephrin signalling is to mediate cell segregation to form sharp borders. This is important during development to ensure that cells are organised into tissues or within tissues (Fagotto et al., 2014). There are many examples of cell segregation, including: separation of the ectoderm and mesoderm, their roles in the notochord-presomitic boundary, the formation of somites, hindbrain segmentation and cell segregation in the eye field (Fagotto et al., 2014). The segmentation of the hindbrain neural epithelium into rhombomeres will be discussed in detail in Chapter 1.2.4. Another example of cell segregation is in neural crest cells, which migrate to form many tissues in the embryo, including the bones and cartilage in the head. One mechanism involved in the segregation of this cell population is driven by Eph-ephrin signalling. In Xenopus, EphA4 and EphB1 are expressed in a complementary pattern

to their ligand ephrinB2 in branchial neural crest and are required for the cells to migrate in to the correct locations (Smith et al., 1997).

During neural circuit formation, Eph-ephrin signalling contributes to guiding axons to the correct locations (Cramer and Miko, 2016). This was discovered in early experiments investigating topographic maps, in which it was identified that axons were directed to the correct region of the brain by a gradient of Eph receptor and ephrin expression (Cheng et al., 1995; Feldheim et al., 2000). There are many examples where Eph-ephrin signalling mediates axon guidance via repulsion. For example, studies have shown that in the limb mesenchyme, Eph-ephrin signalling acts to guide motor neurons to their target muscles, with EphA4 being expressed in motor neurons and ephrins in the mesenchyme (Kao et al., 2012).

Vasculogenesis is the process by which the vasculature network is laid down by differentiation of angioblasts into endothelial cells and angiogenesis is the process by which new blood vessels branch from the already present vasculature (Patan, 2004). During these processes EphB4 is expressed in venous endothelial cells, while ephrinB2 is expressed in the arterial endothelial cells (Wang et al., 1998), and when the two cell types come into contact with one another, Eph-ephrin signalling results in repulsion which sculpts the capillary network (Oike et al., 2002). Mutants of both *EphB4* and *ephrinB2* gave the same developmental defects in cardiovascular development with veins and arteries not forming the correct morphology (Gerety et al., 1999).

In the intestine, the stem cells in the crypts proliferate and undergo differentiation as they move up through the villus, before being shed into the lumen (Yen and Wright, 2006). Eph-ephrin signalling regulates cell segregation between the stem cells and differentiating cells which express Eph receptors and ephrins, respectively in a graded complementary pattern along the crypt-villus axis (Batlle et al., 2002). This is important to ensure that progenitor cells are maintained in the crypts and differentiating cells migrate towards the villus. Experiments blocking Eph-ephrin signalling causes cells to be mispositioned along the crypt-villus axis (Holmberg et al., 2006; Jurek et al., 2016). In addition, Eph-ehprin signalling contributes to the control of cell proliferation in parallel to Wnt signalling.

There are some examples showing Eph-ephrin signalling can regulate apoptosis (Magal et al., 1996; Park, 2013). For example, a decrease in apoptosis is observed when EphA7, a receptor for ephrinA5, is knocked out, which results in an increase in neural progenitor cells and a larger cortex in mice (Depaepe et al., 2005). A similar effect is found in the mouse diencephalon and mesencephalon. When *ephrinA5* is mutated, there is a decrease in apoptosis of EphA7-expressing cells, causing an increase in cells at the dorsal midline (Park et al., 2013). In contrast, another study showed increased apoptosis when *EphA7* was knocked down in human lung carcinoma cells (Li et al., 2016). Together these studies demonstrate that Eph-ephrin signalling is important for regulating size via apoptosis and ensuring that the correct number of cells are maintained.

In addition to the roles described above in morphogenesis, there has been increasing evidence that Eph-ephrin signalling can control cell differentiation in some tissues. As the main focus of this project is to identify novel Eph-ephrin transcriptional targets in the hindbrain, a more comprehensive review of the known effects of Eph-ephrin signalling on differentiation will be covered in Chapter 1.3.

1.2 Hindbrain development

1.2.1 Hindbrain specification and segmentation

The hindbrain is segmented which underlies neuronal patterning and neural crest specification. The hindbrain is specified in the neural plate as a result of anterior and posterior signals that give cells positional information and induce specific identities along the anterior-posterior (A-P) axis (Kiecker and Lumsden, 2012). The neural plate initially has an anterior identity and the combined input of retinoic acid (RA), Wnt and fibroblast growth factor (FGF) signalling results in the specification of posterior regions (Kudoh et al., 2002). The result is the specification of the forebrain, midbrain, hindbrain and spinal cord. FGF signalling in the hindbrain induces the expression of RA degrading enzymes, one of which is Cyp26a (White et al., 2007). This results in gradients of FGF, and RA, from posterior to anterior (

Figure 4).

The neural epithelium is segmented into seven regions, called rhombomeres (r1-r7), each with a distinct identity and different pattern of gene expression (Lumsden and Krumlauf, 1996). This segmentation process is regulated by the integration of different signalling mechanisms leading to specific patterns of transcription factor expression which give unique identity to the different rhombomeres (White et al., 2007; Hernandez et al., 2007; Walshe et al., 2002). One key transcription factor is Krox20, which is expressed in rhombomeres 3 (r3) and 5 (r5) (Wilkinson et al., 1989a), and its discrete expression pattern is visible before the morphological segments have formed (Irving et al., 1996). Krox20 regulates the expression of many genes including *EphA4*, which is expressed in r3 and r5 (Theil et al., 1998). EphA4 then plays a key role in border sharpening along with other Eph receptors and ephrins. Krox20 also regulates Hoxa2 and Hoxb2 expression in r3 and r5 by binding upstream enhancers of these genes (Maconochie et al., 1996; Nonchev et al., 1996).

There are other transcription factors involved in specifying segment identity, which act as part of the gene network and are important for the development and segmentation of the rhombomeres (Tumpel et al., 2009; Krumlauf, 2016). This includes variant hepatocyte nuclear factor 1 (vHnf1), which is important for specifying the posterior regions of the hindbrain and in combination with RA and FGF signalling induces MafB expression (Hernandez et al., 2004). MafB is required for hindbrain segmentation and acts to specify r5 and r6 by acting in combination with vHnf1 to give posterior hindbrain identity and repress r4 neuronal fates (Moens et al., 1996; Hernandez et al., 2004).

The *hox* genes are also part of the gene network and specify A-P identity in the hindbrain (Tumpel et al., 2009; Krumlauf, 2016). The *hox* genes are a set of transcription factors that are conserved across vertebrates and invertebrates and their overlapping expression patterns result in specific identities for the different segments (Wilkinson et al., 1989b; Hunt et al., 1991; Tumpel et al., 2009). The expression of *hox* genes is regulated by various factors including the gradients of FGF and RA as well as other transcription factors in the hindbrain. *hox* genes can also repress the expression of other transcription factors, such as the repression of

krox20 by Hoxb1a and Hoxa1 (Helmbacher et al., 1998). Mutational analysis of the *hox* genes has shown that they are required for hindbrain segmentation (Waskiewicz et al., 2002), as well as A-P identity (Bell et al., 1999).

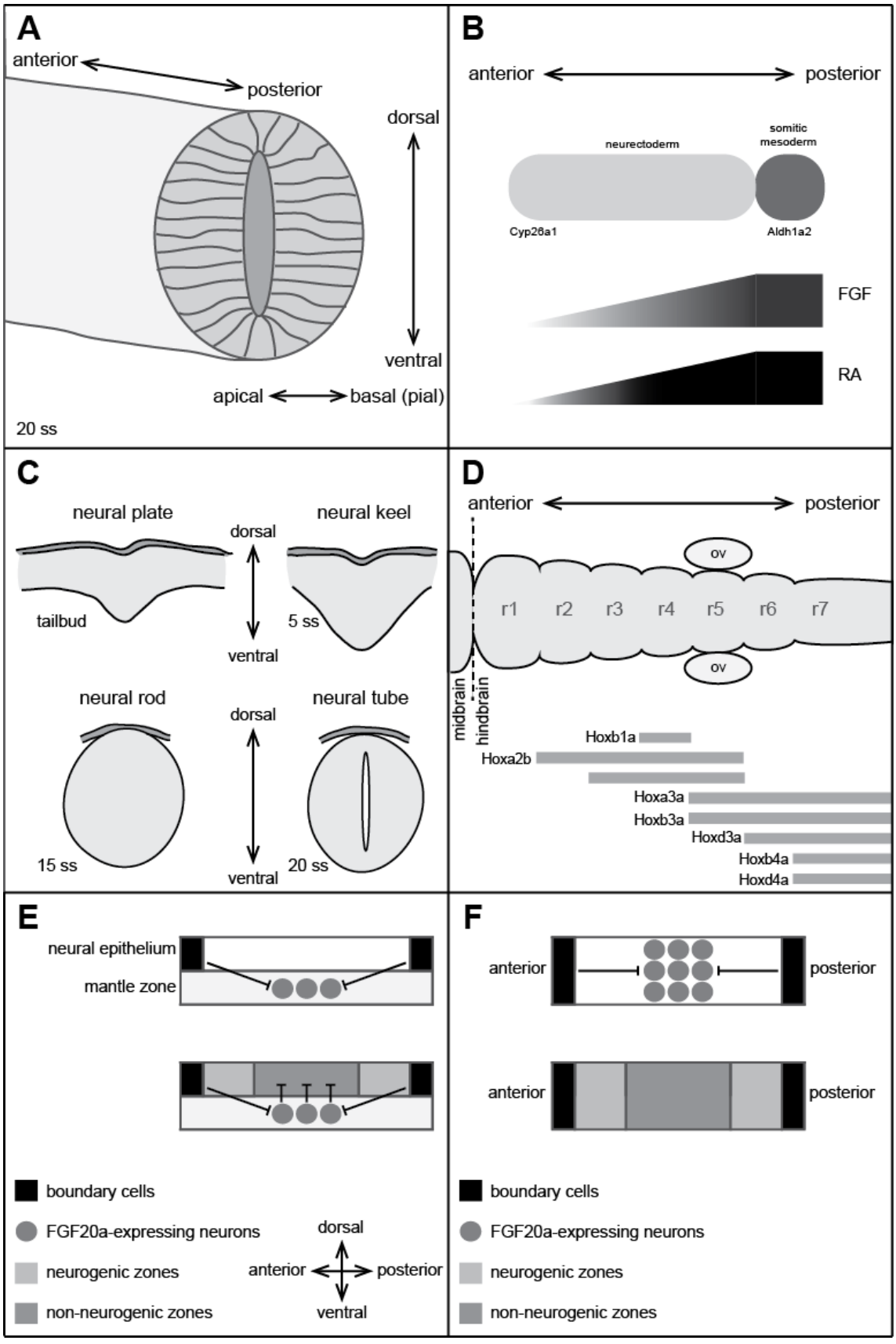
A
anterior
posterior
dorsal
ventral
apical
basal (pial)
20 ss
B
anterior
posterior
neurectoderm
somitic mesoderm
Cyp26a1
Aldh1a2
FGF
RA
C
neural plate
neural keel
dorsal
tailbud
5 ss
ventral
neural rod
neural tube
dorsal
15 ss
20 ss
ventral
D
anterior
posterior
ov
r1
r2
r3
r4
r5
r6
r7
ov
midbrain
hindbrain
Hoxb1a
Hoxa2b
Hoxa3a
Hoxb3a
Hoxd3a
Hoxb4a
Hoxd4a
E
neural epithelium
mantle zone
boundary cells
FGF20a-expressing neurons
neurogenic zones
non-neurogenic zones
dorsal
anterior
posterior
ventral
F
anterior
posterior
anterior
posterior
boundary cells
FGF20a-expressing neurons
neurogenic zones
non-neurogenic zones

Figure 4 Hindbrain patterning and morphology

(A) Three-dimensional schematic of a cross-section of the hindbrain at 20 ss showing the anterior-posterior, dorsal-ventral and apical-basal axes. (B) Schematic showing FGF and RA gradients as hindbrain identity is specified. Aldh1a2 is expressed in the somatic mesoderm and produces RA, which then diffuses across the neurectoderm. Cyp26a1 is expressed in the anterior and degrades RA, resulting in a RA gradient across the hindbrain and gives different identities to rhombomeres. FGF also interacts with Cyp26a1 and Aldh1a2. The regulation of the RA gradient is robust and elongates with the anterior-posterior axis as the embryo develops. (C) Schematic of neural tube formation in zebrafish from neural plate (tailbud stage), neural keel (5 ss), neural rod (15ss) to neural tube formation (20ss). Illustrations are cross-sections with the dorsal-ventral axis labelled. (D) Schematic of hindbrain showing the regions of Hox factor expression that are responsible for segmentation of the hindbrain. Illustration is from a dorsal view and the anterior-posterior gradient is labelled, rhombomeres are labelled r1-r7 and otic vesicle (ov). (E,F) Schematics of a rhombomere and surrounding boundary cells to show the role of hindbrain boundaries in patterning neurogenesis from lateral (E) and ventral (F) views. The boundary cells position FGF20a-expressing neurons to the centre of segments in the mantle zone. Signalling via FGF20a then inhibits neurogenesis in the overlying neural epithelium, known as the non-neurogenic zone, and restricts neurogenesis to the adjacent region, known as the neurogenic zone. Figure based on Clarke (2009),White et al. (2007), Moens and Prince (2002) and Terriente et al. (2012).

1.2.2 Hindbrain boundary cells

Hindbrain boundary cells arise at the border of rhombomeres and are a distinct cell population from the other cells of the hindbrain segments. The boundary region is comprised of a two-cell layer that spans the dorsal-ventral axis. In chick embryos, there is a larger extracellular space between the boundary cells and the arrangement of these cells is different from those that comprise the rhombomeres (Lumsden and Keynes, 1989; Heyman et al., 1993). Experiments in chick found that the S-phase nuclei of boundary cells are situated closer to the basal surface, whereas in the rhombomeres they are at the pial surface. In addition, the boundary cells have a lower rate of cell division (Guthrie and Lumsden, 1991). At the hindbrain boundaries, the neural epithelium is constricted and experiments in zebrafish show that increased myosin phosphatase results in altered cell morphology in the hindbrain as a result of increased cortical tension. This suggests that during normal development, tension and cell shape are different at the boundaries (Gutzman and Sive, 2010).

During hindbrain development, the boundary cells arise in a non-sequential order with respect to the A-P axis, but following a specific and reproducible pattern (Fraser et al., 1990). The boundaries either side of r4 are specified first, with the r3/r4 boundary initially, followed by the r4/r5 boundary. The remaining four boundaries arise in the following order: r1/r2, r2/r3, r6/r7 and r5/r6 (Moens and Prince, 2002).

Cell transplantation experiments have shown that juxtaposed odd and even segments induce boundary formation (Guthrie and Lumsden, 1991).

Currently, the genetic markers that have been identified for hindbrain boundary cells are expressed in all six boundaries, suggesting that all boundaries are the same cell type. Such markers include *wnt1* and *wnt8b* at early stages, from 14 hours post fertilisation (hpf) (Riley et al., 2004; Amoyel et al., 2005), and radical fringe (*rfng*), which is expressed in the boundaries from 16 hpf (Cheng et al., 2004). *pax6* is expressed at higher levels in the boundaries than the rest of the rhombomeres (Xu et al., 1995).

Rfng is expressed by the boundary cells, and promotes Notch activation, which in turn prevents neurogenesis, enabling the boundary cells to be maintained since differentiation is inhibited (Cheng et al., 2004; Qiu et al., 2004; Qiu et al., 2009). The boundary cells act as signalling centres in the hindbrain (Walshe et al., 2002; Riley et al., 2004), and regulate neuronal patterning by positioning FGF20a-expressing neurons in segment centres. These neurons then provide a concentrated source of FGF20 signalling (Gonzalez-Quevedo et al., 2010; Terriente et al., 2012), which acts to locally inhibit neurogenesis and restrict it to regions flanking the boundaries (Figure 4). Consequently, the neurogenic zones are adjacent to the boundary cells and neurogenesis is excluded from the centre of rhombomeres (Gonzalez-Quevedo et al., 2010) (Figure 4). Previous studies where boundary cell formation is prevented have shown that neurons are no longer organised in the correct way and that neuronal subtypes which should be separated are adjacent in the hindbrain (Terriente et al., 2012).

1.2.3 Eph receptors and ephrins during zebrafish hindbrain development

Signalling by Eph receptors and ephrins is important during hindbrain development. Two separate roles have been identified in hindbrain segmentation in which Eph-ephrin signalling is responsible for border sharpening and for boundary cell formation (Xu et al., 1995; Heyman et al., 1995; Irving et al., 1996). To investigate border sharpening, EphA4 signalling was blocked by a dominant negative form of the

receptor, which showed that the borders of r3 and r5, where EphA4 is expressed, no longer sharpen (Xu et al., 1995). When antisense morpholino oligonucleotides (MOs) against *EphA4* were injected into embryos, the expression of *krox20* was found to be fuzzy at the borders of r3 and r5 (Cooke et al., 2005). Another study showed that mosaic ectopic expression of *EphA4* or *ephrinB2* was able to drive cell sorting within hindbrain segments (Xu et al., 1999).

The role of Eph-ephrin signalling in regulating hindbrain boundary cell formation was identified in similar experiments to those described for border sharpening. Injection of dominant negative EphA4 to block Eph-ephrin signalling found that the formation of certain boundaries was disrupted (Xu et al., 1995). In addition, boundary cell markers, such as *rfng* and *sema3Gb*, are no longer expressed after knockdown of *EphA4*, *ephrinB3* or *ephrinB2* (Cooke et al., 2005; Terriente et al., 2012). The boundaries that are disrupted are specific to the location of signalling by the Eph-ephrin binding pair that has been blocked. For example, experiments using MOs against *EphA4* or *ephrinB3* found that the hindbrain boundaries at r2/r3, r3/r4 and r5/r6 are lost (Cooke et al., 2005; Terriente et al., 2012). When *ephrinB2* is knocked down, there is only a slight disruption to the hindbrain boundaries. However, when *ephrinB2* function is blocked in combination with *EphA4* there was a greater disruption to boundaries and increased loss of the boundary cell marker, *sema3Gb*, than when targeting *EphA4* alone (Cooke et al., 2005). Henceforth, the point at which rhombomeres are in contact with one another will be referred to as the border and the cell population that arises at the border will be referred to as the boundary.

Although Eph receptors and ephrins can bind multiple partners, they have higher affinity for specific ephrins or Eph receptors, respectively. In the hindbrain, there are three Eph-ephrin binding pairs, based on affinity and their expression in segmented and complementary patterns (Figure 5). For example, ephrinB3b is expressed in rhombomeres 2 (r2), 4 (r4) and 6 (r6), whilst EphA4a is expressed in a complementary pattern in the adjacent rhombomeres, r3 and r5. As signalling is contact dependent, Eph-ephrin signalling is strongly activated at the border of rhombomeres in which the binding partners are expressed (Figure 5: yellow). There is also likely to be weaker activation within the segments due to overlapping expression with binding partners that can be bound at a lower affinity. Whilst

EphA4a-ephrinB3b and EphB4a-ephrinB2a binding pairs have been shown to be involved in border sharpening and boundary cell formation, the role of EphB3a-ephrinB1a has not been determined (Figure 5).

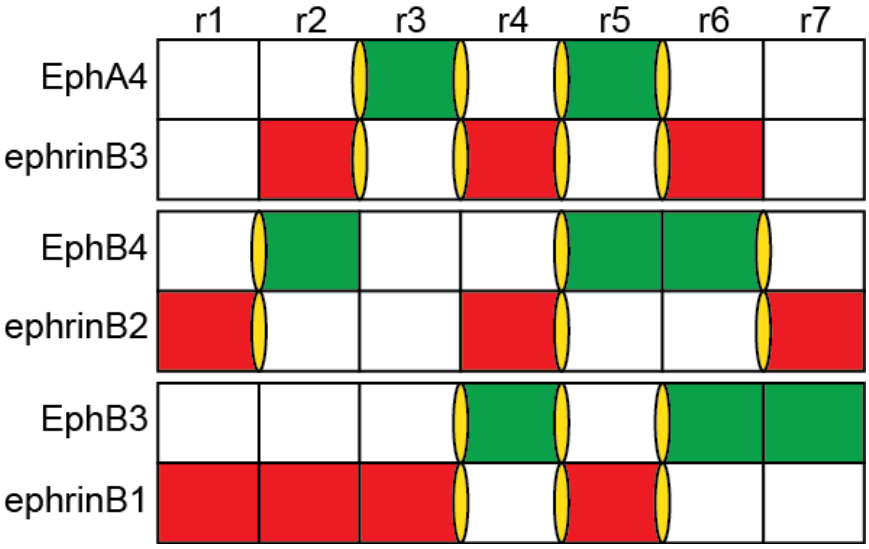

Figure 5 Eph receptor and ephrin expression in the zebrafish hindbrain

The three Eph-ephrin binding pairs expressed in the zebrafish hindbrain are labelled vertically and the seven rhombomeres are represented in vertical columns (r1-r7). The expression of Eph receptors and ephrins is shown in green and red, respectively. Locations where strong signalling occurs are shown in yellow. This is only where an Eph receptor and ephrin of a binding pair are expressed in adjacent rhombomeres, due to the contact dependent nature of signalling. Expression patterns based on Xu and Wilkinson (2013), and Jordi Cayuso, Wilkinson Lab (unpublished).

1.3 Transcriptional regulation by Eph receptor and ephrin signalling

In addition to the well described roles of Eph-ephrin signalling that have been previously discussed (Chapter 1.1.5), there is increasing evidence that Eph-ephrin signalling is also able to regulate gene expression, although this is less understood. This section will focus on experiments that have found Eph-ephrin signalling to have roles in transcriptional regulation and will include both *in vitro* and *in vivo* studies as well as in a variety of tissues and organisms. This will focus initially on examples of Eph-ephrin signalling acting via another receptor or pathway, which regulates gene expression, and then examples where Eph-ephrin signalling directly controls cell differentiation.

1.3.1 Direct versus indirect transcriptional regulation

Before discussing examples of transcriptional regulation by Eph-ephrin signalling, one aspect to address is whether the effect on gene expression is direct or indirect (Wilkinson, 2014). When Eph-ephrin signalling is disrupted there can be change in the position of a cell, for example, from cell migration, resulting in altered cell-cell contacts. This would mean that any alteration in gene expression could be indirect as the cell is now in a new location and receiving different signals. An example of this is in the intestine where double *EphB2* and *EphB3* mutants have mis-positioned cells, which results in cell proliferation and differentiation (Genander et al., 2009). The alternative situation would be changes to gene expression that are a direct consequence of Eph-ephrin signalling. This would include examples where cells do not change their location and are receiving the same external stimuli but still alter their expression. In the hindbrain, a direct consequence of losing Eph-ephrin signalling is the absence of boundary cell marker expression (Xu et al., 1995; Cooke et al., 2005; Terriente et al., 2012).

1.3.2 Transcriptional regulation via other signalling pathways

One mechanism whereby Eph receptors and ephrins can regulate gene expression is by activating other receptors that have known roles in regulating gene expression. It has been shown that Eph-ephrin signalling can result in phosphorylation and subsequent activation of the NMDA receptor. This receptor regulates calcium influx in neurons, which results in the activation of signalling pathways that cause changes to gene expression (Ghosh and Greenbery, 1995). EphB2 is clustered with the NMDA receptor at excitatory synapses and upon ephrinB binding and activation of EphB2 there is an interaction between EphB2 and the NMDA receptor (Dalva et al., 2000). This interaction results in phosphorylation of the NMDA receptor at the NR2B subunit, leading to calcium influx which induces the expression of genes involved in synaptic remodelling (Takasu et al., 2002).

1.3.3 Activation of transcription factors by Eph receptors and ephrins

Some of the previously identified phosphorylation targets of Eph-ephrin signalling have an established role in regulating transcription. One example is EphA4 which is upstream of the Janus kinase-signal transducer and activator of transcription (Jak-Stat) pathway in muscle cells. The Jak-Stat signalling pathway relays the extracellular signal to the nucleus via the activation of Jak, which in turn phosphorylates and activates the Stat transcription factors (Aaronson and Horvath, 2002). In the neuromuscular junction, EphA4 activation by ephrinB1 causes EphA4 to associate with Jak2, leading to its phosphorylation and subsequent activation. This results in the phosphorylation of Stat1 and Stat3, which leads to the up-regulation of acetylcholinesterase (Lai et al., 2004).

1.3.4 Cell fate specification in *Ciona*

There are several examples that demonstrate how Eph-ephrin signalling can regulate cell fate decisions during cell lineage specification in *Ciona*. FGF is a diffusible ligand that causes the widespread activation of MAPK signalling which induces specific cell fates during *Ciona* development. This is inhibited locally by Eph-ephrin signalling, which blocks MAPK activation and results in a mesodermal fate. On the other hand, if there is an absence of Eph-ephrin signalling then MAPK signalling can persist and the cell will be driven down an endodermal fate (Shi and Levine, 2008). Other cell fate decisions driven by Eph-ephrin signalling in *Ciona* include neural and notochord (Picco et al., 2007), and motor ganglion neuronal subtypes (Stolfi et al., 2011).

1.3.5 Survival, proliferation and differentiation of neural progenitors

A number of studies suggest that signalling by Eph receptors and ephrins is important in some contexts for maintaining the balance of neural progenitors and differentiating neurons during neurogenesis. This balance is maintained by ensuring that neural progenitor proliferation and cell differentiation are tightly regulated. A study of the EphA7 mutant, a receptor for ephrinA5, showed a phenotype of a larger forebrain which was found to be due to a reduction in apoptosis of neural progenitors

(Depaepe et al., 2005). The number of progenitor cells can also be regulated by inhibiting or increasing cell proliferation. A study investigating the role of EphB1-ephrinB3 signalling in the hippocampus shows that activation maintains neural progenitors and in *EphB1* mutant mice there is a depletion of this cell population (Chumley et al., 2007). In contrast, neural progenitor cell proliferation is inhibited by ephrinB3-EphB3 signalling in the subventricular zone. EphB3 is expressed by the neural stem cell precursors and ephrinB3 in the adjacent cells. When *EphB3* is knocked out in mice there is an increase in proliferation of the progenitor cells (del Valle et al., 2011). These examples demonstrate that Eph-ephrin signalling can have opposing effects on neural progenitor cell proliferation.

Neuronal differentiation is also regulated by Eph-ephrin signalling, both downstream of forward and reverse signalling. When EphA receptors are activated by ephrinA1, this promotes the differentiation of neural progenitors to neurons. In cell culture, experiments where neurospheres were treated with ephrinA2 found that there was an increase in markers for neural differentiation, and the reverse was observed when treated with a dominant negative form of the ligand. This mechanism acts via the MAPK pathway which is induced by EphA activating Rap1, a small G protein (Aoki et al., 2004). Similarly, in stem cell niches of the adult hippocampus, Eph-ephrin signalling promotes differentiation. When EphB2, expressed by neural stem cells, is activated by ephrinB2, proneural transcription factors are up-regulated to drive neuronal differentiation (Ashton et al., 2012). In the cerebral cortex, ephrinB1 reverse signalling is responsible for maintaining neural progenitors, and blocking signalling with a dominant negative form of ephrinB1 induces differentiation to cortical neurons (Qiu et al., 2008).

1.3.6 Keratinocyte development

Cell differentiation in the skin is regulated by Eph-ephrin signalling via desmoglein1 up-regulation to inhibit MAPK signalling, leading to keratinocyte differentiation (Getsios et al., 2004; Lin et al., 2010). Desmoglein1 is a desmosomal cadherin that binds to other desmogleins or desmocollins in epithelial cells membranes, to form desmosomes, enabling epithelial cells to anchor together (Nekrasova and Green,

2013). Eph-ephrin signalling induces the differentiation of keratinocytes as well as a decrease in proliferation, as they move outwards to the superficial layers where proliferation is not required (Genander et al., 2010). The Eph-ephrin binding pair responsible for this behaviour is ephrinA1 which activates EphA2. EphA2 activation leads to the up-regulation of desmoglein1 expression, which supports keratinocyte differentiation (Lin et al., 2010).

1.3.7 Bone remodelling

Bone remodelling is the process by which bone matrix is resorbed by osteoclasts, and replaced with new bone by osteoblasts. The transition of bone removal to bone production is mediated by differentiation of osteoclasts to osteoblasts (Sims and Martin, 2014). During the later stages of bone development EphB-ephrinB signalling plays the predominant role through both forward and reverse signalling. Osteoclasts are ephrinB2-expressing and osteoblasts are EphB4-expressing. EphB4 activation in osteoblasts by ephrinB2 promotes cells to differentiate to osteoblasts, maintaining this fate. Reverse signalling through ephrinB2 in osteoclasts inhibits differentiation to osteoblast (Zhao et al., 2006). Signalling by EphA-ephrinAs has also been implicated in this process in bone remodelling; EphA2 activation by ephrinA2 leads to osteoclast differentiation (Irie et al., 2009). In combination, forward and reverse signalling help to maintain the necessary balance for bone homeostasis.

1.4 Aims

This study has focused on identifying transcriptional targets of Eph-ephrin signalling in the hindbrain. Previous studies have identified that Eph-ephrin signalling can induce changes in gene expression in a variety of cell types leading to changes in cell fate, cell proliferation and synaptic remodelling. During hindbrain development, there is evidence that Eph-ephrin signalling is essential to induce a cell population, called the boundary cells, which express specific markers. When Eph-ephrin signalling is blocked, expression of these genes is no longer induced.

In order to further understand the role of Eph-ephrin signalling in hindbrain development, this project has set out to identify the transcriptional targets of this signalling. The first aim of this project was to explore different techniques to find the best method to disrupt Eph-ephrin function in the hindbrain as measured by loss of boundary cells. Once this was in place the method was then used to identify the target genes of Eph-ephrin signalling. Finally, the target genes that had been identified were investigated to further understand the role of Eph-ephrin signalling in the hindbrain.

Chapter 2. Materials and Methods

2.1 Solutions and Reagents

2.1.1 General Solutions

Agarose gel
Agarose gels were made with 1% agarose in 1X Tris-acetate (TAE) run at 120 V and 120 mA unless otherwise stated.

Phosphate Buffered Saline with Tween-20 (PBST)
PBST was made to 1 µl/ml of Tween-20 (Sigma Aldrich, UK) in 1 x PBS.

Danieau's solution
1X Danieau's solution is comprised of 58 mM NaCl, 0.7 mM KCl, 0.4 mM $MgSO_4$, 0.6 mM $Ca(NO_3)_2$ 5 mM HEPES in 1 x PBS and pH adjusted to 7.6.

E3 media
1X E3 media is comprised of 5 mM NaCl, 0.17 mM KCl, 0.33 mM CaCl, 0.33 mM $MgSO_4$ in dH_2O and pH adjusted to 7.4.

L Broth (LB)
10 g Tryptone, 10 g NaCl and 5 g yeast extract was dissolved in a final volume of 1L ddH_2O and sterilized by autoclave at 20 PSI for 15 minutes.

2.1.2 Fish Husbandry

Zebrafish embryos were obtained by natural spawning as described (Westerfield, 2000) and maintained between 23 °C and 28.5 °C. Embryos were staged by hours post fertilisation (hpf) or the number of somites, somite stage (ss) (Kimmel et al., 1995).

2.1.3 Zebrafish strains

The following strains were used:

Wild types:

LonAB

Transgenics:

HSP70 Gal4 (*HS-Gal4)* (Scheer and Campos-Ortega, 1999)

UAS-ephrinB1-DN1-ACC (*UAS-soluble ephinB1*) (Jordi Cayuso, Francis Crick Institute)

Mutants:

tp53 mutant (Berghmans et al 2005)

EphA4 crispr1 mutant (mut_EphA4a_e3) *EphA4a*^{fci503} (Jordi Cayuso, Francis Crick Institute)

EphB4a^{hu3378} (Sanger Institute)

ephrinB2a^{hu3393} (Sanger Institute)

EphrinB3b TALEN mutant (mut_efnB3b_e1(2bpdel)) *EphrinB3b*^{fci502} (Megan Addison, Francis Crick Institute)

2.1.4 Genotyping

Fin-clipping protocol

Adult zebrafish were treated with 0.02% 3-aminobenzoic acid ethyl ester (MS-222) before clipping the end of the caudal fin with surgical scissors. DNA was lysed in 50 µl of 0.02% proteinase K (Thermo Fisher, UK) and incubated at 65 °C for 16 hours.

PCR and restriction digest

The primers used for genotyping are shown in Table 1 Primers used for genotyping. Unless otherwise stated, reagents used for PCR and restriction digestion were purchased from New England Biolabs, UK.

Gene	Forward primer 5'-3'	Reverse primer 5'-3'
tp53	ACATGAAATTGCCAGAGTATGT	TCGGATAGCCTAGTGCGAGC
EphA4a	GCTCCGCAGTACATTTTAGGG	GTCTTTCCTCTCACAGTGGGA
EphB4a	AGGCGGAGAGAAGAAAGTCAA	TGTTACCTGCATTGCCAAAGG
ephrinB2a	TTTTGATCTAGAGAGAAATGCGAGT	TAGAGGCGTGTCTGCTTTTGACACCTG
ephrinB3b	GAGAGAGTATCCCGCACACACG	TAGATGGGCTCCATGTTGGT

Table 1 Primers used for genotyping

The PCR reaction to identify *tp53* mutants was set up as shown in Table 2. The reaction was incubated at 95 °C for 30 seconds, then 35 cycles of 95 °C for 30 seconds, 53 °C for 30 seconds and 68 °C for 20 seconds, followed by a final incubation at 68 °C for 2 minutes.

The PCR reaction to identify *EphA4a* mutants was set up as shown in Table 3. The reaction was incubated at 98 °C for 1 minute, then 40 cycles of 98 °C for 10 seconds, 67 °C for 20 seconds and 72 °C for 20 seconds, followed by a final incubation at 72 °C for 2 minutes.

The PCR reaction to identify *EphB4a* mutants was set up as shown in Table 4. The reaction was incubated at 98 °C for 1 minute, then 40 cycles of 98 °C for 10 seconds, 67 °C for 20 seconds and 72 °C for 20 seconds, followed by a final incubation at 72 °C for 2 minutes.

The PCR reaction to identify *ephrinB2a* mutants was set up as shown in Table 5. The reaction was incubated at 94 °C for 90 seconds, then 44 cycles of 94 °C for 30 seconds, 64 °C for 30 seconds and 68 °C for 20 seconds, followed by a final incubation at 72 °C for 7 minutes.

Reagent	Volume
cDNA (diluted DNA digest 1:10)	1.0 µl
10X Standard *Taq* Reaction Buffer	2.0 µl
10mM dNTPs	0.4 µl
***tp53* Forward primer (10 µM)**	1.0 µl
***tp53* Reverse primer (10 µM)**	1.0 µl
***Taq* DNA polymerase**	0.3 µl
DEPC-treated water	14.3 µl
Total volume	20.0 µl

Table 2 PCR reaction for *tp53* genotyping

Reagent	Volume
cDNA (diluted DNA digest 1:50)	4.0 µl
5X Q5 Reaction Buffer	5.0 µl
10mM dNTPs	0.5 µl
***EphA4a* Forward primer (10 µM)**	1.0 µl
***EphA4a* Reverse primer (10 µM)**	1.0 µl
Q5 High-Fidelity DNA polymerase	0.1 µl
DEPC-treated water	13.4 µl
Total volume	25.0 µl

Table 3 PCR reaction for *EphA4a* genotyping

Reagent	Volume
cDNA (diluted DNA digest 1:50)	4.0 µl
5X Q5 Reaction Buffer	5.0 µl
10mM dNTPs	0.5 µl
***EphB4a* Forward primer (10 µM)**	1.0 µl
***EphB4a* Reverse primer (10 µM)**	1.0 µl
Q5 High-Fidelity DNA polymerase	0.1 µl
DEPC-treated water	13.4 µl
Total volume	25.0 µl

Table 4 PCR reaction for *EphB4a* genotyping

Reagent	Volume
cDNA (diluted DNA digest 1:50)	2.0 µl
5X Q5 Reaction Buffer	5.0 µl
10mM dNTPs	0.5 µl
***ephrinB2a* Forward primer (10 µM)**	1.0 µl
***ephrinB2a* Reverse primer (10 µM)**	1.0 µl
Q5 High-Fidelity DNA polymerase	0.1 µl
DEPC-treated water	13.4 µl
Total volume	25.0 µl

Table 5 PCR reaction for *ephrinB2a* genotyping

PCR products were visualised by agarose gel electrophoresis before restriction digestion, set up as shown in Table 6. The reaction was incubated at 37 °C for 3 hours before being visualised by agarose gel electrophoresis to determine the genotype. The enzymes used and the interpretation of the restriction digest are shown in Table 7.

Reagent	Volume
PCR product	5.0 µl
CutSmart Buffer	1.5 µl
Restriction enzyme	1.0 µl
DEPC-treated water	7.5 µl
Total volume	15.0 µl

Table 6 Restriction digest for genotyping

Gene	Restriction enzyme	Mutated gene cut or uncut?
tp53	MboII	cut
EphA4a	AleI	uncut
EphB4a	AlwNI	cut
ephrinB2a	PshAI	cut

Table 7 Restriction enzyme used and interpretation of genotyping result

High Resolution Melt Curve (HRM) analysis

HRM was used to identify *ephrinB3b* mutants and has been previously described in (Dahlem et al. 2012). RT-PCR was carried out using the *ephrinB3b* primers shown in Table 1, and in the presence of MeltDoctor^{TM} HRM Dye (applied Biosystems) using an ABI 7900 qPCR machine according to the manufacturer' instructions. This was

followed by a melt curve analysis using HRM Software V2.0.2 from Life Technologies.

2.1.5 Microinjection with morpholino oligonucleotides

MOs (GeneTools, USA) were re-suspended to a final concentration of 1 mM in ddH_2O as described (Gerety and Wilkinson, 2011), and stored at RT. MOs were injected up until the 2-cell stage and into p53 homozygous mutants to avoid the effects of toxicity that can result from MO use. MOs used are listed in Table 8.

MOs	Translation blocking (TB) or splice blocking (SB)	Sequence 5'-3'	References
EphA4a	TB	AACACAAGCGCAGCCATTGGTGTC	(Cooke et al., 2005)
EphB4a	TB	TAAAATGAGTGAGTTACCTTCCTCC	
ephrinB2a	TB	CGGTCAAATTCCGTTTCGCGGGA	(Cooke et al., 2005)
ephrinB3b	SB	TTGCGGCTCTTACCTTTTGTTCAAG	(Terriente et al., 2012)

Table 8 MOs used for knockdown experiments

2.1.6 Heat shock

Embryos were collected at the desired stage and subjected to heat shock in 0.6X Danieau's solution at 38 °C for 1 hour before returning to 28.5 °C.

2.2 Analysis of gene expression

2.2.1 Whole embryo and hindbrain tissue dissections

Embryos were collected at 19 hpf or 20 ss, dechorionated, de-yolked, and hindbrains dissected using forceps in autoclaved PBS. Dissected hindbrains were transferred to Non-Stick RNase-Free 1.5 ml Microfuge Tubes (Ambion, UK) and centrifuged at

0.3 xg for 30 seconds. The supernatant was discarded and 350 µl lysis buffer (The Epigenetics Company, USA) added.

Whole embryos were collected at 19 hpf or 20 ss, dechorionated then transferred to Non-Stick RNase-Free 1.5 ml Microfuge Tubes (Ambion, UK) and centrifuged at 0.3 xg for 30 seconds. The supernatant was discarded and 350 µl lysis buffer added prior to RNA extraction.

2.2.2 RNA extraction

RNA was extracted following the protocol described by Lan et al. (2009) using the RNeasy® Micro Kit (Qiagen, Netherlands) or Quick-RNA Microprep (The Epigenetics Company, USA) and the manufacturer's recommended protocol.

2.2.3 cDNA synthesis

cDNA was synthesised using SuperScript® III First-Strand Synthesis System for RT-PCR (Invitrogen, USA) following the manufacturer's protocol. The reaction was set up with 100 ng RNA, 1 µl oligo$(dT)_{20}$ and 1 µl dNTP mix made up to 10 µl with DEPC-treated water and incubated at 65 °C for 5 minutes followed by incubation on ice for 1 minute. The cDNA synthesis mix was then added in the following order: 2 µl RT buffer, 4 µl $MgCl_2$, 2 µl DTT, 1 µl RNaseOUT™, 1 µl SuperScript III RT and incubated at 50 °C for 50 minutes then 85 °C for 5 minutes followed by an incubation on ice for 1 minute. 1 µl of RNaseH was added before incubating at 37 °C for 20 minutes. cDNA was used for RT-qPCR or stored at -20 °C.

2.2.4 Reverse transcriptase – quantitative polymerase chain reaction (RT-qPCR)

A dilution series of the cDNA synthesised was used to confirm the amplification efficiency of each primer pair using the following dilutions: 1:3, 1:6, 1:12, 1:24 and 1:48. A no template control was also used to determine any contamination and primer dimer formation. qPCR analysis was carried out using Platinum® SYBR®

Green qPCR Supermix-UDG and reagents unless otherwise stated (Invitrogen, USA). A typical RT-qPCR reaction is shown in Table 9. The reaction was incubated at 50 °C for 2 minutes, 95 °C for 2 minutes, then 40 cycles of 95 °C for 15 second and 60 °C for 30 seconds, followed by a melting curve analysis.

Reagent	Volume
cDNA (diluted)	1.0 µl
SYBR mix	10.0 µl
ROX	0.4 µl
Forward primer (10 µM)	0.5 µl
Reverse primer (10 µM)	0.5 µl
DEPC-treated water	7.6 µl
Total volume	20.0 µl

Table 9 RT-qPCR reaction

2.2.5 RT-qPCR primer sequences

The primers used for RT-qPCR are shown in Table 10. These were all designed for this project except for β-actin which was the same as for previously published work (Lan et al., 2009).

Gene	Forward primer 5'-3'	Reverse primer 5'-3'
β-actin	CGAGCTGTCTTCCCATCCA	TCACCAACGTAGCTGTCTTT
six3a	AAGCCACTGGACTCACTCCT	CTGCCCTATTGCTTGATGCT
hoxB6a	GGGAAAAGCATCTACCCTGA	CGACCAGCGTTACCGAAG
krox20	GGACATTACGAGCAGATAAACG	CTGCTGGAGTAGGCTAAGTCG
otx2	CAAGCAACCACCTTACACGG	TCGTCTCTGCTTTCGAGGAG
cd9a	AAGTGGCTGCTGGAATTTGG	TGCTTTGTTGGTAGGTGTCG
ppfia4	GTCCGGGGTCTCTAGTGAAG	AGTCACCCTTTCAAGAGCCA
tmppe	GGGACAAATGAAGCCTCGAC	TGCCCATTGAGTGTAAGAGC
dnm2a	GGTACAGATGCCCGGGATAT	CAGCACGAATGTCCTTACGG
ube2_z	TACCATAACGAGCCGGGTTT	ACCCTCCAGCATATCACACA
ttc32	ACACACAGTTCATCGAGTCCT	CCACCCGGAGATACTTCACC
akr7a3	CTTCGGCAACAATTGGGCTA	CCGTACGCTGATTCTAGAGC
Stx4	ACTCAGAGAAGACATCAAAGGGA	CCTCATTCTTACATTCACTGGGA
hmgb2a	AGGGACCTCGGTGAACTTTT	GCGAACCTTATCAGTCTTAGCC
hnrnpaba	GCAGTATGGAGGTCGCTTTG	CCTTGGTTTCCGTAGCCTTG
nap1l1	TCACACAAACAATCCTGACAAAA	TAGTCCAGTCGATCGTGCA
tubb2b	TCTTCAAGCTGGACAATGCG	TTGAAGGTCGCTGTCTCCAT
mdka	AGGCTCTCTTCAACGTCGAA	TAGTTCCCTTTCCCCTTGCC
marcksb	CGGAGCAAAAGACGAGACTG	TCCCGTTGGTTTTAGCATGG
ybx1	ATATCTCCGTAGCGTTGGGG	GGGCCGGTAACATTTGCTG
rpl15	ACCAGATCAAGTTTGCACGC	CAGTAGGAGTTCAGGACCCG
fubp1	ACTACTCTAACGTGGCTCCG	GTACCCCATCACCTCCTATTTT
col15a1b	GAGGCTCCAAGGGTCACC	CCCAAAAGAGTAGGCAGGGT
fam117aa	GCCTGTTACCTGTGTCAACG	TCTCGTAGGTGTTCGGCG
abi1b	CCTCAGCCCCACCTAAACG	CAGTGAGGGGAATCTGGGG
wsb1	AGGACATCGGATTGTGAGACT	ACTGTTCTGCCGAGAGAGTC

Table 10 RT-qPCR primers

2.2.6 Statistical significance

Statistical significance was determined by one-way ANOVA test or Pearson's Chi-square test using Microsoft Excel.

2.3 In situ hybridisation

2.3.1 Cloning new *in situ* hybridisation probes

PCR of probe sequence

In situ hybridisation probe sequences were amplified by PCR from a cDNA library generated from whole wild type zebrafish embryos at 20 ss. The primer sequences in Table 11 and the reaction was set up as described in Table 12. Reagents were purchased from New England Biolabs, UK, unless otherwise stated. The reaction was initiated with an incubation at 98 °C for 30 seconds, followed by 35 cycles of: 98 °C for 10 seconds, 57 °C for 20 seconds and 72 °C for 20 seconds, then a final extension step of 72 °C for 2 minutes.

***In situ* hybridisation probe**	**Forward primer 5'-3'**	**Reverse primer 5'-3'**
nestin	GGCCAACTCTGAGTGCAATAG	TTGGCGGGATCATAAGTAGCT
hmgb2a	TAATCAAGTTTGTGCGCGCA	GCTTCTGCCTTCTTTCCTGC
mdka	TAGTTCAGCCACTCCTCTGC	GACTTGTCTACCACTGCCCT
tubb2b	GTGTCTACTCCCAGCCAGTT	TTCATGATGCGGTCGGGATA
nap1l1	TCCCTCGAAGCATGACACTT	CTCAGGGCAAAACTCGCAAT

Table 11 Primers for *in situ* hybridisation probes

Reagent	**Volume**
cDNA library (diluted 1:3)	1.0 µl
10X Standard buffer	2.5 µl
dNTPs (2 mM)	0.5 µl
forward primer (10 µM)	0.1 µl
reverse primer (10 µM)	0.1 µl
DEPC-treated water (Sigma Aldrich, UK)	20.6 µl
Taq polymerase	0.2 µl
Total volume	25.0 µl

Table 12 *In situ* hybridisation probe PCR

Purification of PCR product

The PCR reaction products were then run on an agarose gel and purified using the MiniElute ® Gel Extraction Kit (Qiagen, Netherlands) and the recommended protocol. DNA eluted in a final volume of 15 µl DEPC-treated water (Sigma Aldrich, UK).

Ligation of probe sequence into vector

The vector and insert were ligated at a ratio of 1:3 with a 7.5 µl reaction set up as follows: 0.5 µl insert, 5.8 µl vector, 0.7 µl 10X buffer and 0.5 µl T4 DNA ligase. A control reaction was set up in which the insert was replaced with DEPC-treated water (Sigma Aldrich, UK). The reactions were incubated at room temperature (RT) for 16 hours.

Transformation to competent cells

2 µl of the ligation product was transformed to Library Efficient® DH5αTM Competent Cells (Invitrogen, USA) and incubated on ice for 30 seconds before being subject to heat shock at 42 °C for 1 minute. The cells were then incubated on ice for 1 minute and 1 ml LB added before incubation at 37 °C for 1 hour. The cells were centrifuged at 0.4 xg for 1 minute and all except 150 µl LB was removed. The cells were re-suspended in the liquid and all 150 µl plated onto pre-warmed LB agar supplemented with 100 µg/ml ampicillin at 37 °C for 16 hours.

Colony selection

Single colonies were selected using a sterilised pick and inoculated in LB with the addition of 100 µg/ml ampicillin, cultures were incubated at 37 °C with gentle shaking for 16 hours.

Preparation and isolation of plasmid DNA

Plasmid DNA was extracted from E. coli cells using the QIAprep® Spin Miniprep Kit (Qiagen, Netherlands) following the recommended protocol and eluted in 50 µl DEPC-treated water (Sigma Aldrich, UK).

Confirmation of insert sequence

Constructs that had the expected molecular weight visualised by agarose gel electrophoresis, after restriction digestion with NotI (New England Biolabs, UK) were selected for sequencing by Source Biosicence sequencing services (Nottingham, UK) for confirmation of sequence.

RNA probes were then synthesised from the plasmid DNA as described below.

2.3.2 Synthesising *in situ* hybridisation probes

Some probes have been previously published (Table 13).

Gene	Publication
rfng	(Terriente et al., 2012)
deltaD	(Amoyel et al., 2005)
neurogenin1	(Gonzalez-Quevedo et al., 2010)
neuroD4	(Terriente et al., 2012)
huC/D	Wilkinson Lab, Francis Crick Institute

Table 13 Probes used for *in situ* hybridisation

2-5 µg of plasmid DNA containing the probe was linearised with the appropriate restriction enzyme. The reaction is shown in Table 14.

Reagent	Volume
DNA plasmid	3 µl
10X Buffer H (New England Biolabs, UK)	4 µl
BSA (Promega, USA)	0.4 µl
EcoRI (New England Biolabs, UK)	2 µl
DEPC-treated water (Sigma Aldrich, UK)	48.4 µl
Total volume	40 µl

Table 14 Linearisation of plamid DNA

The reaction was incubated at 37 °C for 16 hours before purifying the linearised DNA using the Illustra GFX PCR DNA and Gel Band Purification Kit (GE Healthcare) and their suggested protocol. DNA was eluted in DEPC-treated water (Sigma Aldrich, UK) into a final volume of 30 µl. The RNA synthesis reaction was set up as shown in Table 15, using reagents purchased from New England Biolabs, UK, unless otherwise stated. The reaction was incubated at 37 °C for 3 hours before purifying the RNA probe. The following were added to the finished reaction in order: 60 µl DEPC-treated water (Sigma Aldrich, UK), 10 µl 10 M ammonium acetate, 2 µl glycogen and 130 µl isopropanol. The reaction was mixed by pipetting and incubated at -20 °C for 30 minutes then centrifuged at 16 xg at 4 °C for 30 minutes. The supernatant was removed and 500 µl 70% ethanol in DEPC-treated water (Sigma Aldrich, UK) added to the pellet. The liquid was pipetted up and down without

disrupting the pellet and removed before centrifugation at 4 xg at 4 °C for 30 seconds. The pellet was dried then re-suspended in 40 µl DEPC-treated water (Sigma Aldrich, UK) and 160 µl hybridisation solution added for long-term storage.

Reagent	Volume
Linearised DNA (1 µg)	*x* µl
10X buffer	4 µl
DTT	4 µl
DIG/F labelled NTPs	2 µl
RNase	1 µl
T7 Polymerase	4 µl
DEPC-treated water (Sigma Aldrich, UK)	x µl
Total volume	40 µl

Table 15 RNA synthesis reaction

2.3.3 *In situ* hybridisation solutions

Hybridisation solution

50% formamide (Ambion, UK), 5XSSC, 50 µg/ml heparin (Sigma Aldrich, UK), 500 µg/ml tRNA (Roche, Switzerland), 0.1% Tween-20 (Sigma Aldrich, UK), 5% dextran sulphate (Sigma Aldrich, UK), 92 mM citric acid, pH adjusted to 6.0.

Solution I

25% formamide (Sigma Aldrich, UK), 2X SSC

Solution II

2X SSC

Solution III

0.2X SSC

Solution IV

0.1X SSS

Blocking solution

2 mg/ml BSA (Sigma Aldrich, UK), 2% sheep serum (Life Technologies, USA).

Colouration buffer

100 mM Tris-HCl (pH 9.5), 50 mM $MgCl_2$, 100 mM NaCl, 0.1% Tween-20 (Sigma Aldrich, UK).

Colouration solution

45 µl NBT (Roche, Switzerland), 35 µl BCIP (Roche, Switzerland) in 10 ml colouration buffer.

2.3.4 *In situ* hybridisation protocol

All washes and incubations were carried out with gentle shaking unless otherwise stated. Embryos were collected in a 2 ml microcentrifuge tube at the stage of interest and fixed in 4% PFA for 3 hours. Embryos were washed 3 times in PBST and dechorionated before dehydration in each of the following for 10 minutes: 2 times 1 ml 75% MeOH, 2 times 1 ml 100% MeOH. Embryos can be stored long term in 100% MeOH at -20 °C prior to *in situ* hybridisation.

Embryos were rehydrated in a 2 ml microcentrifuge tube and washed in each of the following for 10 minutes: 1 ml 75%, 50%, 25% MeOH in PBST. Embryos were washed 5 times in PBST for 5 minutes and dechorionated. Embryos were then pre-hybridized in 1 ml Hybridization Solution at 65 °C for a minimum of 1 hour. Probes were diluted at 1-4/200 µl in Hybridization Solution and pre-warmed to 65 °C before being used for embryo incubation at 65 °C for 16 hours.

Solutions I-IV were pre-warmed to 65 °C. Washes were carried out at 65 °C with 1 ml of solution as follows: 3 washes in Solution I for 10 minutes, 2 washes in Solution II for 10 minutes, 2 washes in Solution III for 20 minutes and one wash in Solution IV for 20 minutes. Embryos were washed 3 times in 1 ml PBST at RT for 5 minutes before incubation in blocking solution at RT for a minimum of 1 hour. Samples were then incubated in 200 µl 37.5 U/ml anti-digoxigenin AP (Roche, Switzerland) at 4 °C for 16 hours.

Embryos were then washed 10 times in 1 ml PBST at RT for 15 minutes before 4 washes in Colouration Buffer for 5 minutes. Embryos were transferred to a 12 well

plate and the Colouration Buffer was replaced with 1 ml Colouration Solution and kept in the dark to develop for around 1-4 hours.

After development, embryos were washed 4 times in 1 ml PBST at RT for 5 minutes before fixation in 1 ml 4% PFA at RT for 30 minutes. Embryos were washed 4 times in 1 ml PBST at RT before long-term storage in 75% glycerol in PBST. Embryos were prepared for image analysis by de-yolking and flat or side mounting onto slides in 75% glycerol in PBST. Imaging was carried out using Zeiss AxioCam High Resolution microscope and Zen pro 2012 software.

2.4 Whole mount immunofluorescence

2.4.1 Whole mount immunofluorescence protocol

All washes and incubations were carried out with gentle shaking unless otherwise stated. Embryos were collected in a 2 ml microcentrifuge tube at the stage of interest and fixed in 4% PFA for 3 hours. Embryos were washed 3 times in PBST and dechorionated prior to whole mount immunofluorescence.

Embryos were blocked in 10% goat serum in PBST for a minimum of 1 hour before replacing with primary antibodies in 5% goat serum and 1% DMSO (Table 16) and incubating at 4 °C for 16 hours. Embryos were then washed 10 times in 1 ml PBST at RT for 15 minutes before replacing with secondary antibodies (Invitrogen, USA) in 5% goat serum and 1% DMSO (Sigma Aldrich, UK) (Table 17) and incubating at 4 °C for 16 hours.

Embryos were washed 3 times in 1 ml PBST at RT for 15 minutes then, if used, incubated with 4',6-diaminodino-2-phenylindole (DAPI) at RT for 45 minutes. Embryos were washed 3 times in 1 ml PBST at RT for 15 minutes before long-term storage in 75% glycerol in PBST.

Antigen (clone)	Species	Dilution	Source (Cat. No.)
ephrinB1a	Rabbit	1:1000	Wilkinson Lab
EphB4a	Guinea pig	1:500	Wilkinson Lab
EphA4a	Rabbit	1:500	Wilkinson Lab
HuC/D (16A11)	Mouse IgG2b	1:200	Molecular Probes (A-21272)

Table 16 Primary antibodies used for immunofluorescence

Embryos were prepared for image analysis by de-yolking and flat mounting onto slides in 75% glycerol in PBST. Imaging was carried out using a Leica TCS SP2 confocal microscope.

Antibody	Dilution	Source (Cat. No.)
Goat Anti-Rabbit Alexa Fluor® 488 (IgG H + L)	1:500	Molecular Probes
Goat Anti-Mouse Alexa Fluor® 488 (IgG H + L)	1:500	Molecular Probes
Goat Anti-Guinea Pig Alexa Fluor® 594 (IgG H + L)	1:500	Molecular Probes
Goat Anti-Rabbit 594 Alexa Fluor® 594 (IgG H + L)	1:200	Molecular Probes

Table 17 Secondary antibodies used for immunofluorescence

2.5 RNA-sequencing

2.5.1 Library preparation

RNA samples underwent quality control and the concentration determined by using the 2100 Bioanalyser and recommended protocol (Agilent Genomics). RNA samples of high enough quality were used to generate cDNA libraries using the Ovation® RNA-Seq System V2 and recommended protocol (NuGEN, The Netherlands).

2.5.2 RNA-sequencing

cDNA libraries were sequenced using a HiSeq 2000 (Illumina) performed by the High Throughput Sequencing facility at The Francis Crick Institute. This protocol gave paired end 50 bp reads.

2.5.3 Bioinformatic analysis of RNA-sequencing data

RNA-sequencing data analysis was performed by Probir Chakravarty (Francis Crick Institute Bioinformatic Platform). The quality of the RNA-sequencing data for each sample was determined using FASTQC before aligning the reads to the zebrafish genome version 10 using STAR. The number of reads per gene were counted using RSEM and quantified with genes less than 1 transcript per million (TPM) being removed. The samples were then normalised using DESeq2 and clustered based on the normalised genes. Pairwise comparisons were made between samples of different conditions using DESeq2 by carrying out a Wald Test. Heat maps and MAplots of differentially expressed genes were constructed using DESeq2.

Chapter 3. Blocking Eph-ephrin signalling in the zebrafish hindbrain

3.1 Introduction

The aim of this project is to discover which genes are downstream of Eph receptor and ephrin signalling in the zebrafish hindbrain. One way of identifying transcriptional targets is to block a signalling event from occurring and compare the difference in transcripts between this situation to the wild type signalling state. In order to identify downstream target genes, the first aim of this project was to block Eph-ephrin signalling in the zebrafish hindbrain.

Previous studies have shown that using MOs against various Eph receptors and ephrins known to be expressed in the hindbrain results in the selective loss of hindbrain boundaries (Cooke et al., 2005; Terriente et al., 2012). This demonstrates that Eph-ephrin signalling is upstream of boundary cell formation and the absence of hindbrain boundaries can be used as a readout of whether Eph-ephrin signalling has been blocked.

This chapter will focus on the different techniques explored in an attempt to block Eph-ephrin signalling in the zebrafish hindbrain. MOs, mutant zebrafish lines and soluble ephrin ligands will be used as methods to block Eph-ephrin signalling. These techniques will be used in combination with *in situ* hybridisation to identify changes to rfng expression, a marker of hindbrain boundaries which is downstream of Eph-ephrin signalling and will determine if signalling has successfully been blocked. Each technique has advantages and disadvantages, making it necessary to evaluate whether one, or a combination of these, would be needed to give the desired phenotype of complete hindbrain boundary cell loss. It will be shown that expressing soluble ephrinB1a ligand at specific times during development is the optimal technique to remove all *rfng* expression, and therefore block Eph-ephrin signalling in the hindbrain.

3.2 Morpholino oligonucleotides

Morpholino oligonucleotides (MOs) are short nucleotide sequences around 25 base pairs in length that bind complementary RNA sequences, thus blocking translation or splicing of transcripts and prevents protein expression. The MO structure differs from that of RNA as the ribose backbone is substituted for morpholine rings and hydroxyl containing phosphodiester bonds are replaced by neutral phosphodiamidate linkers. This ensure that they are stable and unable to be degraded by nucleases (www.gene-tools.com).

Using MOs to knockdown gene function in zebrafish is a well-established technique which has several advantages for blocking Eph-ephrin signalling. Firstly, this method is rapid because rather than generating stable lines, which can take several months, Eph receptors and ephrins can be knocked down in transient in the embryo from MO injection at the 1-cell stage. Another advantage is that several different MOs can be injected in one cocktail to block multiple Eph receptors and ephrins in the hindbrain. Finally, some of the MOs that target the Eph receptors and ephrins of interest have already been verified and the phenotypes are documented.

The main disadvantage of using MOs is that they can cause off-target effects due to toxicity. There is a major known effect mediated by Tp53 activation, which leads to the activation of the cell death pathway and the expression of many genes. This can be suppressed by knockdown or in a *tp53* mutant background (Robu et al., 2007; Gerety and Wilkinson, 2011). In addition, there is also the uncertainty of how to interpret MO data after several reported phenotypes from blocking gene function with MOs differing from the phenotypes found in mutants. This could be the result of off-target effects of MOs or genetic compensation occurring in the mutants (Rossi et al., 2015).

3.2.1 Individual morpholino oligonucleotide knockdown

In order to block Eph-ephrin signalling in the hindbrain, MOs against *EphA4a*, *EphB4a*, *ephrinB2a* and *ephrinB3b* were used. These Eph receptors and ephrins were targeted because of their complementary segmented expression in the

hindbrain (Figure 5), as well as their known role in boundary cell formation (Xu et al., 1995; Xu et al., 1999; Cooke et al., 2001). MOs were injected individually into zebrafish embryos at the 1-cell stage. The concentrations were optimised in an attempt to give the predicted phenotype based on where the Eph-ephrin binding pairs are expressed and on previous observations (Cooke et al., 2005; Terriente et al., 2012). Knocking down individual Eph receptors or ephrins had different efficiencies in giving hindbrain boundary loss phenotypes, depending on which Eph-ephrin binding pair is targeted. The embryos developed normally after treatment and no gross morphological phenotypes were observed (data not shown).

Targeting either *EphA4a* or *ephrinB3b* with MOs individually resulted in the same phenotype. In these embryos, *rfng* expression is lost at the boundaries of rhombomeres 2 and 3 (r2/r3), r3/r4 and r5/r6 (Figure 6: C and D); the boundaries at which EphA4a and ephrinB3b are exclusively expressed and signal without redundancy by EphB4a and ephrinB2a. This was seen in 82% of embryos when using EphA4a MO and 36% of embryos when using ephrinB3b MO. The difference in penetrance could be due to the efficiency of the MOs.

However, targeting either *EphB4a* or *ephinB2a* with MOs individually resulted in embryos that displayed weak *rfng* expression in affected hindbrain boundaries whilst the remaining embryos maintained wild type *rfng* expression. Embryos that displayed the phenotype had weaker expression of rfng at one or both of the boundaries of r1/r2 and r6/r7 (Figure 6: E and F); the boundaries at which EphB4a and ephrinB2a are exclusively expressed and signal without redundancy by EphA4a and ephrinB3b. This was seen in 36% of embryos when using EphB4a MO and 69% of embryos when using *ephrinB2a* MO.

It is evident from individual knockdown experiments that there is redundancy of signalling by Eph-ephrin binding pairs in the hindbrain because the r4/r5 boundary remains when either EphA4a-ephrinB3b or EphB4a-ephrinB2a binding pairs are targeted individually. In addition, the r1/r2 and r6/r7 boundaries have weak *rfng* expression when either *EphB4a* or *ephrinB2a* is targeted yet this pair are the only identified Eph-ephrins at these boundaries, highlighting that there may be undiscovered Eph-ephrin binding pairs. Despite this, in an attempt to remove all

hindbrain boundary cells, both known Eph-ephrin binding pairs were targeted by MOs. As previously mentioned with individual MO knockdowns, morphant embryos developed normally after treatment and no gross morphological phenotypes were observed (Figure 7: C, E, G).

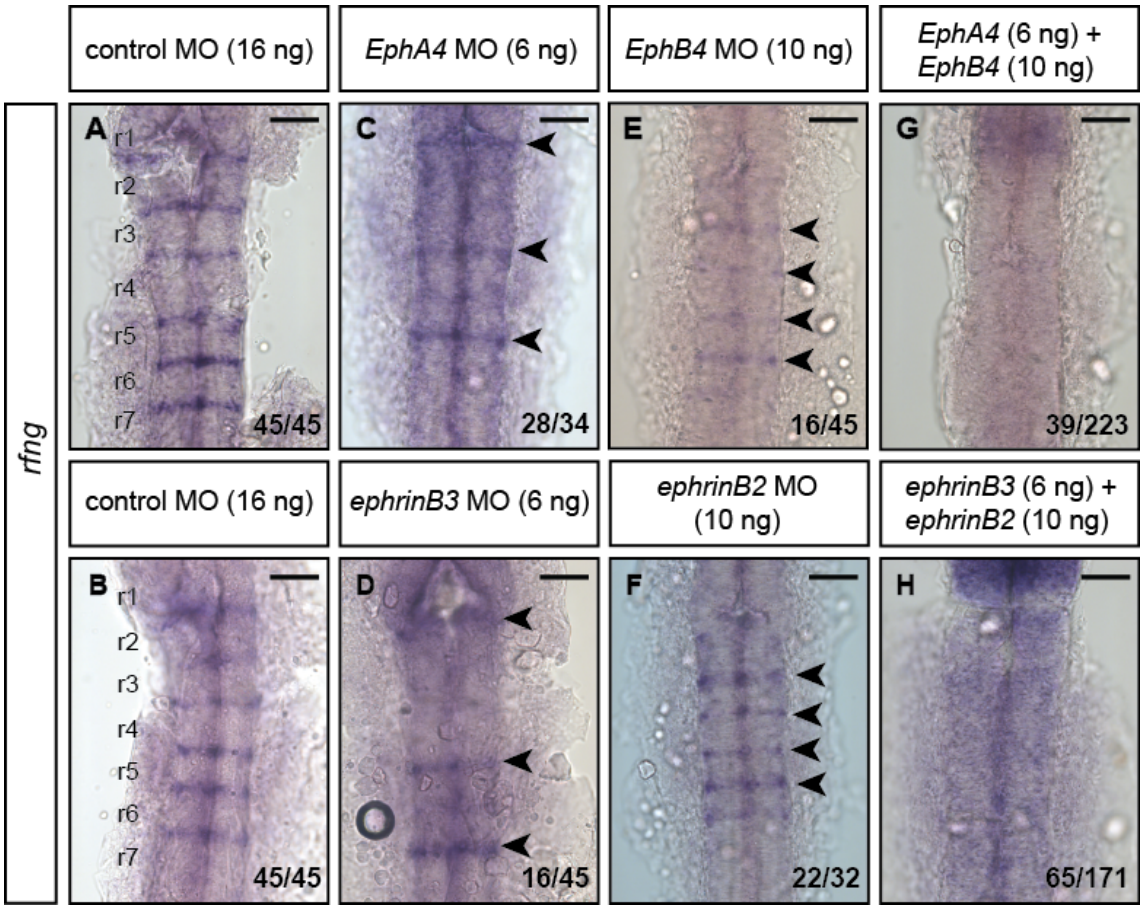

Figure 6 *rfng* expression after MO mediated knockdown

(A-H) Embryos with homozygous background for *tp53-/-* at 19 hpf after *in situ* hybridisation for *rfng* to mark the hindbrain boundary cells. Arrowheads point to boundaries that are not affected by MO knockdown. Numbers indicate the number of embryos that show this phenotype; the remainder have wild type *rfng* expression. The scale bar represents 50 μm.

3.2.2 Combined morpholino oligonucleotide knockdown

Individual MOs against Eph receptors or ephrins were able to prevent specific hindbrain boundaries from forming. In order to remove all the boundaries and completely block Eph-ephrin signalling in the hindbrain, MOs were used in combination to target either *EphA4a* and *EphB4a* or *ephrinB2a* and *ephrinB3b*. Using a combination of MOs to knockdown both *EphA4a* and *EphB4a* or *ephrinB3b* and

ephrinB2a successfully prevented *rfng* expression in the hindbrain (Figure 6: G, H). However, this was observed in a low percentage of embryos: 18% when targeting Eph receptors and 38% of embryos for ephrins. The remaining embryos have a mixture of phenotypes with wild type or partial boundary loss phenotypes. This suggests that although it is possible to completely block Eph-ephrin signalling in the hindbrain by using a combined MO approach, it is not consistent. In light of this and despite the low penetrance, this approach has had some success in blocking Eph-ephrin signalling in the hindbrain and if the relevant embryos could be identified they may be suitable for RNA-sequencing.

3.2.3 Hindbrain morphology phenotypes

In order to identify the embryos with absent hindbrain boundaries, a specific hindbrain morphology was used. Eph-ephrin signalling causes constrictions to arise in the hindbrain, which is likely to be the result of increased cortical tension at the interface of rhombomeres (Sela-Donenfeld et al., 2009; Calzolari et al., 2014). In embryos where Eph-ephrin signalling is absent, the constrictions will not arise. It has previously been observed that the constrictions are visible from 14ss (16 hpf) (Kimmel et al., 1995) and therefore, the experiment was repeated with embryos selected based on hindbrain morphology at 14 ss (Figure 7), before carrying out *in situ* hybridisation for *rfng*.

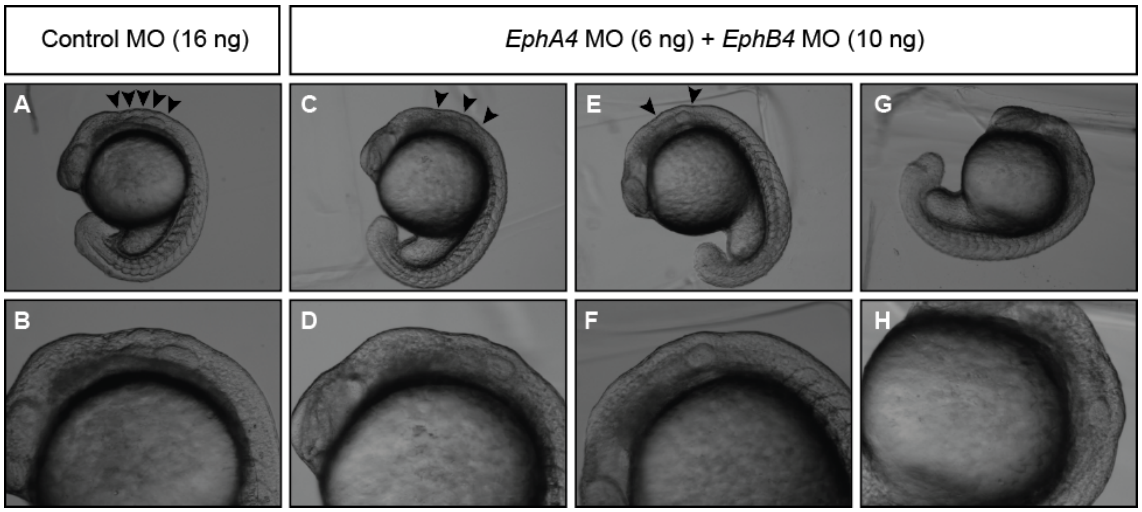

Figure 7 Morphological differences between control and knockdown embryos

(A-H) Embryos at 17 hpf taken in brightfield, arrowheads point to the visible constrictions of the hindbrain where the boundaries arise. (A-B) Embryos when a control MO has been injected and has wild-type morphology and five constrictions can be seen. (C-H) Embryos after MO knockdown for both *EphA4* and *EphB4*. (C-D) shows three constrictions, (E-F) shows two constrictions with a less defined constriction between, and G-H shows smooth hindbrain morphology with no constrictions.

When embryos are selected with the smooth hindbrain phenotype, there is an increase in the percentage of embryos with the loss of *rfng* from 18% (Figure 6: G, H) to 67% (Table 18). However, 18% of embryos that were selected in this group have partial boundary loss and 15% have all the boundaries present (Table 18). Due to the similarity between morphological phenotypes and the lack of a robust and reproducible process to characterise them, this is an error-prone method to select embryos where Eph-ephrin signalling is blocked. Consequently, alongside the known problem of off-target effects of MOs, other techniques were explored in order to find a more reliable method for blocking Eph-ephrin signalling.

Hindbrain morphology	Complete boundary loss	Partial boundary loss	All boundaries present
Smooth hindbrain	22/33	6/33	5/33
Intermediate morphology	1/22	21/22	0/22
Defined rhombomeres	0/117	99/117	18/117

Table 18 Correlation between hindbrain morphology and boundary loss

Embryos with homozygous background for *tp53-/-* were injected with 6 ng *EphA4a* MO and 10 ng *EphB4a* MO before sorting into groups at 17 hpf based on hindbrain morphology. The 'smooth hindbrain' embryos showed no constrictions where rhombomere boundaries form, the 'intermediate morphology' group showed two constrictions and the 'defined rhombomeres' group showed multiple constrictions. After *in situ* hybridisation for *rfng* embryos in each group were counted to determine the boundary phenotypes. Pearson's Chi-square test showed that sorting hindbrains based on morphology and the boundary loss phenotype are dependent on one another (P value of less than 0.05).

3.3 Mutant zebrafish lines

The second approach tested to block Eph-ephrin signalling in the zebrafish hindbrain was to use mutant zebrafish lines. For this, four individual mutant lines were used: *EphA4a-/-* (Jordi Cayuso, Wilkinson Lab), *EphB4a-/-* (Sanger Institute), *ephrinB3b-/-* (Megan Addison, Wilkinson Lab), *ephrinB2a-/-* (Sanger Institute). The *EphA4a* mutant was generated by CRISPR and has a nonsense mutation caused by a 4 bp deletion an early stop codon and truncates the protein in the ligand binding domain and is a null mutant (Jordi Cayuso, unpublished). The *EphB4a* mutant line was generated as part of the Zebrafish Mutation Project and has a nonsense mutation by substitution of base A to T at residue R238, which lies just after the ephrin binding domain and lacks EphB4a expression (Kettleborough et al., 2013). The *ephrinB3b* mutant was generated using transcription activator-like effector nucleases (TALENs) which introduced a 2 bp deletion and 2 bp substitution at residue R5 and residue R6, respectively resulting in a null mutant (Megan Addison, unpublished). The *ephrinB2a* mutant was generated as part of the Zebrafish Mutation Project and has a nonsense mutation by substitution of base T to A at residue R86, which lies in the extracellular domain and results in a null mutant (Kettleborough et al., 2013).

The main advantage of using mutant zebrafish lines is that there is no issue of off-target effects, unlike when using MOs. When using homozygous adults all embryos in a clutch will carry the same mutations giving reliable biological replicates for the experiment. On the other hand, the main disadvantage is that generating mutants can be time consuming and several generations of breeding are needed to obtain homozygous mutants, which were not available when this project began. Another disadvantage of this approach is that it relies on all the Eph receptors and ephrins that signal in the hindbrain being known so that they can be targeted for mutation. There is the possibility that other Eph-ephrin binding pairs could compensate for signalling lost by those targeted. This compensation could be by other Eph receptors and ephrins that do not usually have a role in boundary cell formation and have not been identified as present in the hindbrain. Furthermore, if all the Eph receptors and ephrins that signal in the hindbrain were targeted by this approach it could be lethal due to the multiple roles of Eph-ephrin signalling during development.

These data shown here focus on individual or double homozygous mutants as the heterozygous mutants showed varied phenotypes of hindbrain boundary loss. The homozygous mutants for *EphA4a* and *ephrinB2a* as well as the mutant line for *ephrinB3b* were not available at the beginning of this project and were generated in parallel to other experiments.

3.3.1 Individual Eph receptor and ephrin mutants

First, this project set out to determine which Eph receptor and ephrin mutants disrupt the formation and maintenance of the different hindbrain boundaries. It then went on to generate double mutants aiming to remove all hindbrain boundaries and completely block Eph ephrin signalling in the hindbrain.

Individual homozygous Eph receptor and ephrin mutant lines were in-crossed and the embryos collected at 20 ss (19 hpf) to assess the hindbrain boundary phenotypes. For *EphA4a* and *ephrinB3b*, the phenotypes were similar showing the selective loss of boundaries r2/r3, r3/r4 and r5/r6 (Figure 8: D, E). This is in

agreement with the hindbrain boundary phenotypes after knockdown of either Eph or ephrin of this binding pair individually using MOs (Figure 6: C, D).

In contrast, for individual *EphB4a* and *ephrinB2a* homozygous mutants there was no complete loss of the predicted hindbrain boundaries at r1/r2 and r6/r7 (Figure 8: B, C). *EphB4a* homozygous mutants showed weaker *rfng* expression at the r6/r7 boundary, but *ephrinB2a* showed wild type *rfng* expression. This is different from the MO knockdown experiments where the r1/r2 and r6/r7 boundaries were sometimes seen to be weaker in *EphB4a* and *ephrinB2a* morphants (Figure 6: E, F).

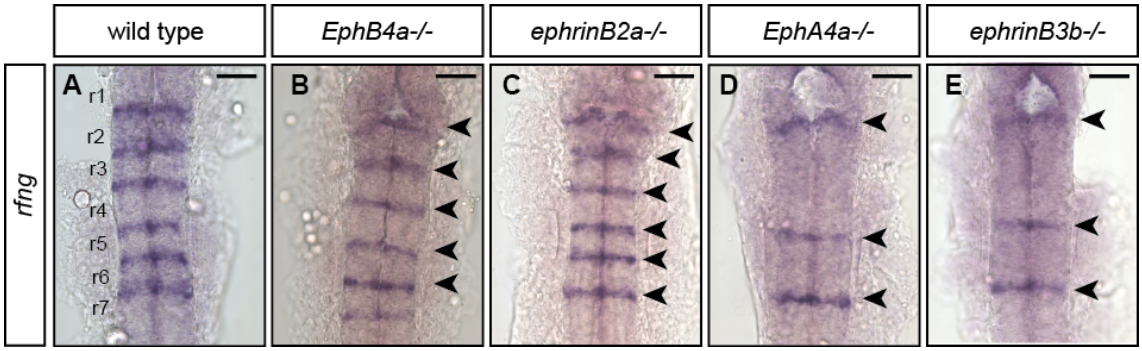

Figure 8 Hindbrain boundary phenotypes of individual Eph receptor and ephrin mutants

(A-H) Embryos at 19 hpf after *in situ* hybridisation for *rfng* to mark the hindbrain boundary cells. Arrowheads point to boundaries that are not affected in the mutant embryos (B-E). The scale bar represents 50 μm.

3.3.2 Double Eph receptor and ephrin mutants

In attempts to block Eph-ephrin signalling in the hindbrain and lose all hindbrain boundaries, double mutants were generated for *EphA4a* plus *EphB4a* and for *ephrinB2a* plus *ephrinB3b*. By targeting either both receptors or both ligands it should prevent any compensation by the Eph receptor or ephrin from the other of the two Eph-ephrin binding pairs. Double homozygous Eph or ephrin mutants were generated by out-crossing homozygous fish of each mutation together (Figure 9: A*)* raising the double heterozygous embryos then in-crossing these (Figure 9: B) to generate a mixture of phenotypes and identify the double homozygous mutants (Figure 9: C). The double homozygotes were then in-crossed (Figure 9: D) and the embryos collected to determine the hindbrain boundary phenotypes (Figure 9: E).

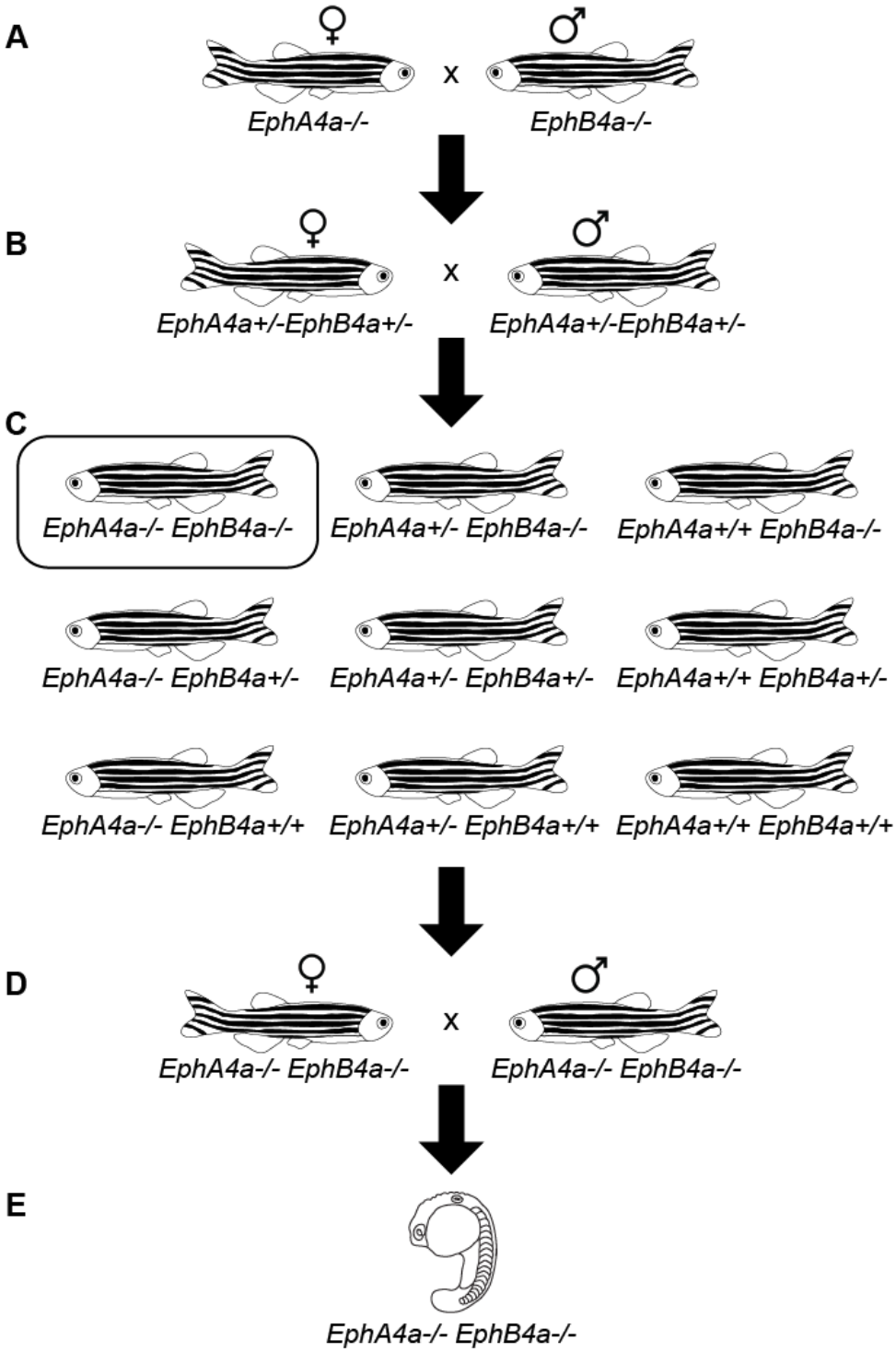

Figure 9 Generation of double homozygous mutant embryos

This schematic demonstrates how homozygous double mutant embryos were generated. This example shows *EphA4a* and *EphB4a* double mutants. The protocol was the same for *ephrinB2a* and *ephrinB3b* double mutants. (A) Single heterozygous mutant lines are crossed and (B) the double heterozygous embryos are raised to adults and in-crossed. (C) The embryos are then raised to adults and genotyped to identify double homozygous mutants (highlighted by box). (D) The double homozygous mutants are then in-crossed and (E) the embryos collected at 20 ss for downstream analysis.

The double homozygous mutants of *EphA4a* and *EphB4a* or *ephrinB2a* and *ephrinB3b* showed the same hindbrain boundary phenotype as the individual homozygous mutants *EphA4a* and *ephrinB3b*. The remaining boundaries are r1/r2, r4/r5 and r6/r7 (Figure 10). This is surprising because in the equivalent double Eph receptor and ephrin morphants there is a subset that completely lacks rfng expression in the hindbrain.

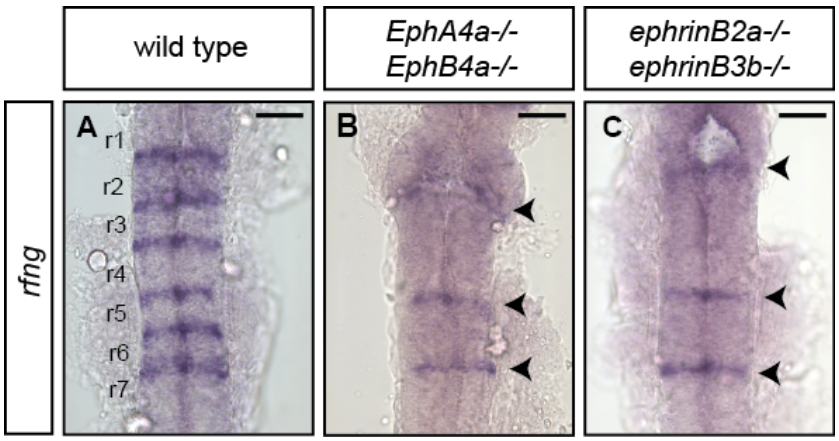

Figure 10 Hindbrain boundary phenotypes of double Eph receptor and ephrin mutants

(A-H) Embryos at 19 hpf after *in situ* hybridisation for *rfng* to mark the hindbrain boundary cells. Arrowheads point to boundaries that are not affected in the mutant embryos (B-E). The scale bar represents 50 µm.

This suggests there is redundancy and that another Eph-ephrin pair is able to induce hindbrain boundary formation in addition to EphA4a-ephrinB3b and EphB4a-ephrinB2a. One potential mechanism is the ephrinB1a-EphB3a binding pair, which also has a segmental and complementary expression pattern in the hindbrain and was identified after the multiple mutant lines had started to be generated. It has been shown that genetic compensation occurs in some mutants but not in morphants (Rossi et al., 2015). It is therefore possible that genetic compensation occurs in Eph-ephrin mutants and not in the morphants.

These experiments have shown that it would be necessary to generate further mutants in order to completely block Eph-ephrin signalling in the hindbrain. Individual mutants of *EphA4a*, *EphB4a*, *ephrinB2a* and *ephrinB3b* or double mutants of the Eph receptors or ephrins are not sufficient to remove all hindbrain boundaries. Generating a mutant that completely lacks all hindbrain boundaries has not yet been achieved

at the time of writing. However, the double Eph receptor or ephrin mutants will provide a useful tool for confirming transcriptional targets identified by RNA-sequencing. There are likely to be other Eph receptors and ephrins signalling redundantly in the hindbrain, in which case a broadly blocking method would be a more useful approach than targeting a specific Eph-ephrin binding pair by MOs or mutation.

3.4 Soluble ephrin ligands

Soluble ephrins are C-terminally truncated so that they lack the intracellular and transmembrane domains and as a result are not membrane bound. Upon binding to an Eph receptor, soluble ephrins cannot initiate the clustering needed to activate downstream signalling, resulting in signalling inhibition (Davis et al., 1994). Due to the promiscuous binding of Eph receptors and ephrins, this technique has the advantage that one ephrin can be over-expressed to bind and block signalling through multiple Eph receptors.

The UAS promoter can be cloned upstream of the soluble ephrin enabling over-expression to be controlled both spatially and temporally. This becomes advantageous in the event that blocking Eph-ephrin signalling globally has a lethal effect on embryonic development, because blocking signalling can be postponed to a later stage of development. In addition, with the use of a hindbrain specific promoter, blocking of Eph-ephrin signalling can be targeted to the hindbrain. This avoids disruption to other areas of the embryo during development as well as ensuring any effects to gene expression which are specific to the hindbrain. The disadvantage of this technique is that there is not a hindbrain only promoter line available, so the expression of the soluble ephrin cannot be spatially controlled.

Previous experiments measuring the binding affinity of ephrin-Fc fusion proteins to Eph receptors suggested that ephrinB2a would be the most suitable candidate for blocking Eph-ephrin signalling (Noberini et al., 2012) (Table 19). Several ephrin ligands were measured and ephrinB2a had the highest binding affinity for the three Eph receptors known to be expressed in the hindbrain (EphA4a, EphB4a and

EphB3a) and high binding affinity for other EphB receptors. Consequently, if there is redundant signalling by other Eph-ephrin binding partners that have not been identified, this gives the highest chance of blocking Eph-ephrin signalling. However, there was already a zebrafish line available that expressed soluble ephrinB1a under the control of a UAS promoter (Jordi Cayuso, Wilkinson Lab). Preliminary experimentation was carried out using this line, which showed it was possible to block Eph-ephrin signalling using soluble ephrinB1a and further experiments were carried out with this transgenic line.

	m-ephrinB1	**m-ephrinB2**	**h-ephrinB3**
m-EphA4	13 ± 0.84	4.2 ± 0.44	12 ± 3.1
r-EphB1	2 ± 0.23	0.88 ± 0.14	6.3 ± 0.85
m-EphB2	3.5 ± 0.23	0.73 ± 0.09	7.1 ± 1.5
m-EphB3	2.5 ± 1.1	1.2 ± 0.18	2.9 ± 0.21
m-EphB4	18 ± 3.0	2.3 ± 0.58	>50
m-EphB6	8.3 ± 4.0	1.6 ± 0.58	11 ± 4.5

Table 19 Binding affinities of Eph receptors and ephrins

Published dissociation constant (K_D) for different Eph receptors and ephrins (Noberini et al., 2012) measured using biotinylated ephrin-Fc fusion proteins and Eph receptor-Fc fusion proteins. Fusion proteins are human (h), mouse (m) or rat (r).

3.4.1 Optimisation of heat shock protocol

The optimised protocol for over-expressing soluble ephrinB1a in embryos is shown in Figure 11. Due to the *HS-Gal4* line having multiple integrations of the transgene as a result of prolonged breeding, the inheritance of both transgenes varies from 25-50%, and therefore the maximum number of embryos with complete hindbrain boundary cell loss is between these values. Initial experiments were carried out crossing the UAS-soluble ephrinB1a line to a heat shock inducible Gal4 driver and a tamoxifen inducible Gal4 driver, to see which was most effective.

For the heat shock induction experiments, the length of heat shock was tested for 30 minutes and 1 hour. The time of heat shock was also optimised by testing heat shock at 6 ss, or at bud, or at bud followed by 12 ss. These experiments showed that in order to obtain the maximum number of embryos possible with no hindbrain boundaries it is more efficient to use the heat shock inducible Gal4 line and it was

necessary to perform two heat shocks that lasted for 1 hour at 38°C, the first at bud stage, then the second at 12 ss (Figure 11).

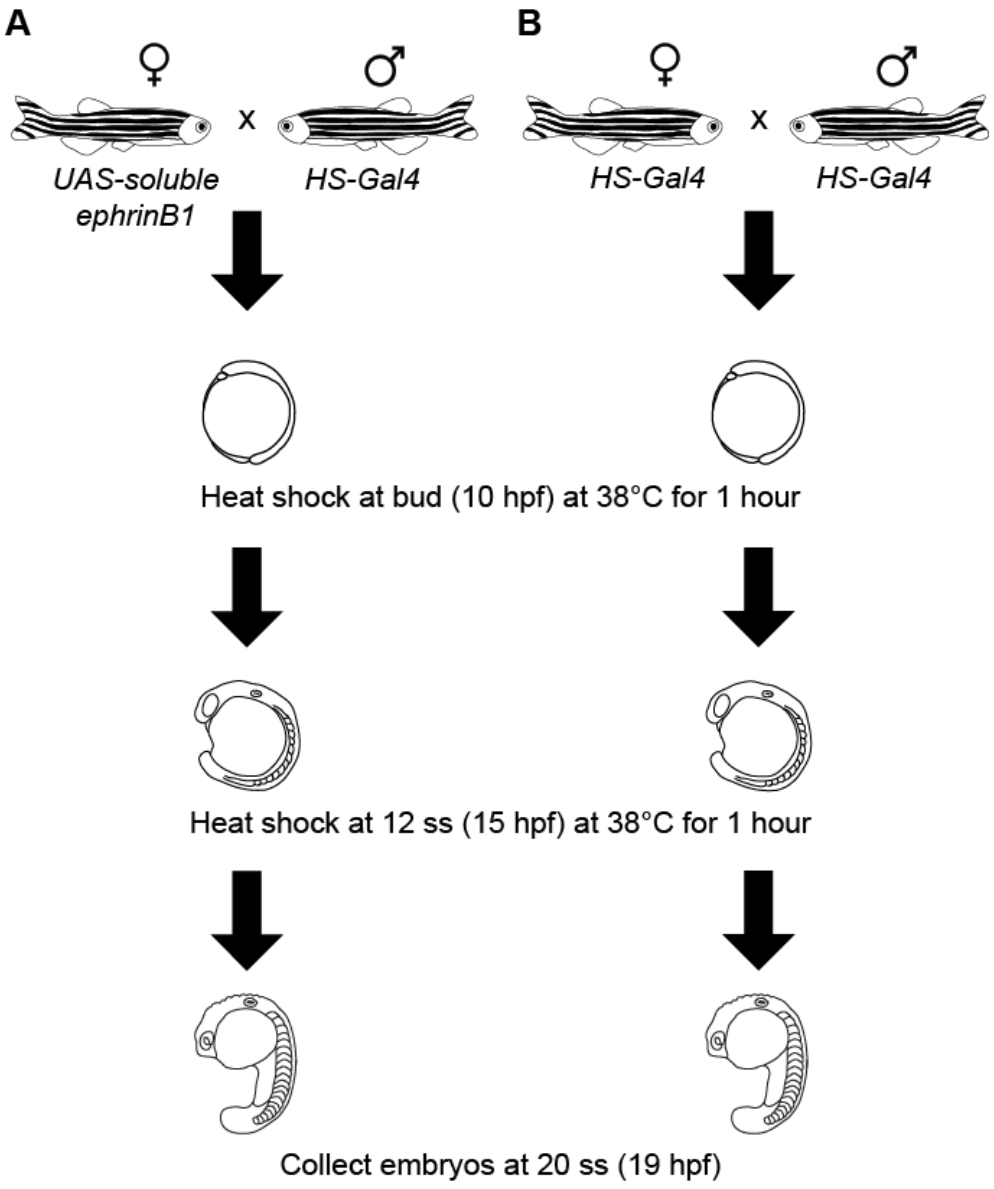

Figure 11 Heat shock protocol for over-expressing *soluble ephrinB1a*

Two crossed were set up: (A) UAS-soluble ephrinB1a fish crossed to *HS-Gal4* fish or (B) *HS-Gal4* fish in-crossed as a control. Embryos were collected and subject to two heat shocks: at bud, then at 12 ss, before collecting at 20 ss for analysis.

When *HS-Gal4* fish are out-crossed to *UAS-soluble ephrinB1a* fish and the embryos are heat shocked twice (Figure 12: C-D), 58% of embryos show complete boundary cell loss and the remaining 42% show no loss of boundary cells (Figure 12: C-F). 100% of control embryos have all hindbrain boundaries present (Figure 12: A-B).

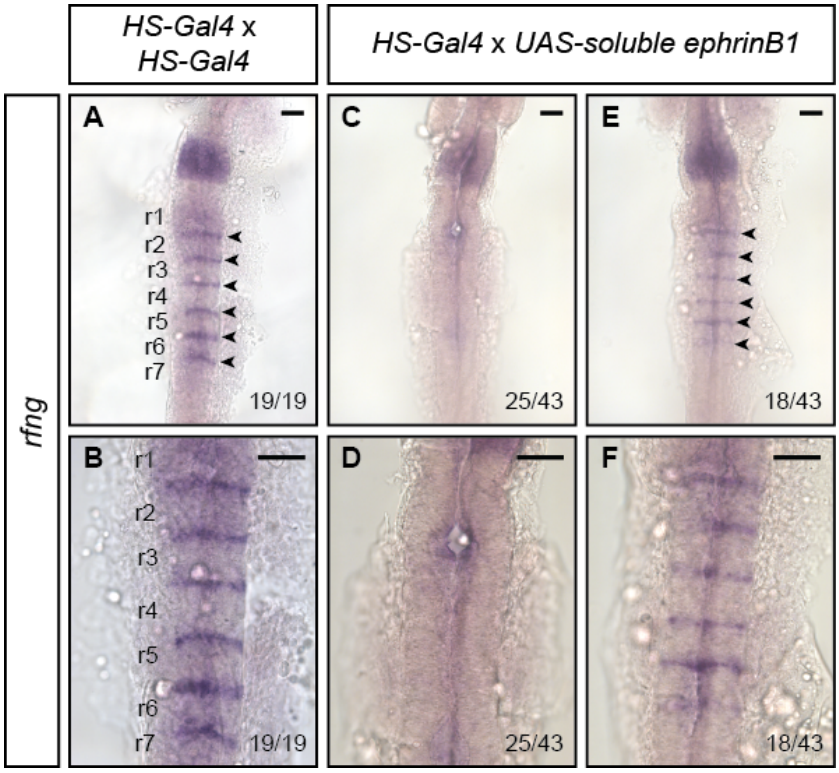

Figure 12 Hindbrain boundary phenotypes after *soluble ephrinB1a* expression

(A-H) Embryos at 19 hpf after *in situ* hybridisation for *rfng* to mark the hindbrain boundary cells. Arrowheads point to boundaries that remain after heat shock. A-B, C-D, E-F are of the same embryo at different magnifications. A-B are control embryos where the *HS-Gal4* line has been in-crossed, C-F are two different phenotypes from the *HS-Gal4* x *UAS-soluble ephrinB1a* cross. The scale bar represents 50 μm.

3.4.2 Confirmation of soluble ephrinB1a over-expression

As it is not possible to simultaneously detect ectopic ephrinB1a and *rfng* expression, the percentage of embryos expressing soluble ephrinB1a and the percentage of embryos lacking *rfng* expression was determined to ensure that they correlated. The antibody used to detect soluble ephrinB1a can also recognise the endogenous ephrinB1a. The expression of the soluble protein thus led to an increase in staining in comparison to wild type.

First, it was ascertained that heat shock is inducing *ephrinB1a* transcript (Figure 13), but it is important to know whether the soluble ephrinB1a protein is expressed since this is the blocking reagent. Therefore, immunostaining for ephrinB1a expression was carried out (Figure 14).

At 20 ss, endogenous ephrinB1a is expressed broadly across the hindbrain in the dorsal region, shown in control embryos (Figure 13: C). In 41% of embryos from the *HS-Gal4* cross with *UAS-soluble ephrinB1a* there is strong *ephrinB1a* expression across the whole embryo (Figure 13: F; Figure 14: F). The percentage of embryos over-expressing soluble ephrinB1a protein was found to be 43-64% (Figure 14: D-F) and the percentage of embryos with absent hindbrain boundaries was 50-67% (over three experimental replicates) (Figure 12: C-D).

A time course was conducted in order to see if soluble ephrinB1a protein was degraded during the time of the experiment. Embryos were collected 1 hour after the first heat shock at bud, at 5 ss, and 1 hour after the second heat shock at 15 ss and finally at 20 ss. 43%, 57% and 41% of embryos from the *HS-Gal4* cross with *UAS-soluble ephrinB1a* showed over-expression of ephrinB1a protein, at 5 ss, 15 ss and 20 ss, respectively (Figure 14: D-F). This demonstrates that soluble ephrinB1a does not degrade during the time embryos will be collected for RNA-sequencing.

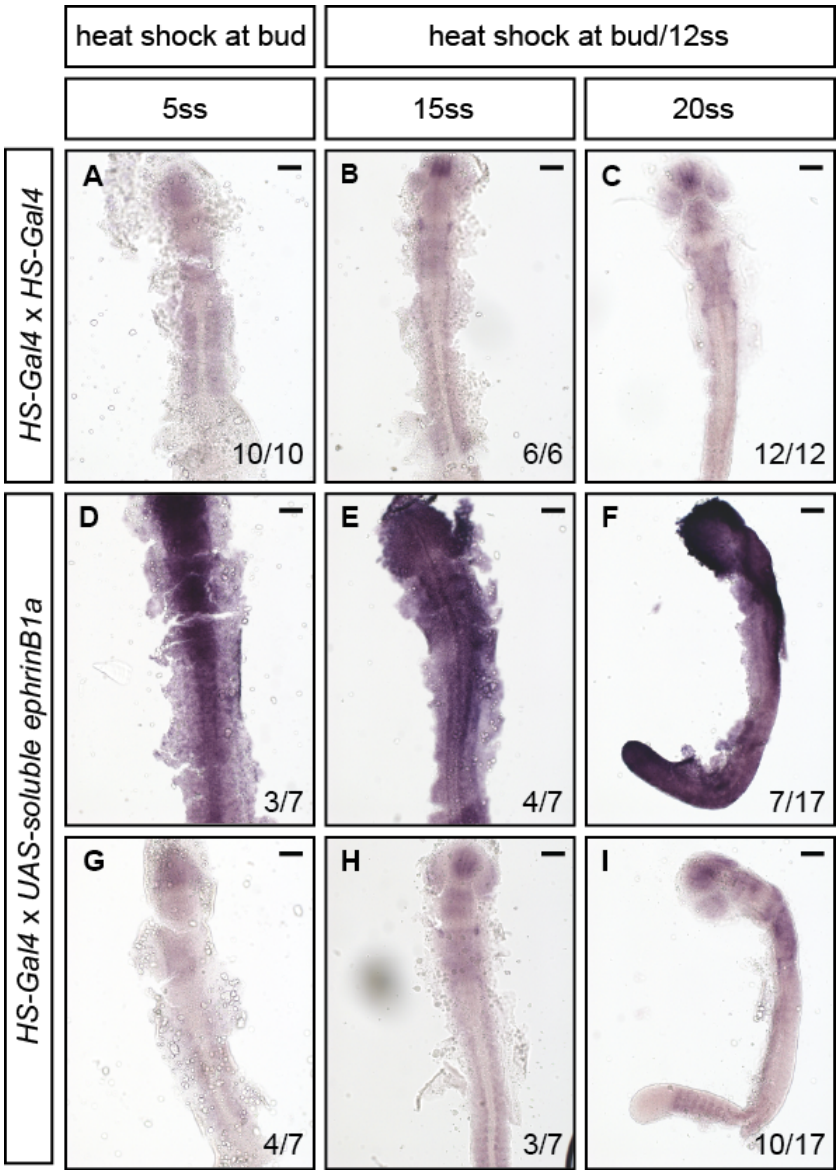

Figure 13 Confirming *soluble ephrinB1a* expression by *in situ* hybridisation

A-I) Embryos at 5 ss (A, D, G), 15 ss (B, E, H), or 20 ss (C, F, I) after *in situ* hybridisation for *ephrinB1a*. A-C Control embryos from HS-Gal4 in-cross and D-I embryos from *HS-Gal4* x *UAS-soluble ephrinB1a* out-cross. The scale bar represents 100 µm.

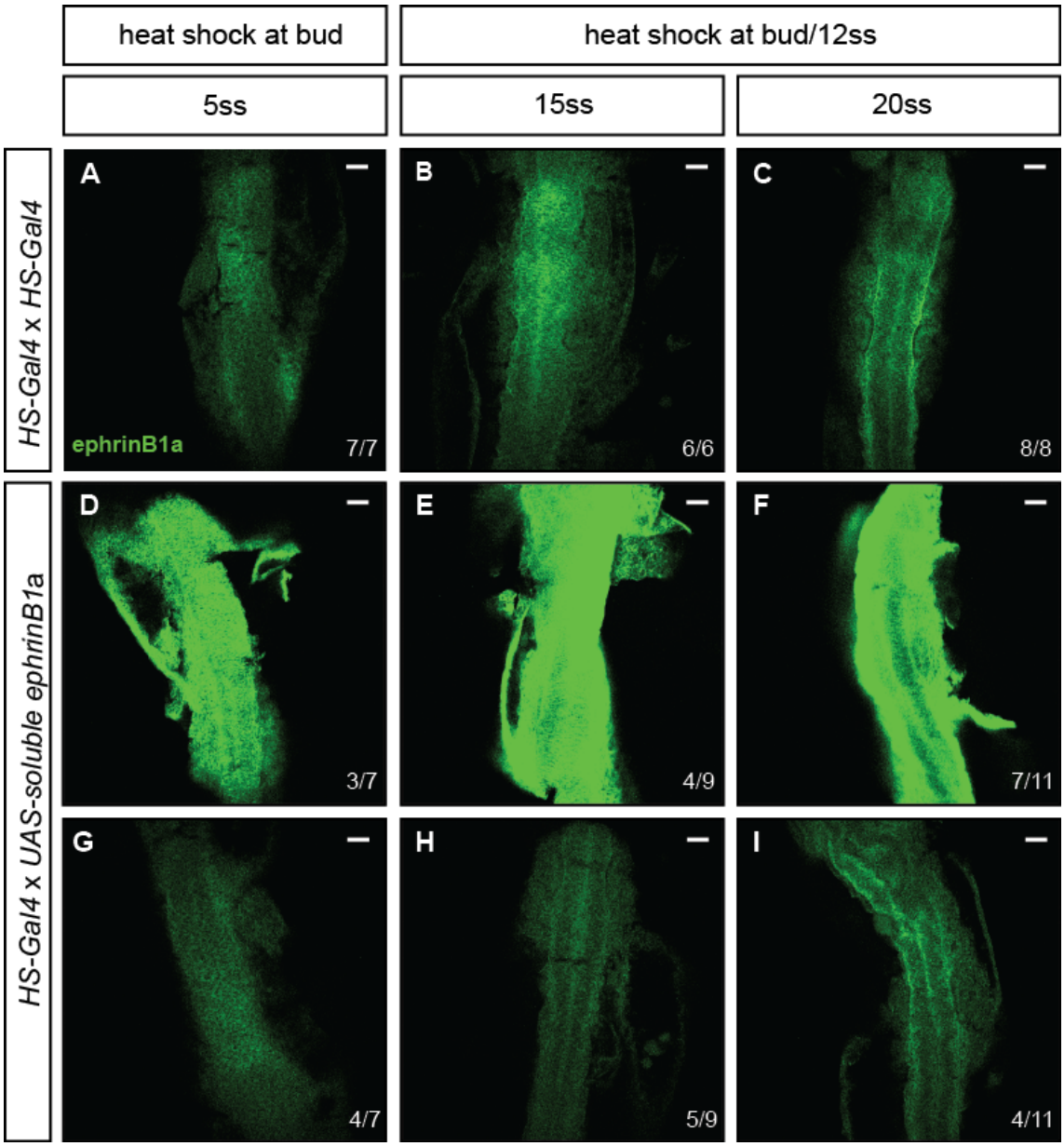

Figure 14 Confirming soluble ephrinB1a expression by immunofluorescence

(A-I) ephrinB1a expression detected by immunofluorescence in embryos at either 5 ss (A, D, G), 15 ss (B, E, H), or 20 ss (C, F, I). A-C are control embryos from *HS-Gal4* in-cross and D-I are from *HS-Gal4* x *UAS-soluble ephrinB1a* out-cross, all embryos have been heat shocked at bud and 12 ss. The scale bar represents 50 µm.

It was observed that when soluble ephrinB1a protein is expressed there is a down-regulation of EphB4a protein (Figure 15). It is well established that when signalling is activated it leads to internalisation of the receptor-ligand complex (Marston et al., 2003; Zimmer et al., 2003; Mann et al., 2003; Lauterbach and Klein, 2006; Goh and Sorkin, 2013). This is a surprising observation because over-expression of soluble ephrinB1a is thought to block signalling and the loss of

boundary cells would support this (Figure 12). In contrast, EphA4a protein was also investigated and was not found to be down-regulated upon soluble ephrinB1a over-expression. This suggests that activation may be selective for specific Eph receptors. Further evidence to support that soluble ephrinB1a is acting as a blocking or activating reagent has not been found and will be discussed in Chapter 7.3.

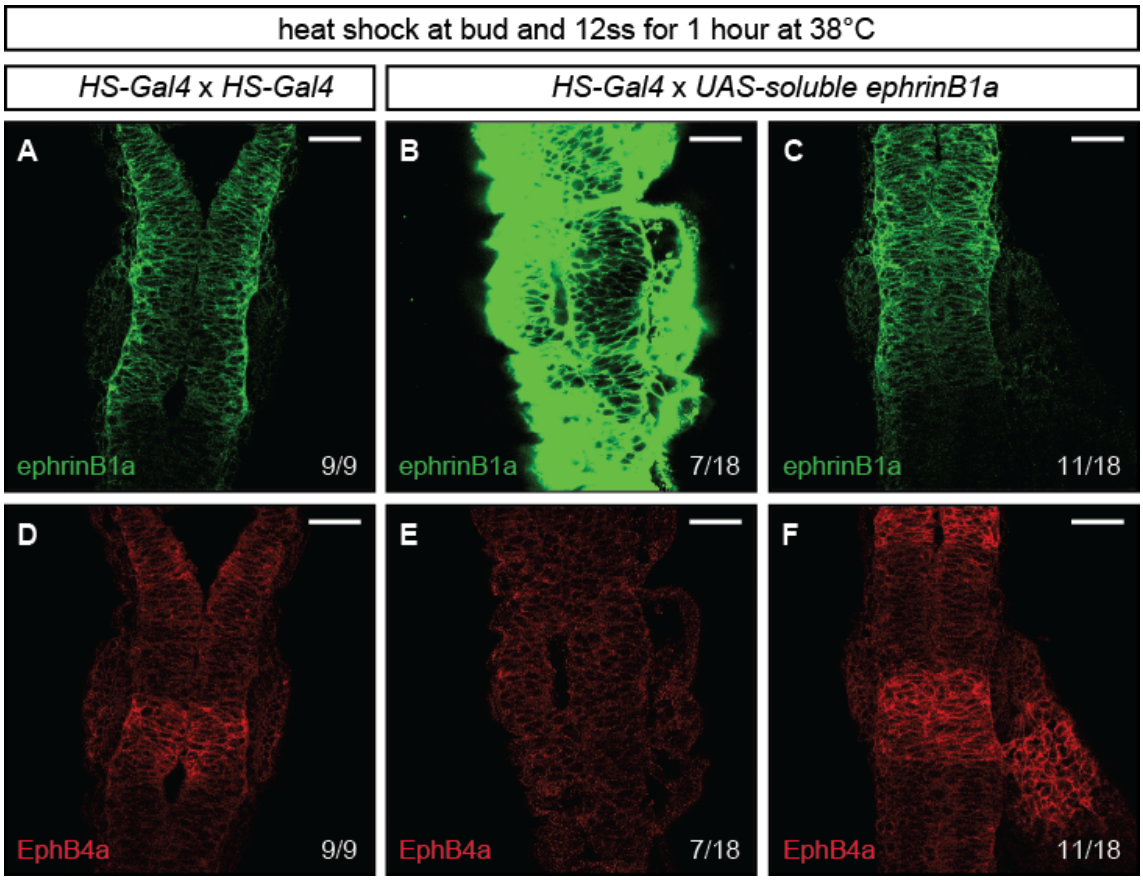

Figure 15 The effect of ephrinB1a expression on EphB4a

(A-E) Immunofluorescence at 20 ss detecting either ephrinB1a (A-C) or EphB4a (D-F). A, D are control embryos from *HS-Gal4* in-cross and B, C, E, F are from *HS-Gal4* x *UAS-soluble ephrinB1a* out-cross, all embryos have been heat shocked at bud and 12 ss. The scale bar represents 100 µm.

3.5 Discussion

From the experiments described in this chapter, it has been shown that the most effective way to block Eph-ephrin signalling in the hindbrain is to use a soluble ephrin approach to globally block Eph-ephrin signalling in the embryo. The readout used to determine if Eph-ephrin signalling had been blocked was to look at *rfng* expression

by *in situ* hybridisation, to see if the hindbrain boundary cells had been lost. Absence of hindbrain boundary cells shows that Eph-ephrin signalling has successfully been blocked (Xu et al., 1995; Cooke et al., 2005; Terriente et al., 2012).

Use of a cocktail of MOs generated embryos with the desired phenotype of complete hindbrain boundary cell loss. However, this was inconsistent within a clutch of injected embryos as there was a mixture of phenotypes ranging from complete boundary loss to wild type hindbrain boundary cell phenotypes. By sorting embryos at 17 hpf on the basis of hindbrain morphology, the hindbrain boundary loss phenotype could be enriched. Unfortunately, this only increased the percentage of embryos with complete hindbrain boundary loss from 18% to 67%. The remaining embryos had partial hindbrain boundary loss or were the same as wild types. This, in combination with the off-target effects of MOs resulted in this technique being abandoned for RNA-sequencing. However, targeting individual Eph receptors or ephrins with MOs could be a useful tool for the confirmation of target genes identified by RNA-sequencing.

Using mutant zebrafish lines was unsuccessful at giving the desired phenotype of complete hindbrain boundary cell loss. However, the double mutant lines did highlight that there is further redundancy of signalling in the hindbrain that is able to induce boundary cell formation. This was shown by the persistence of the r4/r5 hindbrain boundary when signalling through both EphA4a-ephrinB3b or EphB4a-ephrinB2a binding pairs was interfered with by mutating both these Eph receptors of ephrins. One beneficial outcome was that this generated a useful tool for validating transcriptional targets that are identified from RNA-sequencing. In particular, the double Eph receptor and ephrin homozygous mutants give partial hindbrain boundary loss phenotypes which can be used to investigate if more broadly expressed transcriptional targets have altered expression in localised regions of the hindbrain. Moreover, it may highlight target genes that are downstream of forward and reverse signalling.

The chosen method to block Eph-ephrin signalling was to use a soluble ephrin approach. For this approach, it is not a prerequisite to know all of the Eph-ephrin interactions in the hindbrain, unlike with the targeted approaches of MOs and mutant

lines. By using soluble ephrins, it is possible to target Eph-ephrin signalling in a non-biased way, by globally blocking signalling from multiple Eph receptors. This ensures that any compensatory signalling by other Eph-ephrin binding pairs, that are not known, will also be blocked. Using this approach with temporal control also avoids lethality from early blocking of Eph-ephrin signalling. From these experiments, it was found that blocking Eph-ephrin signalling before bud stage resulted in the death of around 50% of embryos which correlates to the number that would inherit both the transgenes and be capable of over-expressing soluble ephirnB1. This is likely to be because of roles of Eph-ephrin signalling in early embryonic development.

To block Eph-ephrin signalling using the soluble ephrin approach, two transgenic lines were out-crossed. This gave rise to a clutch of embryos in which 25-50% contain both the *HS-Gal4* and *UAS-soluble ephrinB1a* transgenes, while the remaining 50-75% of embryos will contain one or none of the transgenes. This has the advantage that if the embryos can be sorted according to their transgenic inheritance then one subset of the clutch can be used for the controls with normal Eph-ephrin signalling, and the remainder for the experimental sample in which Eph-ephrin signalling has been blocked. This should minimise inter-clutch background gene expression differences.

When collecting samples for RNA-sequencing it will be important to ensure that there are enough biological replicates so that there are sufficient numbers for the control and experiments groups. It will also be important to identify a way of screening the samples prior to RNA-sequencing so that the genetic background of the samples can be confirmed.

3.6 Conclusion

In this chapter, three different methods were tested to block Eph-ephrin signalling in the hindbrain. It was discovered that the best approach is to use soluble ephrins to globally block Eph-ephrin signalling in the embryo, eliminating any redundancy in signalling by other Eph receptors and ephrins. This technique has also enabled any potential problems of lethality to be avoided by inducing soluble ephrinB1a

expression, to block Eph-ephrin signalling at a time where endogenous Eph-ephrin signalling is initiated in the hindbrain. Therefore, earlier Eph-ephrin signalling for other roles during development is not disrupted. This minimises changes in gene expression resulting from blocking Eph-ephrin signalling outside the hindbrain that is not of interest in this project.

The next chapter will focus on the second aim of the project ‘to identify the transcriptional targets of Eph receptor and ephrin signalling’. In order to do this, firstly the best sample type for RNA-sequencing will be investigated. Secondly, a quality control protocol was developed in order to ensure that differences between samples are minimised. Finally, a method was set up to identify the control samples from the samples over-expressing soluble ephrinB1a. The findings from the RNA-sequencing screen will also be presented.

Chapter 4. Preparation of zebrafish hindbrains for RNA-sequencing

4.1 Introduction

RNA-Sequencing is a highly sensitive technique that for the scope of this study could enable the transcriptome of samples to be comparatively quantified, generating a list of potentially interesting candidate genes for investigation. Previous experiments have identified transcriptional targets of Eph-ephrin signalling, in the gut and keratinocytes, some of which were also carried out *in vitro* (Genander et al., 2009; Walsh and Blumenberg, 2011; Walsh and Blumenberg, 2012). The focus of this study is to identify target genes specific to Eph-ephrin signalling in the hindbrain.

In this chapter, preparative investigations are undertaken to determine the optimal number of embryos per sample and whether dissection is required for the identification of hindbrain specific Eph-ephrin target genes. After deciding that hindbrain dissections are more appropriate, methods were developed for screening samples to ensure the least contamination from tissues surrounding the hindbrain. These experiments were carried out using RT-qPCR and exploited the knowledge of genetic markers for specific regions in the embryo.

As discussed in Chapter 3.4.1, expression of soluble ephrinB1a will be used to block Eph-ephrin signalling in embryo. This is achieved by crossing the transgenic line HS-Gal4 with the transgenic line UAS-soluble ephrinB1a, which will give a clutch of embryos that inherit one, both or none of the transgenes. In this chapter, an RT-qPCR protocol has been designed in order to differentiate between control hindbrains and hindbrains that express soluble ephrinB1a. This enables the hindbrains in which Eph-ephrin signalling is blocked to be selected and by RNA-sequencing and comparing transcripts to the control group, genes that are differentially expressed can be identified.

4.2 Optimisation of sample

The first question addressed was whether it was necessary to dissect out the hindbrain from zebrafish embryos or whether using whole embryos would suffice. The latter would ensure that the hindbrains remain undamaged and the sample can be replicated reliably because there is no manipulation to the embryo. However, this could result in global gene expression diluting acute effects occurring specifically in the hindbrain, as it is a small region of tissue in comparison to the embryo as a whole.

To investigate whether hindbrain dissection is essential, 40 whole embryos and 40 hindbrain dissections were pooled into their respective groups and converted into cDNA libraries for analysis by RT-qPCR. Three genes, *krox20*, *six3a* and *hoxB6a*, were profiled to examine any differences in relative expression between the two batches. *krox20* is expressed in r3 and r5 and was used to determine if hindbrain specific genes were enriched when hindbrains were dissected. *six3a* is expressed anteriorly to the hindbrain and *hoxB6a* is expressed posteriorly to the hindbrain; both of these were used to determine if genes that are not expressed in the hindbrain could be eliminated or decreased in the hindbrain dissected sample.

In the sample comprised of dissected hindbrains, there is a 4.9-fold enrichment of *krox20* transcripts in comparison to whole embryos. This reflects the proportion of total embryo tissue in the hindbrain sample. Although *six3a* and *hoxB6a* are not expressed in the hindbrain, there is still some expression detected in the hindbrain dissections. There is a 6.7-fold and 1.2-fold decrease of *six3a* and *hoxB6a* transcripts, respectively, in the hindbrain dissections in comparison to the whole embryos (Figure 16). This shows that the hindbrain dissections contain more tissue that is posterior to the hindbrain than anterior. This is likely to be due to the difficulty of dissections as a result of the morphological markers in the posterior of the hindbrain being less defined than in the anterior.

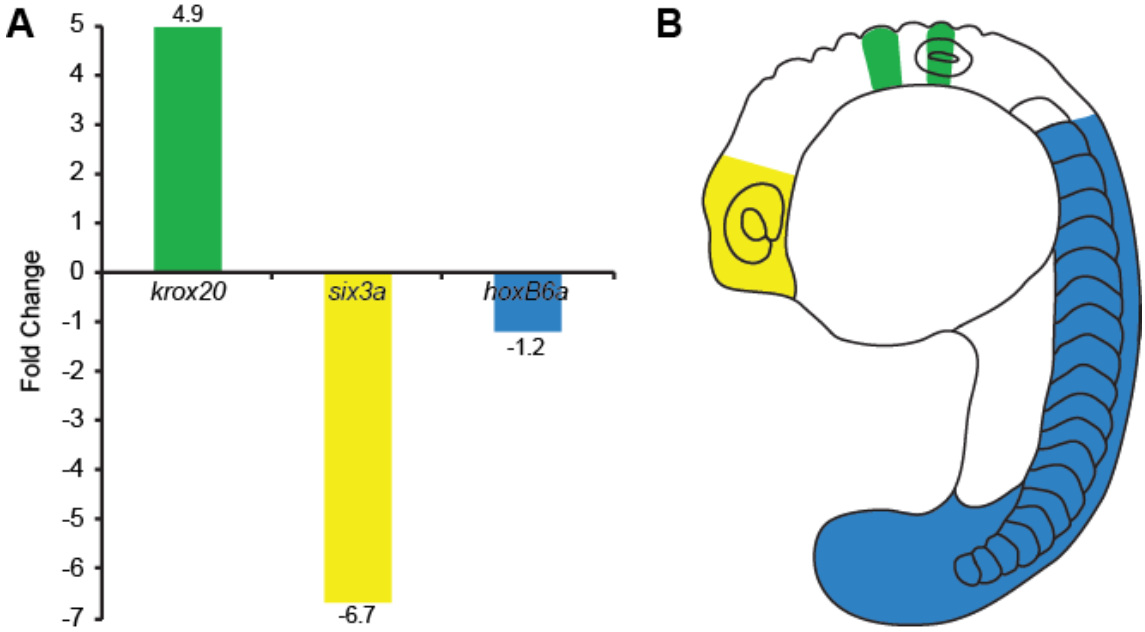

Figure 16 Comparison of gene expression in whole embryos and hindbrain dissections

(A) Fold change of gene expression in hindbrain samples in comparison to whole embryos. Each sample contains 40 embryos or 40 dissected hindbrains at 19 hpf. (B) Schematic of a zebrafish embryo at 19 hpf showing the expression pattern of *krox20* (green), *six3a* (yellow) and *hoxB6a* (blue).

Any contamination in the hindbrain dissections could mean that there are false positives or negatives of transcripts. For example, it has been observed that *rfng* expression in the midbrain-hindbrain boundary (MHB) remains when Eph-ephrin signalling is blocked by soluble ephrinB1a (Figure 12). If this tissue is not eliminated from the samples it could make the data difficult to interpret, since it could mean that target genes with lower expression when Eph-ephrin signalling is blocked may not be identified as expression in the MHB will mask this loss. In addition, Eph-ephrin signalling is active in many tissues with different roles, such as angiogenesis and somite formation (Gerety and Anderson, 2002; Davy and Soriano, 2007), thus making it important to collect only the relevant tissue. To maximise the quantity of relevant material in samples collected for RNA-sequencing it was important to ensure that high quality, uncontaminated RNA could be extracted from zebrafish hindbrains. Therefore, it is also important that the dissections are consistent across all hindbrain samples.

An additional problem with pooling embryos is that there will be a mixture of transgenic backgrounds. Only a subset of these embryos will contain both the transgenes *HS-Gal4* and *UAS-soluble ephrinB1a* and over-express soluble ephrinB1a when heat shocked. If embryos are pooled then this will weaken the signal of differentially expressed genes when Eph-ephrin signalling is blocked.

Embryos were therefore collected individually after hindbrain dissection in order to determine if all, or some, of the dissections have contamination from surrounding tissue. The expression profile of five genes that are expressed in the hindbrain and the adjacent tissues were quantified by RT-qPCR to measure the consistency between dissections (Figure 17).

There is variation between the dissected hindbrains in the number of transcripts from genes that are not expressed in the hindbrain. The dissections are technically challenging and performed manually with forceps, which is likely to give rise to some differences from one dissection to the next. In some cases, there are higher levels of *six3a* detected than *otx2*, despite *otx2* being expressed in tissue adjacent to the hindbrain and *six3a* further towards the anterior. This may be a result of tissue fragments contaminating hindbrain dissections. However, this variation can be kept to a minimum and similar level by setting a defined threshold that contamination must be less than in order to qualify for RNA-sequencing. The level of contaminating genes was measured in eight hindbrain dissections to determine the variation between samples (Figure 17). From the maximum level of expression detected of the three contaminating genes, a threshold was set to 25% of the highest levels of contamination detected for *six3a*, *otx2* and *hoxB6a* (Figure 17).

In some samples, there were undetectable levels of contaminating transcripts, which is characterised as undetected in the raw RT qPCR data. To enable comparative quantification of these samples against samples with detectable levels, the CT values were adjusted to 40 which corresponds to the maximum number of cycles in the protocol, representing the lowest detectable amount. In all of the sets of data analysis there were transcripts with undetected CT values that were altered to a value of 40, reflecting that dissections reproducibly eliminated unwanted tissue.

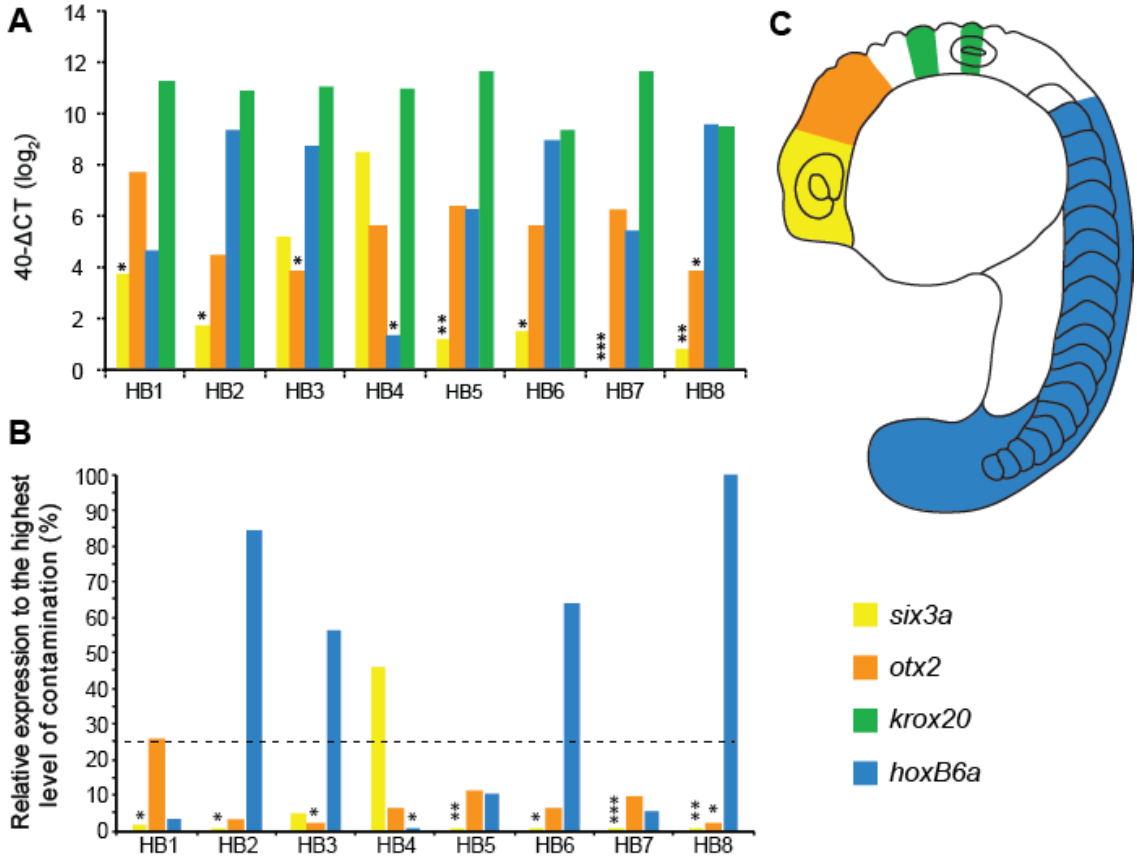

Figure 17 Expression profiles of genes representing contamination in wild type hindbrains

(A) 40-ΔCT values to show higher expression as a higher value, expression is shown as Log_2. (B) Expression of the genes on a linear scale, shown as a percentage of the gene with contaminating samples at the highest level, in this case *hoxB6a* in HB8. (A-B) The ΔCT is calculated by normalising to *β-actin* expression in each hindbrain. Undetected gene expression was given the maximum cycle value 40 and the number of undetected triplicates is marked with *. (C) Schematic of a zebrafish embryo at 19 hpf showing where the four genes are expressed in the embryo at this stage.

4.3 Sample selection for RNA-sequencing

Three separate sets of dissections were carried out and hindbrains collected by crossing *HS-Gal4* fish with *UAS-soluble ephrinB1a* fish, heat-shocking at bud and 12 ss for 1 hour and collecting at 20 ss (Figure 11). RNA was then extracted from these hindbrains, and used to generate cDNA which was then screened for contamination with markers of tissues anterior and posterior to the hindbrain and for soluble ephrinB1a expression by RT-qPCR. The data presented in Figure 18 and Figure 19 is of hindbrain dissections that were selected for RNA-sequencing as they have low

expression of genes representing contamination. This dataset excludes additional replicates that were collected.

4.3.1 Identifying samples over-expressing *soluble ephrinB1*

RT-qPCR was carried out for *soluble ephrinB1a* to determine the relative levels of expression (Figure 18). The primers used to detect *soluble ephrinB1a* expression were designed to bind downstream of the soluble ephrinB1a construct and in the SV40 polyadenylation site. This ensures that the endogenous *ephrinB1a* transcript is not amplified. There is no detection of soluble ephrinB1a in heat shocked controls (CH) and high expression of *soluble ephrinB1a* in the remaining samples (E) (Figure 18). The large increase in expression of soluble ephrinB1a means that one can be confident that these are the samples where Eph-ephrin signalling is blocked.

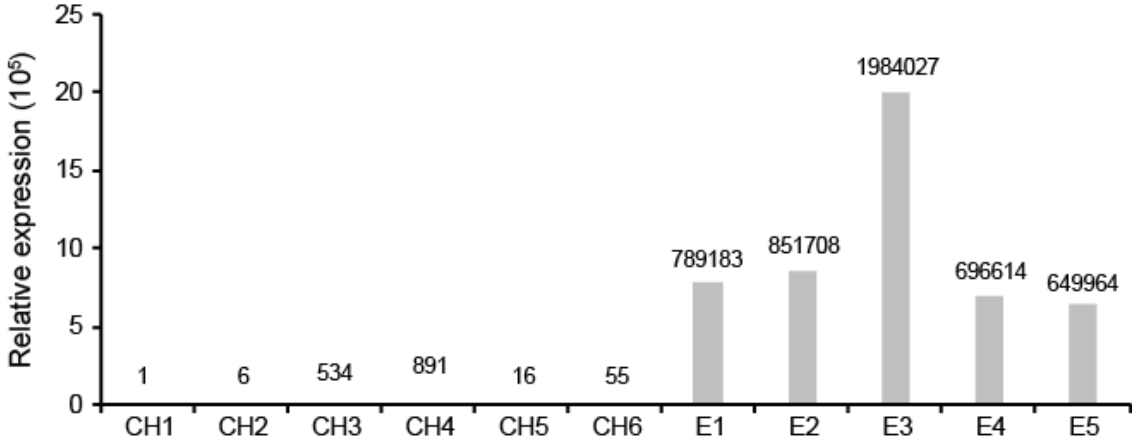

Figure 18 Expression of *soluble ephrinB1a* in hindbrains used for RNA-sequencing

Relative expression of *soluble ephrinB1a* in individual hindbrain samples used for RNA-sequencing. CH1-6 are heat shocked controls that do not express *soluble ephrinB1a* and E1-5 express *soluble ephrinB1a*. The ΔCT is calculated by normalising to *β-actin* expression in each hindbrain.

4.3.2 Identification of uncontaminated samples

The expression profiles of the dissected hindbrains used for RNA-sequencing are all below the threshold contamination level (Figure 19: A). This level is 25% of the amount of the highest level of contamination found previously (Figure 17). The samples sequenced from biological replicates two and three were found to contain

only control hindbrains or hindbrains over-expressing *soluble ephrinB1a*, respectively (Table 20).

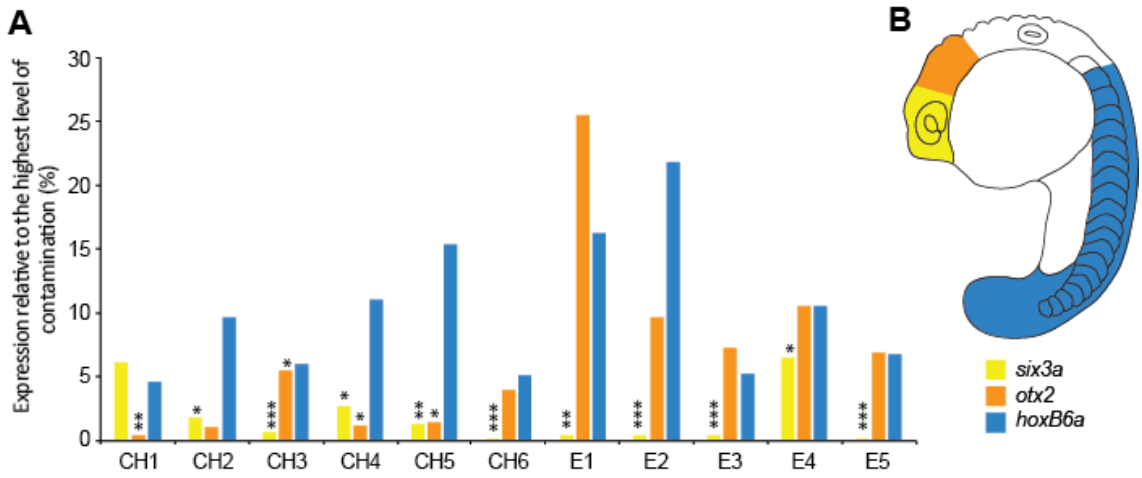

Figure 19 Gene expression profiles of hindbrains used for RNA-sequencing

(A) Relative expression profiles of three genes representing contamination from the forebrain (*six3a*), the midbrain (*otx2*) and the neural epithelium and spinal cord (*hoxB6a*) in individual hindbrain samples used for RNA-sequencing. CH1-6 are heat shocked controls that do not express soluble ephrinB1a and E1-5 are over-expressing *soluble ephrinB1a*. The ΔCT is calculated by normalising to *β-actin* expression in each hindbrain. Undetected gene expression was given the maximum cycle value 40 and the number of undetected triplicates is marked with *. (B) Schematic of a zebrafish embryo at 19 hpf showing where the three genes are expressed in the embryo at this stage.

Sample name	Biological replicate	Expression of soluble ephrinB1a? (Y/N)
CH1	2	N
CH2	2	N
CH3	1	N
CH4	1	N
CH5	1	N
CH6	2	N
E1	1	Y
E2	1	Y
E3	1	Y
E4	3	Y
E5	3	Y

Table 20 Biological replicates to collect RNA-sequencing samples

Each sample is a dissected zebrafish hindbrain CH1-6 are heat shock controls that do not express soluble ephrinB1a and E1-5 over-express *soluble ephrinB1*. Three biological repeats of the experiment were carried out from separate zebrafish breeding pairs on different days, labelled biological replicates 1-3.

4.4 RNA-sequencing

4.4.1 Data quality and alignment

The 11 hindbrains with low contamination described in Figure 19 were selected for RNA-sequencing. The sequencing data were analysed and comparisons were made between the control hindbrains and hindbrains over-expressing *soluble ephrinB1a* in order to identify potential transcriptional targets of Eph-ephrin signalling. Initially, the raw RNA-sequencing data were assessed to ensure that the quality was high enough for future analysis. This was done using FastQC (Babraham Institute), which assigns a value of confidence that the base in the sequence is correct. For this analysis, all samples had a base quality value of greater than 20 (out of 40) and were used for further analysis.

Following quality control, the data were aligned to version 10 of the zebrafish genome using Spliced Transcripts Alignment to a Reference (STAR) which enables spliced transcripts to be mapped to the genome as it allows for intronic gaps (Dobin et al.,

2013). At this stage, there was an additional assessment for data quality to ensure that a threshold level of transcripts had aligned to the reference genome. For all of the samples, between 70-90% of transcripts aligned to the zebrafish genome, which was sufficient for further analysis.

4.4.2 Differentially expressed genes

The aligned reads were counted for each gene per hindbrain sample and the genes with less than 1 transcript per million were subsequently removed. Following this, the differences in gene expression between control hindbrains and hindbrains over-expressing *soluble ephrinB1a* could be identified by carrying out a Wald Test, where pairwise comparisons are made between the level of transcripts, in the two experimental groups. This was performed using DESeq2, a programme that is used to estimate expression values of genes and calculate differential expression (Love et al., 2014). There were 1216 genes that were significantly differentially expressed between the control and experimental conditions (Figure 20), of which 585 of these genes were more highly expressed and 631 had lower expression when soluble ephrinB1a is over-expressed. Genes that were found to be significantly differentially expressed had a q-value < 0.05. The q-value is the adjusted p-value and is used to remove genes that are false positives from the differential expression data as it enables the false discovery rate to be calculated.

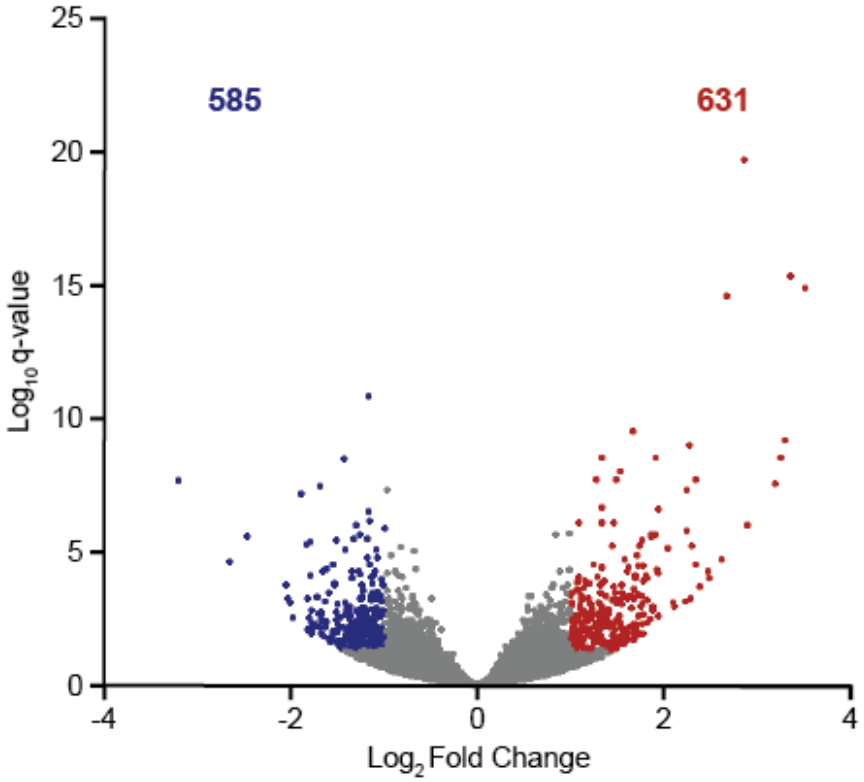

Figure 20 Volcano plot of differentially expressed genes

Volcano plot of differentially expressed genes between control hindbrains and hindbrain over-expressing *soluble ephrinB1a*. Every dot represents one gene and genes in red are up-regulated and genes in blue are down-regulated in *soluble ephrinB1a* expressing hindbrains. The *x*-axis shows the log fold change of each gene and the and the y-axis shows the log q-value.

To find out whether genes were consistently up- or down-regulated in the different experimental conditions, the distance from the median expression value for statistically significantly differentially expressed genes is presented in a heat map (Figure 21). This displays that for the 1216 genes there is an overall pattern where genes that are more highly expressed in one sample are lower in the other. However, there are some genes with varied expression that does not correlate with the expression of *soluble ephrinB1a*. This occurs more frequently for hindbrain samples CH6 and E1 and could be the result of low level contamination by surrounding tissues that were not detected in the RT-qPCR screen. For example, it could be that the otic vesicle has not been consistently removed in all hindbrain dissections given this was not screened for by RT-qPCR.

After identifying differentially expressed genes between the control group and *soluble ephrinB1a* expressing group, the samples can be clustered according to their expression profile. Samples within each group are more similar to each other than samples from the other condition, and this will identify any samples that are different from the rest of the group. The dendrogram (Figure 21) shows that the control samples (CH) cluster together and are more similar to each other than the samples expressing *soluble ephrinB1a* (E), which form a separate cluster. Moreover, it shows that there are not any major batch effects from collecting the samples because the samples from each batch of dissections do not cluster together. This suggests that the significant differences between samples are driven not by the experimental repeat but arise from changes to expression when *soluble ephrinB1a* is expressed, in the experimental group in comparison to the control.

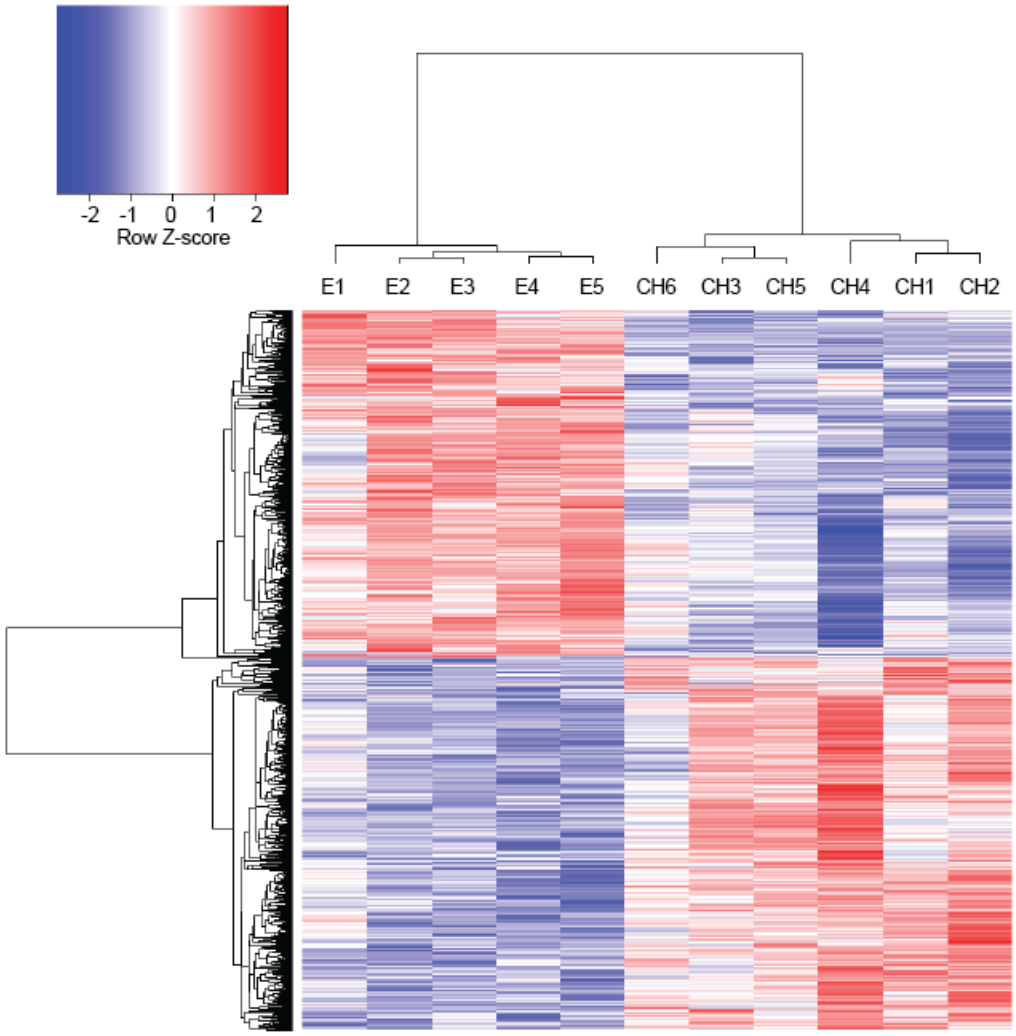

Figure 21 Significantly differentially expressed genes between control hindbrains and hindbrains expressing *soluble ephrinB1a*

Heatmap showing 1216 genes that are differentially expressed and statistically significant between control hindbrains (CH1-6) and hindbrains expressing *soluble ephrinB1a* (E1-5). Genes and hindbrain samples are the rows and columns, respectively. The colour shows the distance from the median for each gene, with red indicating values higher than the median and blue indicating values lower. The left dendrogram shows the average distance per gene and the dendrogram represents the distance between the samples.

Initially, genes were selected for validation by rank of the most statistically significant that are differentially expressed between the two sample groups. The 50 most significant have been represented in a heatmap to show how similar these are within each experimental condition (Figure 22). The genes can be split into two groups: those that are detected at similar levels within a sample group (unlabelled, Figure 22), and those that have variation in relative levels within each group (labelled with *,

Figure 22). The latter group could account for the extent to which Eph-ephrin signalling has been blocked, but, this would only explain the variation within group E. It could also reflect different amounts of contamination from other tissues, for example, samples CH6 and E1 have different levels of expression for several genes than the other samples. As there is little or no expression data on many of these genes it is difficult to draw conclusions from the variation. Some of the genes that vary have widespread expression, such as *tuba1a* and *tuba1b* and could reflect other biological variation. The variation in some genes can also be seen in the heatmap showing all the statistically differentially expressed genes (Figure 21).

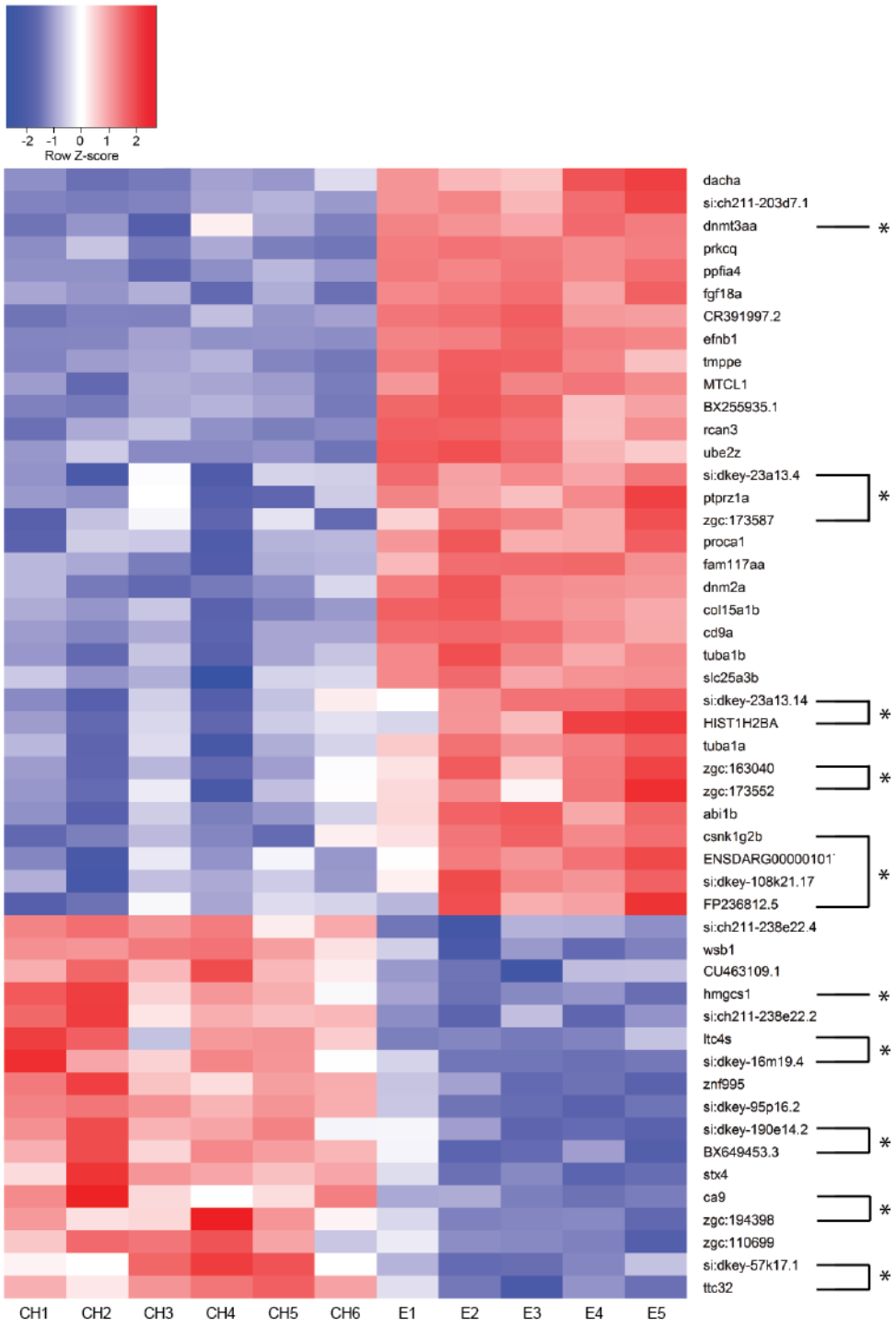

Figure 22 Heatmap of the 50 most statistically significant differentially expressed genes

Heatmap showing 50 genes that are differentially expressed between control hindbrains (CH1-6) and hindbrains expressing *soluble ephrinB1a* (E1-5) that are most statistically significant. Genes and hindbrain samples are the rows and columns, respectively. The colour shows the distance from the median for each gene (Z-score), with red indicating values higher than the median and blue indicating values lower than the median. Genes marker with * have more variation.

The second way in which the data can be organised is to show genes with the highest fold change out of all the statistically significant genes identified between controls and soluble ephrinB1a expressing hindbrains. This is a useful representation as these genes are likely to have the most dramatic change in gene expression by *in situ* hybridisation between the two experimental conditions. The 20 genes with the highest fold change are all statistically significant with an adjusted P value of less than 0.05 (Table 21). From the list of genes with the highest fold change there are 13 genes that are also present in the 50 most statistically significant genes. These genes are as follows: *cd9a*, *ppfia4*, *BX255935.1*, *prkcq*, *tmppe*, *rcan3*, *tmppe*, *rcan3*, *fgf18a*, *zgc:173587*, *zgc:163040*, *FP236812.5* and *HIST1H2BA* (1 to many).

Gene	log_2FoldChange	q-value
efnb1	7.42	0
cd9a	3.51	1.29E-15
ppfia4	3.36	4.36E-16
BX255935.1	3.30	7.13E-10
CR391997.2	3.25	3.45E-09
si:ch211-203d7.1	3.21	3.23E-08
prkcq	2.90	1.14E-06
tmppe	2.87	2.09E-20
rcan3	2.68	2.62E-15
si:dkey-248e17.5	2.62	2.10E-05
pik3cd	2.50	1.03E-04
CR388052.1	2.48	6.28E-05
si:dkey-146c18.6	2.40	2.12E-04
znf1129	2.35	3.25E-05
fgf18a	2.35	2.28E-08
zgc:173587	2.31	6.84E-06
CABZ01077605.1	2.29	5.83E-04
zgc:163040	2.28	1.13E-09
FP236812.5	2.25	1.79E-06
HIST1H2BA (1 to many)	2.25	5.63E-08

Table 21 Genes with highest fold change from RNA-sequencing that are statistically significant

Genes with the highest average fold change (log2FoldChange) in soluble ephrinB1a expressing hindbrains in comparison to control hindbrains out of the statistically significant genes. Adjusted P values show the level of significance of differential expression between control hindbrains and *soluble ephrinB1a* expressing hindbrains.

When selecting candidate genes for validation, another way to categorise the data is to select genes with the highest number of reads, since these are less likely to be falsely identified as differentially expressed. The 20 genes with the highest average expression across the samples were selected from the significantly differentially expressed genes (Table 22). When comparing this list to the top 20 genes with the highest fold change there are no genes that are present in both.

Gene	BaseMean	q-value
si:dkey-153m14.1	613034	5.29E-05
zgc:158463	208087	6.90E-05
efnb1	41650	0
hmgb2a	29943	1.11E-03
hnrnpaba	23597	1.15E-03
tubb2b	20682	2.09E-02
mdka	17240	4.36E-02
zgc:56493	16863	1.40E-02
marcksb	14941	3.95E-03
ybx1	12761	1.08E-03
rpl15	12172	1.18E-03
fubp1	11987	4.64E-04
rps9	10830	4.07E-03
smarce1	10631	1.28E-02
smarca4a	10198	2.98E-02
ahnak	9864	5.00E-02
zbtb16b	9283	1.91E-02
si:ch211-113a14.12	9222	3.74E-04
hmgb3a	9157	3.23E-02
smarcc1a	9006	3.33E-03

Table 22 Genes with highest read counts from RNA-sequencing that are statistically significant

Genes with the highest average of normalised reads across all samples (BaseMean) out of statistically significant genes. Adjusted P values show the level of significance of differential expression between control hindbrains and *soluble ephrinB1a* expressing hindbrains.

A final way to select potential target genes from the list is to identify which genes correlate to the level of ephrinB1a, as *soluble ephrinB1a* is over-expressed to block Eph-ephrin signalling and only present in these samples (E), and is absent in the controls (CH) (Figure 23). This can be used to identify which other genes behave in a similar manner, or the opposite, from control to *soluble ephrinB1a* expressing samples. In this analysis, it is not possible to differentiate between endogenous *ephrinB1a* and the expressed form, so as a result both transcripts will be included.

When comparing the 15 genes with the greatest positive correlation to *ephrinB1a* with the 50 most statistically significant genes, the 11 genes present in both analyses are: *CR391997.2*, *tmppe*, *prkcq*, *ppfia4*, *BX255935.1*, *MTCL1*, *cd9a*, *fgf18a*, *si:ch211-203d7.1*, *tuba1b* and *dnm2a*. When comparing the top 15 genes with the greatest negative correlation to *ephrinB1a* to the 50 most statistically significant genes, the four genes present in both analyses include: *si:ch211-238e22.2*, *znf995*, *ttc32* and *wsb1*. There are also six genes that appear on the list of genes with highest fold change that are also present on the list of genes with the greatest positive correlation to *ephrinB1a*. This includes: *CR391997.2*, *tmppe*, *prkcq*, *ppfia4*, *cd9a* and *fgf18a*. In contrast, there are no genes that overlap between the highest fold change and the genes with the greatest negative correlation to *ephrinB1a*.

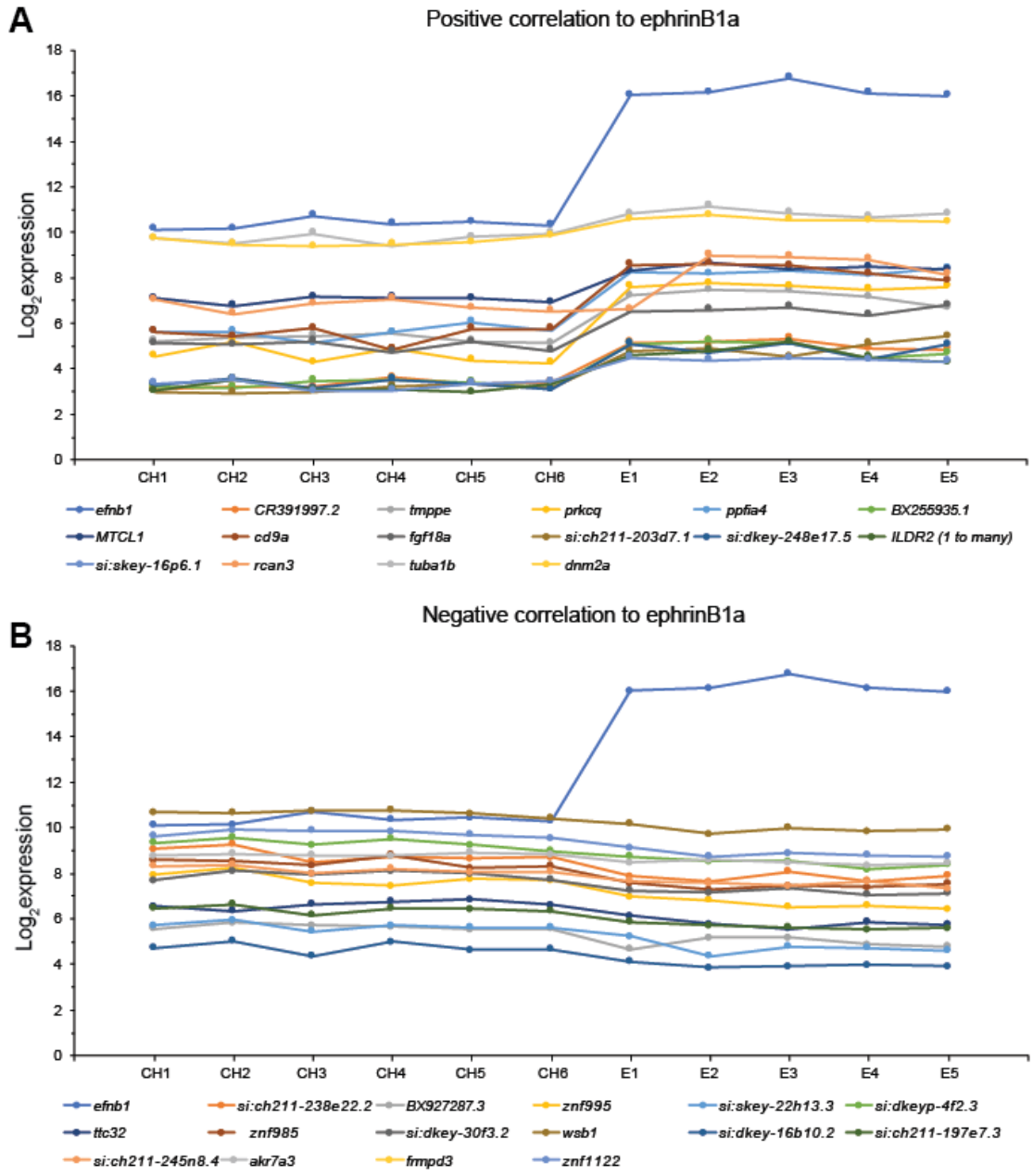

Figure 23 Correlation of gene expression with ephrinB1a across RNA-sequencing samples

Graphs showing differentially expressed genes which have the highest positive correlation (A) and the highest negative correlation (B) to *ephrinB1a* in the RNA-sequencing samples. RNA-sequencing samples are shown on the *x*-axis and the normalised Log_2 expression is shown in the *y*-axis.

4.5 Discussion

In this chapter, the optimal sample type for RNA-sequencing has been determined and a quality control method has been developed to ensure that samples used are

as similar as possible. The ideal sample type is dissected hindbrains, which enables enrichment of hindbrain specific transcripts. Contamination from tissues surrounding the hindbrain can be kept to minimal levels by keeping hindbrain dissections separate and selecting those with the lowest expression of genes which are present in neighbouring tissues.

Within a clutch of embryos there is a mixture of transgene inheritance, with fish that carry one of either the *HS-Gal4* or *UAS-soluble ephrinB1a* transgenes, fish that carry none of the transgenes and fish that carry both. Only the embryos carrying both transgenes will express *soluble ephrinB1a* upon heat shock, which can be retrospectively detected by performing RT-qPCR on RNA that was used for RNA-sequencing. This ensured that control and soluble ephrinB1a expressing embryos come from the same zebrafish cross and have identical treatment by heat shock. As a result, any experimental variation was kept to a minimum and any changes in gene expression arising from heat shock should not be present in the data.

The data generated by RNA-sequencing were of high quality with 70-90% of transcripts aligning to the zebrafish genome. Reassuringly, the samples clustered into two groups based on whether Eph-ephrin signalling had been blocked; the control hindbrains (CH) and hindbrains that expressed *soluble ephrinB1a* (E). This gave confidence that the experimental replicates did not have significant differences in gene expression and that the experimental procedure had not affected overall gene expression. There were 1216 transcripts found to be significantly differentially expressed between control embryos and embryos that express *soluble ephrinB1a*, which is too large to investigate all of them. Therefore, several ways to categorise the data were explored. These were to select the most significantly differentially expressed genes, the genes with the greatest fold change, the genes that behave most similarly across the samples as soluble ephrinB1a and the genes with the highest read count. The different analyses make different assumptions about the expression of the relevant genes and are likely to find different candidates, so genes will be selected from multiple lists for validation.

The first way to categorise the significantly differentially expressed genes was to rank them in order of the most statistically significant. These are the genes that change

the most reliably between the two experimental conditions and provides a starting point for validating targets as they are the most likely to be representative targets. The significance of the change in expression is a reflection of the variation across the samples within each condition. Lower statistical significance for a gene is the result of increased variation and could be due to contamination from surrounding tissues, differences in blocking of Eph-ephrin signalling and unidentified biological variation. Therefore, it is essential that only genes that are significantly different are considered, but the most significant will not necessarily be the most relevant genes. One example is if genes involved in differentiation were to be affected, then a small delay in timing across the samples would affect the level of gene expression. This would mean that the significance of such genes would be lower due to the variability, despite being relevant. In addition, there may be intrinsically variable effects. For example, it is known that the boundary cells are absent when ephrinB1a is over-expressed (Figure 12), which in turn is known to result in the misplacement of FGF20a-expressing neurons and changes in neurogenesis in a variable manner (Terriente et al., 2012).

Secondly, the statistically significant genes were ranked in order from the greatest fold change. The changes in gene expression should be easier to detect by *in situ* hybridisation as the differences will be greater. One issue with this method is that genes with lower fold changes may be those that are biologically relevant. For example, if a gene is expressed in multiple regions of the hindbrain it may only alter at one site, this would result in a lower fold change. In addition, genes that change as a consequence of the rate of differentiation being altered may also be subtle. *rfng* is no longer expressed when Eph-ephrin signalling is blocked, but, this does not appear on the list of significantly differentially expressed genes.

Another way that genes were categorised in order to rule out false positives is to select genes that have a high number of read counts. Genes with a low number of read counts are likely to fluctuate as a result of noise. For example, a change in read count from control to experimental condition of 10 to 12 is a difference of 20%. However, this is a change in 2 transcripts and could just be a natural fluctuation in gene expression, whereas a 20% increase from 1000 to 1200 is a numerically robust difference and more likely to be statistically significant. Despite this, some genes with

a low level of expression may still be relevant. However, selecting genes with only high read counts will favour genes that are widely expressed and not those expressed in specific cell types.

Finally, genes were identified that had the most correlated expression to *ephrinB1a* or had the opposite expression levels across all the hindbrain samples. From the RNA-sequencing data, *ephrinB1* transcripts detected are both the endogenous ephrinB1a and *soluble ephrinB1a*. From the RT-qPCR carried out to identify hindbrains where Eph-ephrin signalling had been blocked it is clear that the levels of *soluble ephrinB1a* expression varies. If there is a dose response effect then by looking at genes that correlate to *ephrinB1a* expression we are likely to identify genes that alter expression downstream of Eph-ephrin signalling. However, *soluble ephrinB1a* expression may be well above the threshold level required to block Eph-ephrin signalling. This would mean that this analysis would identify genes that have the most consistent level of expression across the sample where Eph-ephrin signalling is blocked. Thus, this would be a similar method of categorising the data as ranking by statistical significance. By looking at the normalised read counts in each sample for the genes that correlate most with *ephrinB1a expression*, it is clear that the differences in gene expression are smaller than for *ephrinB1a* (Figure 23). This is unsurprising given that the level of over-expression of ephrinB1a will dwarf changes to endogenous gene expression.

There is overlap in the genes present in the different categories of organising the RNA-sequencing data. There are also several genes that only appear in one of these categories, and it will be useful to be inclusive and take a subset of genes from each list for validation. This will reveal if there is a particular way of categorising the data that identifies validated target genes. The validation will be imperative because even when looking at the most statistically significant genes in the form of a heatmap it is clear that there is some fluctuation in expression levels across the experimental samples (Figure 22). In addition, *in situ* hybridisation validation will also be important to reveal the expression patterns of genes as this will determine if they are relevant. It is important to note that the genes identified as differentially expressed may not be direct transcriptional targets but secondary to other effects of Eph-ephrin signalling.

One example is that the change in expression may be a consequence of the loss of the hindbrain boundary cells or because of effects of altered morphogenesis.

4.6 Conclusion

In this chapter, candidate target genes of Eph receptor and ephrin signalling in the hindbrain have been identified by RNA-sequencing. When Eph-ephrin signalling is blocked, there are 1216 genes that have statistically significant differential expression in comparison to control. A comprehensive analysis of a group of this size is beyond the scope of this study. In order to reduce the number to a manageable figure, genes were categorised in different ways to see if there were genes that were flagged repeatedly as potential targets for validation. The significantly differentially expressed genes were categorised in the following way: the most significantly differentially expressed, the highest fold change, the highest average number of reads and the genes with the most positive or negative correlation to *ephrinB1a* expression across the samples.

In the next chapter, differentially expressed genes identified here will be validated by RT-qPCR to determine which genes are regulated downstream of Eph-ephrin signalling. This technique provides a way to screen through multiple genes from the different categories. Then validated targets will then be screened by *in situ* hybridisation to identify the expression patterns in the hindbrain before determining how the expression changes when Eph-ephrin signalling is blocked.

Chapter 5. Validation of genes regulated downstream of Eph-ephrin signalling

5.1 Introduction

In the previous chapter, genes potentially regulated downstream of Eph-ephrin signalling were identified by blocking signalling and comparing the transcripts present to those without blocking. This identified 1216 candidate genes that have significantly different expression between the two experimental groups. Some of these genes could be the result of slight differences in the amount of contaminating tissues present in the hindbrain dissections of the two conditions. Despite measures being taken to keep this contamination to a minimum, it was notable that for some genes the levels of expression varied within the experimental condition. As a result, before carrying out further investigation, it will be important to validate candidate genes which were selected using four criteria that were discussed in Chapter 4.

RT-qPCR and *in situ* hybridisation were used to validate potential target genes. RT-qPCR can be used to quantify changes in gene expression and compared to the RNA-sequencing results, determining if altered expression of the gene is the same for both techniques. Genes that are validated by RT-qPCR will then be screened using *in situ* hybridisation to determine whether they are expressed in the hindbrain at detectable levels and reveal their expression pattern. To examine how the expression of candidate genes alter when Eph-ephrin signalling is blocked, comparisons will be made between wild type embryos and embryos where Eph-ephrin signalling has been disrupted either by expressing *soluble ephrinB1a* or in double Eph receptor and ephrin mutants. From this dataset, genes with modified expression patterns when Eph-ephrin signalling is blocked will be investigated further.

5.2 Validating changes in gene expression by RT-qPCR

In order to validate changes in gene expression by screening multiple genes, rather than genes individually, RT-qPCR was carried out on whole embryos. Although the

RNA-sequencing was performed on hindbrain dissections, whole embryos have been chosen for several reasons. Firstly, when using whole embryos any genes that were identified from RNA-sequencing as a result of contamination from surrounding tissues should be eliminated, since false positive genes will not be differentially expressed between control whole embryos and whole embryos where Eph-ephrin signalling is blocked. In addition, whole embryos can be collected more easily as there is no manipulation to the embryo. Embryos can then be selected which over-express *soluble ephrinB1a* and controls that do not. This method eliminates the need for embryo dissections that require a quality control step to ensure low contamination from surrounding tissues.

The disadvantage of using whole embryos is that that Eph-ephrin signalling has a variety of roles during development in multiple tissues. For example, for boundary cell formation in the hindbrain and somites (Durbin et al., 1998; Cooke et al., 2005; Terriente et al., 2012), as well as for angiogenesis (Cheng et al., 2002), and in control of cell migration, proliferation and apoptosis (Davy and Soriano, 2007; Holmberg et al., 2006; Park, 2013). Therefore, there is a possibility that changes in gene expression elsewhere in the embryo may mask the changes in expression in the hindbrain. Nevertheless, because of the high throughput nature and the ability to eliminate targets found due to contamination, this technique was used to see if it was possible to validate Eph-ephrin transcriptional targets.

For a gene to be validated as affected by blocking of Eph-ephrin signalling it should firstly have similar levels of expression within each of the two experimental groups. Secondly, the gene should also have different levels of expression between the two conditions, showing that it has changed when Eph-ephrin signalling has been blocked. However, because of the potential effects of blocking signalling elsewhere in the embryo masking changes in gene expression in the whole embryo, the first criterion will be more important than the latter. This will inform us that the expression level of the gene in question is reproducible in each condition and also that the expression is altered when Eph-ephrin signalling is blocked.

5.2.1 Validation in embryos where Eph-ephrin signalling is blocked

Whole embryos for analysis were derived by crossing *HS-Gal4* fish to *UAS-soluble ephrinB1a* fish, carrying out two 1 hour heat shocks at bud and 12 ss, and collecting at 19 hpf (Chapter 3.4.1, Figure 11). The level of *soluble ephrinB1a* expression was quantified to identify which of the embryos were heat shocked controls and which over-expressed *soluble ephrinB1a* (Figure 24). As observed previously with hindbrain dissections used for RNA-sequencing (Chapter 4.3.1, Figure 18), the relative levels of *soluble ephrinB1a* expression vary between the embryos collected. The embryos which express *soluble ephrinB1a* are embryos 7, 16 and 19 (Figure 24), which will now be referred to as wE1, wE2 and wE3, respectively (Figure 26). For the control samples, the three embryos with no expression of *soluble ephrinB1a* were chosen: embryos 6, 14 and 20 (Figure 24), which will now be referred to as wCH1, wCH2 and wCH3, respectively (Figure 26). By choosing samples with similar levels of *soluble ephrinB1a* for E1-3, the validation experiments should be easier to interpret as it would be expected that gene expression changes would be similar. If there is a threshold level of soluble ephrinB1a expression which is sufficient to block Eph-ephrin signalling, this should be reached in all three samples as they are the highest across the 20 embryos and are similar to one another.

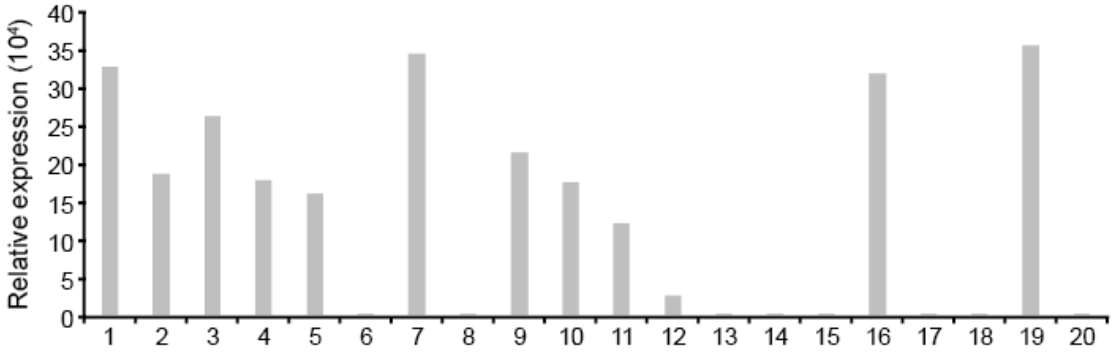

Figure 24 Expression of *soluble ephrinB1a* in individual whole embryos

Relative expression of *soluble ephrinB1a* in individual whole embryos to select samples for validation experiments. ΔCT is calculated by normalising to *β-actin* expression in each hindbrain.

Genes were selected for validation from the four different criteria used to organise the RNA-sequencing data, discussed in Chapter 4.4.2. The 22 genes are listed in Table 23 along with which category they appear.

Gene	Most significantly differentially expressed	Highest fold change	Highest read count	Positive correlation to *ephrinB1a*	Negative correlation to *ephrinB1a*
hmgb2a			✓		
nap1l1		✓			
tubb2b			✓		
ybx1			✓		
mdka			✓		
marcksb			✓		
rpl15			✓		
cd9a	✓	✓		✓	
akr7a3					✓
stx4	✓				
ube2z	✓				
ttc32	✓				✓
hnrnpaba			✓		
fubp1			✓		
abi1b	✓				
col15a1b	✓				
fam117aa	✓				
ppfia4	✓	✓		✓	
tmppe	✓	✓		✓	
dnm2a	✓			✓	
wsb1	✓				✓

Table 23 Criteria of candidate gene selection

Candidate genes were selected for RT-qPCR based on the above criteria.

The first step of validation was to determine if expression of the selected genes changes when Eph-ephrin signalling is blocked, using RT-qPCR in whole embryos (Figure 25). Any genes with less than 1.2-fold increase or decrease in expression when Eph-ephrin signalling was blocked were considered not to alter.

Seven genes did not change in expression (*hmgb2a*, *nap1l1*, *ybx1*, *stx4*, *wsb1*, *rpl15* and *hnrnpaba*). Eight genes had increased expression when Eph-ephrin signalling was blocked (*tubb2b*, *marcksb*, *cd9a*, *ube2z*, *abi1b*, *fam117aa*, *ppfia4* and *tmppe*). Six genes had decreased expression when Eph-ephrin signalling was blocked (*mdka*, *dnm2a*, *ttc32*, *akr7a3*, *col15a1b* and *fubp1*) with *ttc32* being significantly decreased. Three genes had opposing changes in expression when Eph-ephrin signalling was

blocked and quantified in whole embryos in comparison to hindbrain dissections (*mdka*, *dnm2a* and *col15a1b*). In addition, *stx4* and *wsb1* expression does not alter in whole embryos but have lower expression in the hindbrain when Eph-ephrin signalling is blocked. These opposing changes are likely to be the consequence of differences in sample type and reflect changes in gene expression that are occurring elsewhere in the embryo. The lack of significance in the observations made by RT-qPCR in whole embryos could be a result of variation across the replicates of each condition, which may be solved by additional replicates, or could be the result of biological variation.

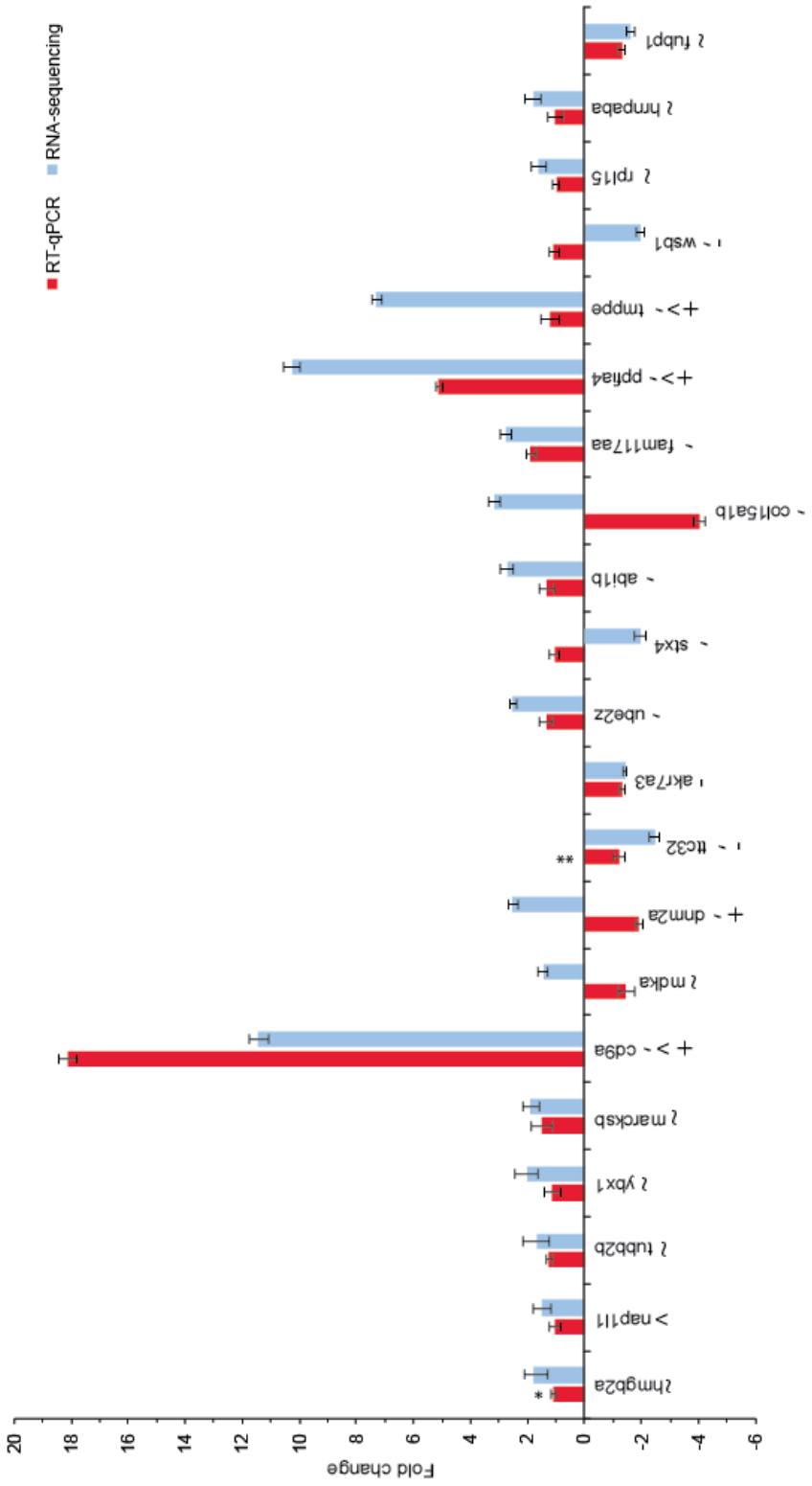

Figure 25 Comparison of RT-qPCR data with RNA-sequencing data

Fold change of gene expression in *soluble ephrinB1a* expressing samples in comparison to control embryos at 19 hpf. Red bars represent RT-qPCR validation in whole embryos (n=3 for control and *soluble ephrinB1a* expressing embryos). Blue bars represent RNA-sequencing normalised reads from hindbrains (n=6 for controls, n=5 for *soluble ephrinB1a* expressing hindbrains). Error bars show standard deviation, ** represents p-value < 0.05, * represents trending towards significance p-value ≤ 0.1 for RT-qPCR data. All RNA-sequencing data has a q-value < 0.05, except for *nap1l1* which has a q-value ≤ 0.07. Categories the genes are selected from are represented by symbols: most significantly differentially expressed (‘), highest fold change (^), highest read count (~), positive correlation to *soluble ephrinB1a* (+), negative correlation to *soluble ephrinB1a* (-).

The normalised read counts of a gene for individual hindbrains, determined by RNA-sequencing, and the relative expression of a gene for individual whole embryos, determined by RT-qPCR, were plotted to compare the similarity between replicates for each gene (Figure 26). This is informative because many of the changes in expression when Eph-ephrin signalling is blocked are not statistically significant when analysed by one-way ANOVA (Figure 25).

When evaluating the RT-qPCR analysis of individual whole embryos (Figure 27), genes could be split into 3 categories: (1) genes that have similar expression levels in all control and *soluble ephrinB1a* expressing embryos, (2) genes that have similar replicates within each experimental condition that is different from the other condition, and (3) genes that do not have similar replicates within the same condition.

stx4, *ybx1*, *rpl15* and *hnrnpaba* have similar expression across the 3 control embryos and 3 embryos expressing *soluble ephrinB1a* (Figure 26). Since no change occurs in whole embryos, the difference found in dissected hindbrains could be due to contamination with other tissues. Alternatively, this could indicate that changes to the expression of these genes in the hindbrain are being equalised by opposing changes elsewhere.

The genes found by RT-qPCR to have fairly similar replicates within each experimental condition and change expression from control to experimental condition (Figure 26), include: *ttc32*, *tmppe*, *hmgb2a*, *tubb2b* and *fubp1*. The RT-qPCR validation shows that *ttc32* and *fubp1* decrease in expression when Eph-ephrin signalling is blocked. In contrast, *tmppe* and *tubb2b* have increased expression, and *hmgb2a* did not alter. These genes will be investigated further.

Finally, there was a subset of genes with variation between replicates within an experimental condition (Figure 26), including: *cd9a*, *ube2z*, *abi1b*, *col15a1b*, *fam117aa*, *ppfia4*, *dnm2a*, *wsb1*, *nap1l1*, *mdka*, *marcksb* and *akr7a3*. For some of these genes there is just one outlier within a sample, such as *ube2z*, *abi1b*, *mdka*, *dnm2a* and *marcksb*. However, for others there is no pattern across the samples within a group, such as the control samples for *col15a1b*, *fam117aa*, *ppfia4*, *wsb1*,

nap1l1 or *akr7a3*. The fluctuations between samples suggests that these genes may not be biologically relevant as they are not similarly modulated within each experimental group. However, it will be informative to investigate a subset of these genes to determine if the expression does vary from one embryo to another.

Consideration should also be taken as to what is known about the candidate genes. This may indicate whether it is likely to have a specific function in the hindbrain or a broader role in the embryo. Previous studies have shown that *hmgb2a* and *tubb2b* are implicated in brain development (Table 24). In addition, the RT-qPCR validation showed that the replicates were similar within the two experimental conditions. *ttc32* and *tmppe* also had similar expression in replicates of each experimental condition but were not chosen to pursue at this time due to a lack of information about what role they may play (Table 24).

nap1l1 and *mdka* did not have similar replicates for the experimental conditions in the RT-qPCR validation, although there was an overall trend of *mdka* gene expression being down-regulated when Eph-ephrin signalling was blocked (Figure 26). This is interesting because this trend is in contrast to the RNA-sequencing data where *mdka* expression is up-regulated. It will be useful to explore this further in order to resolve why there may be differences between what is observed by RNA-sequencing and RT-qPCR. In addition, *mdka* is known to be a marker of neural differentiation, making it an interesting candidate to investigate further (Schafer et al., 2005) (Table 24). *nap1l1* was also selected because of previous work showing that it is expressed in progenitor cells (Yan et al., 2016) (Table 24). *cd9a* and *stx4* are also involved in neuronal development based on previous studies. However, efforts to detect expression by *in situ* hybridisation have been unsuccessful.

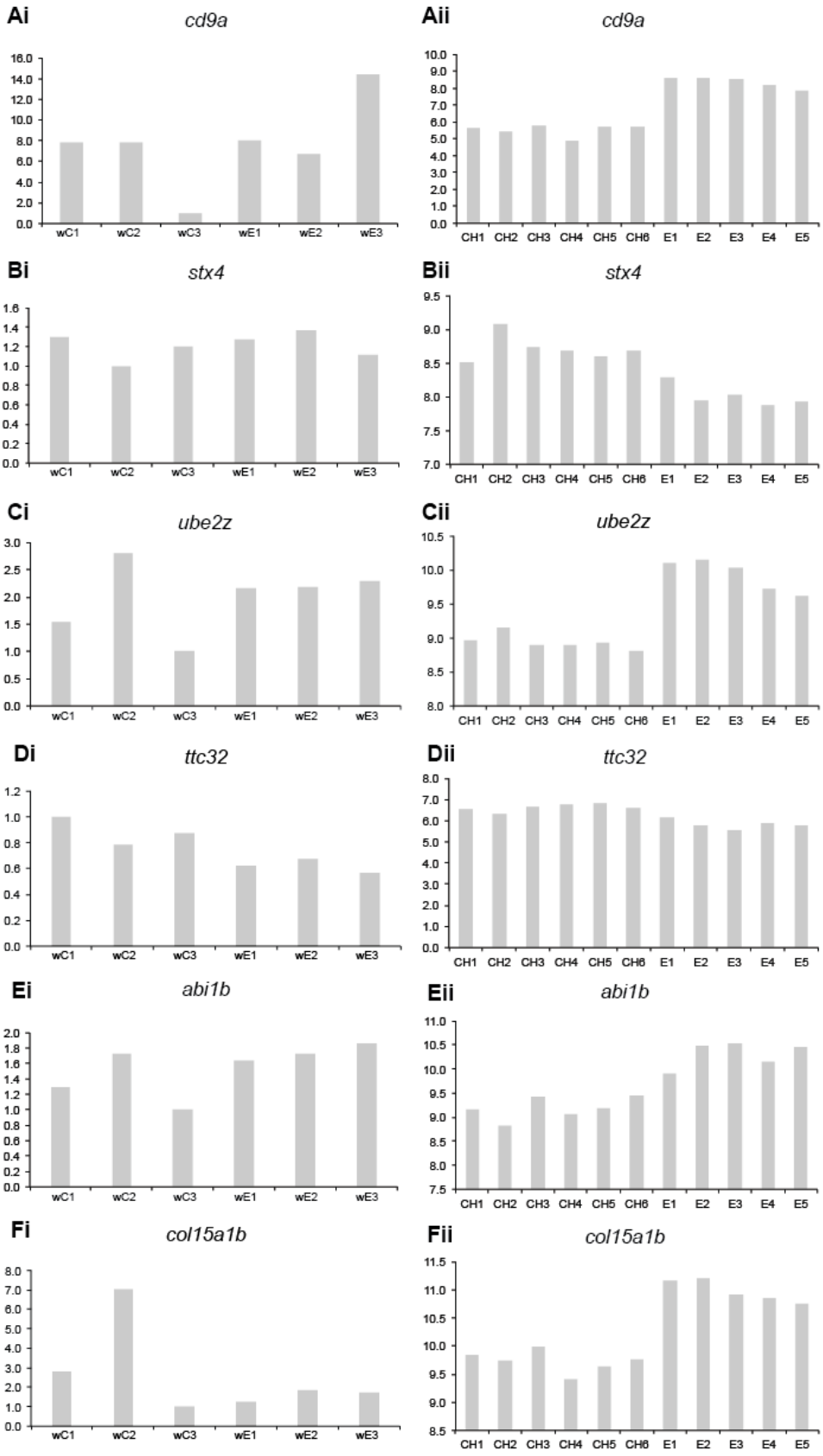
Ai
cd9a
wC1 wC2 wC3 wE1 wE2 wE3
Aii
cd9a
CH1 CH2 CH3 CH4 CH5 CH6 E1 E2 E3 E4 E5
Bi
stx4
wC1 wC2 wC3 wE1 wE2 wE3
Bii
stx4
CH1 CH2 CH3 CH4 CH5 CH6 E1 E2 E3 E4 E5
Ci
ube2z
wC1 wC2 wC3 wE1 wE2 wE3
Cii
ube2z
CH1 CH2 CH3 CH4 CH5 CH6 E1 E2 E3 E4 E5
Di
ttc32
wC1 wC2 wC3 wE1 wE2 wE3
Dii
ttc32
CH1 CH2 CH3 CH4 CH5 CH6 E1 E2 E3 E4 E5
Ei
abi1b
wC1 wC2 wC3 wE1 wE2 wE3
Eii
abi1b
CH1 CH2 CH3 CH4 CH5 CH6 E1 E2 E3 E4 E5
Fi
col15a1b
wC1 wC2 wC3 wE1 wE2 wE3
Fii
col15a1b
CH1 CH2 CH3 CH4 CH5 CH6 E1 E2 E3 E4 E5

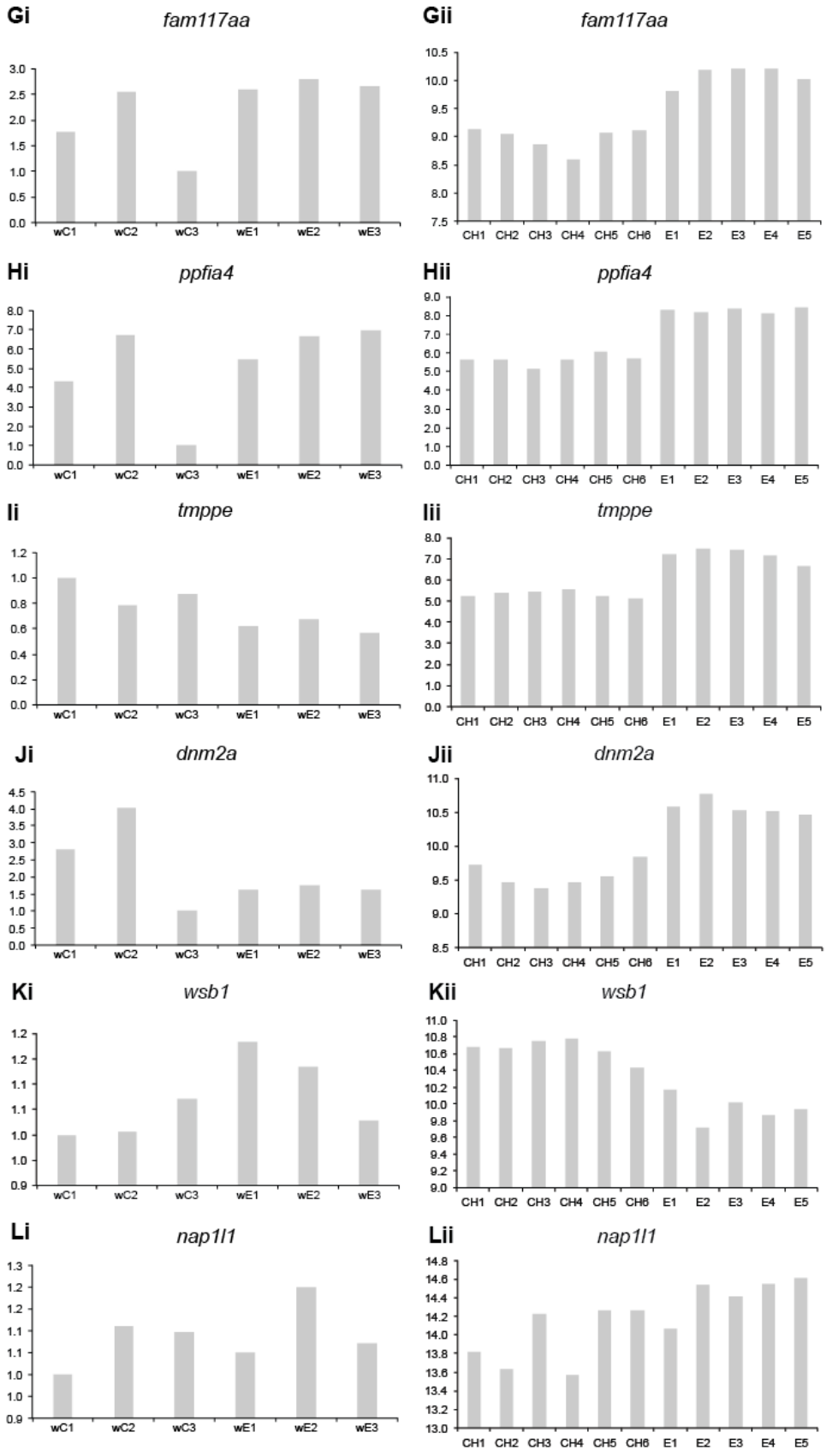
Gi
fam117aa
wC1 wC2 wC3 wE1 wE2 wE3
Gii
fam117aa
CH1 CH2 CH3 CH4 CH5 CH6 E1 E2 E3 E4 E5
Hi
ppfia4
wC1 wC2 wC3 wE1 wE2 wE3
Hii
ppfia4
CH1 CH2 CH3 CH4 CH5 CH6 E1 E2 E3 E4 E5
Ii
tmppe
wC1 wC2 wC3 wE1 wE2 wE3
Iii
tmppe
CH1 CH2 CH3 CH4 CH5 CH6 E1 E2 E3 E4 E5
Ji
dnm2a
wC1 wC2 wC3 wE1 wE2 wE3
Jii
dnm2a
CH1 CH2 CH3 CH4 CH5 CH6 E1 E2 E3 E4 E5
Ki
wsb1
wC1 wC2 wC3 wE1 wE2 wE3
Kii
wsb1
CH1 CH2 CH3 CH4 CH5 CH6 E1 E2 E3 E4 E5
Li
nap1l1
wC1 wC2 wC3 wE1 wE2 wE3
Lii
nap1l1
CH1 CH2 CH3 CH4 CH5 CH6 E1 E2 E3 E4 E5

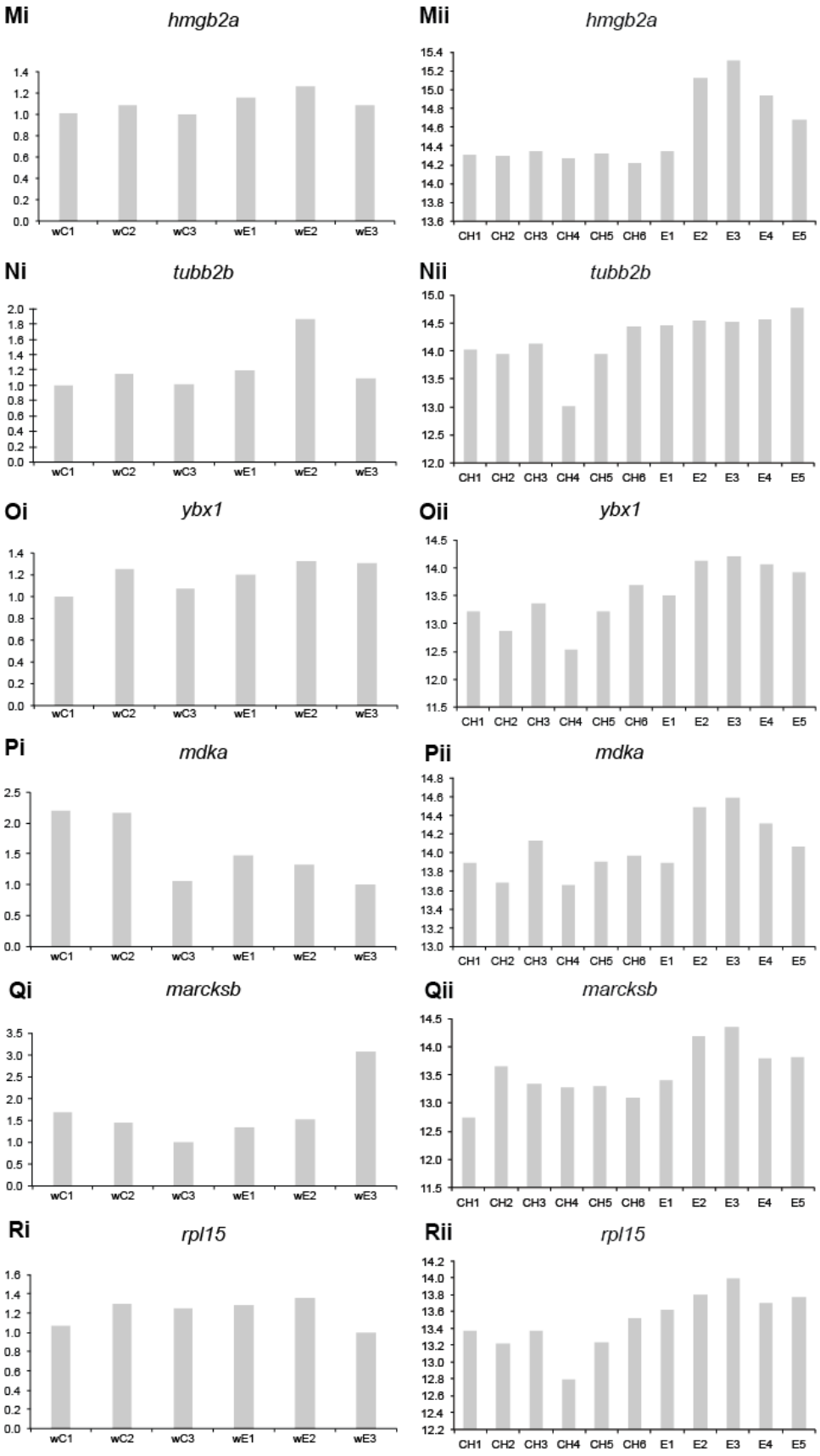
Mi
hmgb2a
wC1 wC2 wC3 wE1 wE2 wE3
Mii
hmgb2a
CH1 CH2 CH3 CH4 CH5 CH6 E1 E2 E3 E4 E5
Ni
tubb2b
wC1 wC2 wC3 wE1 wE2 wE3
Nii
tubb2b
CH1 CH2 CH3 CH4 CH5 CH6 E1 E2 E3 E4 E5
Oi
ybx1
wC1 wC2 wC3 wE1 wE2 wE3
Oii
ybx1
CH1 CH2 CH3 CH4 CH5 CH6 E1 E2 E3 E4 E5
Pi
mdka
wC1 wC2 wC3 wE1 wE2 wE3
Pii
mdka
CH1 CH2 CH3 CH4 CH5 CH6 E1 E2 E3 E4 E5
Qi
marcksb
wC1 wC2 wC3 wE1 wE2 wE3
Qii
marcksb
CH1 CH2 CH3 CH4 CH5 CH6 E1 E2 E3 E4 E5
Ri
rpl15
wC1 wC2 wC3 wE1 wE2 wE3
Rii
rpl15
CH1 CH2 CH3 CH4 CH5 CH6 E1 E2 E3 E4 E5

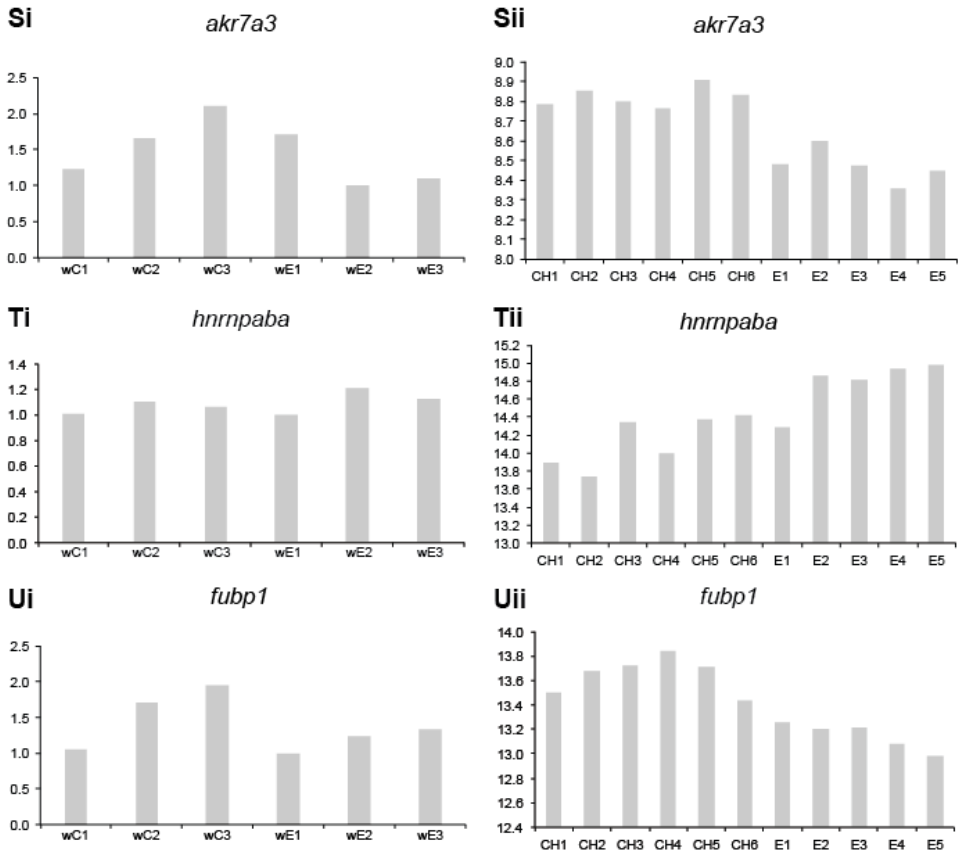

Figure 26 Comparison of individual samples from RT-qPCR validation to RNA-sequencing data

(Ai-Ui) Graphs showing relative levels of gene expression calculated by RT-qPCR in individual whole embryos (Ai-Ui). The ΔCT is calculated by normalising to *β-actin* expression in embryo. C1-3 are control embryos and E1-3 are over-expressing *soluble ephrinB1a* and Eph-ephrin signalling has been blocked. All embryos have been heat shocked. (Aii-Uii) Graphs showing normalised react counts from RNA-sequencing for each gene. Samples are individual hindbrains and CH1-6 are controls and E1-5 are over-expressing *soluble ephrinB1a* and Eph-ephrin signalling has been blocked. All hindbrains have been heat shocked. The whole embryos (i) and hindbrains (ii) are from different experiments and are different embryos.

Gene	Known roles	References
hmgb2a	Regulation of neuronal cell differentiation	(Abraham et al., 2013; Bronstein et al., 2017)
nap1l1	Regulates proliferation in iPSCs	(Yan et al., 2016)
tubb2b	Neuronal migration and differentiation	(Jaglin and Chelly, 2009; Breuss et al., 2015)
ybx1	Regulation of Nodal signalling	(Kumari et al., 2013; Zaucker et al., 2017)
mdka	Neural Tube formation	(Schafer et al., 2005)
marcksb	Gastrulation/cell membrane protrusion	(Wang et al., 2013)
rpl15	Ribosome assembly	(Provost et al., 2013)
cd9a	Regulation of neuronal cell differentiation	(Howe et al., 2013)
akr7a3	Tumour suppressor, blocks ERK/c-jun NFkB	(Chow et al., 2017)
stx4	Membrane trafficking in dendritic spines	(Kennedy et al., 2010)
ube2z	Ubiquitin conjugating enzyme protein	(Gu et al., 2007)
ttc32	No information	N/A
hnrnpaba	Activates EMT and metastasis in hepatocyte cancer	(Zhou et al., 2014)
fubp1	Pro-proliferative and anti apoptotic oncogene	(Wesely et al., 2017)
abi1b	No information	N/A
col15a1b	Type of collagen expressed in slow myosin heavy chain-positive cells	(Bretaud et al., 2011)
fam117aa	No information	N/A
ppfia4	No information	N/A
tmppe	No information	N/A
dnm2a	Cardiac function, neuromuscular development	(Li et al., 2013; Gibbs et al., 2013)
wsb1	Midblastula Transition	(Gibbs et al., 2013)

Table 24 Previously published roles of candidate genes

Review of the literature on known roles of candidate genes.

5.2.2 Validation in Eph receptor and ephrin mutants

The four candidate genes selected were also analysed by RT-qPCR in double Eph receptor and ephrin mutants to quantitate changes in gene expression prior to qualitative analysis by *in situ* hybridisation. The mutants used were: *EphA4a* and

EphB4a double mutants, and *ephrinB2a* and *ephrinB3b* double mutants. In the double Eph receptor mutants signalling will not occur via EphA4a and EphB4a receptors with their respective binding partners. However, other Eph receptors still present in the hindbrain can signal redundantly with the ephrin binding partners of these Eph receptors. In the double ephrin mutants signalling will not occur through ephrinB2a and ephrinB3b with their respective binding partners. Again, other ephrins are able to signal redundantly with the Eph receptors that usually bind these ephrins. As there are only three ephrinBs present in the hindbrain, and in this mutant two are absent, it would be expected that there would be less redundancy of signalling than for the double Eph receptor mutant. Both double mutants have partial boundary loss, with the boundaries of r1/r2, r4/r5 and r6/r7 remaining (Chapter 3.3.2, Figure 10).

There were alterations in gene expression in the Eph receptor and ephrin double mutants in comparison to wild type embryos (Figure 27). Any genes with a less than 1.2-fold increase or decrease in expression were considered not to alter. *nap1l1* and *tubb2b* did not alter in the Eph receptor double mutants in comparison to control embryos, whereas *mdka* and *hmgb2a* decreased significantly by 1.4-fold and 1.5-fold, respectively. In the double ephrin mutants, *hmgb2a* and *tubb2b* expression did not change, *mdka* expression increased by 1.5-fold and *nap1l1* expression decreased by 1.4-fold. The change in expression of *mdka* in double Eph receptor mutants was roughly equal and opposite to the change in double ephrin mutants.

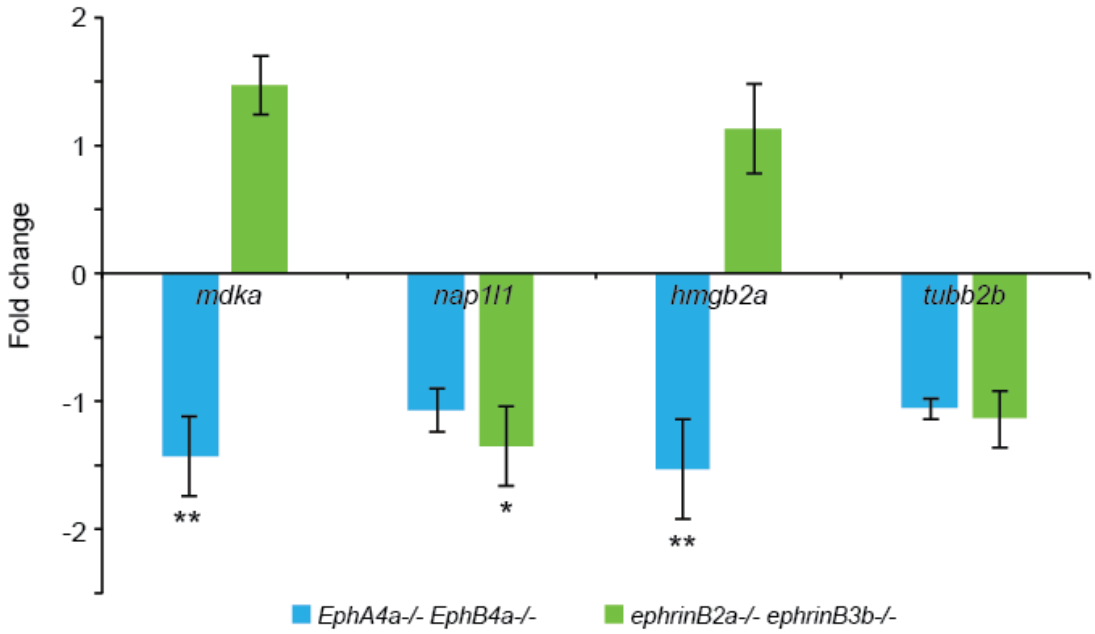

Figure 27 Fold change of genes in double Eph receptor and ephrin mutants

Fold change of gene expression in Eph receptor and ephrin double mutants in comparison to wild type embryos. Analysis was carried out on embryos at 19 hpf, n=3 of pools of 40 whole embryos for each condition. Error bars show standard deviation, ** represents p-value ≤ 0.05, * represents trending towards significance p-value ≤ 0.07 for RT-qPCR data Expression was normalised to *β-actin* for each sample.

5.3 Validating selected genes by *in situ* hybridisation

To further investigate *tubb2b*, *hmgb2a*, *nap1l1* and *mdka*, their expression pattern was determined in wild type embryos. All four of these genes are highly expressed in the hindbrain according to the normalised read counts (baseMean values) determined by RNA-sequencing, which range from 17,000-30,000 transcripts per million. RNA probes were designed for *in situ* hybridisation and expression analysed at 20 ss, the stage that RNA-sequencing was carried out. *In situ* hybridisation can be utilised to detect changes in the pattern of gene expression, but is not sensitive enough to quantitate differences in expression unless this is large.

5.3.1 Expression of candidate genes in wild type embryos

tubb2b expression is mainly uniform along the A-P axis, but with localised expression in lateral regions, which appears to be in neural epithelial cells (Figure 28: A, B). The expression pattern of *hmgb2a* is uniform and the same as previously reported (Moleri

et al., 2011). *nap1l1* expression is higher in some segments than others (Figure 28: E, F), which is in agreement with previous data (Thisse and Thisse, 2014). *mdka* has higher localised expression in the segments and lower expression in what appears to be the hindbrain boundaries (Figure 28: G, H), which is in agreement with previous data (Winkler et al., 2003).

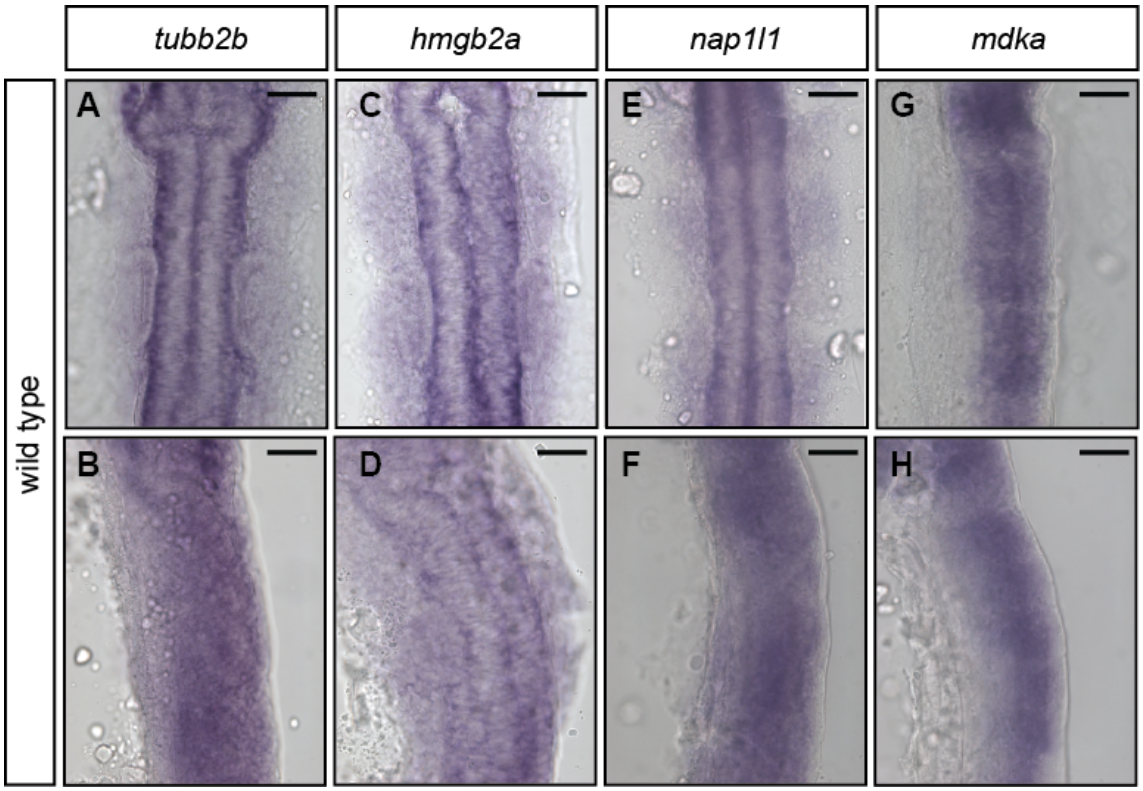

Figure 28 Expression of validated target genes in wild type embryos

(A-H) Embryos at 20 ss / 19 hpf after *in situ* hybridisation for *tubb2b* (A-B), *hmgb2a* (C-D), *nap1l1* (E-F) and *mdka* (G-H). (A, C, E, G) Are flat mounted embryos and (B, D, F, H) are side mouted embryos. Scale bar represents 100 µm.

5.3.2 Expression of candidate genes in embryos where Eph-ephrin signalling is disrupted

In order to determine if the expression of the candidate genes is affected by Eph-ephrin signalling, their expression patterns were identified in embryos where signalling had been blocked. Embryos were collected in the same way that the RNA-sequencing samples were obtained by out-crossing the *HS-Gal4* and *UAS-soluble ephrinB1a* transgenic fish. This induces *soluble ephrinB1a* expression in around 50% of embryos from a clutch to globally block Eph-ephrin signalling

(Chapter 4.3.1, Figure 11). These embryos have complete loss of hindbrain boundaries. The numbers and images depicted in the proceeding figures for this cross are the embryos that have expression patterns that are different from wild type embryos and are predicted to have inherited both transgenes and over-express soluble ephrinB1a. Double Eph receptor or double ephrin mutant embryos were also used, which have partial boundary loss, with the boundaries of r1/r2, r4/r5 and r6/r7 remaining (Chapter 3.3.2, Figure 10). As with previous validation experiments, the embryos were collected at 20 ss, the same stage that the RNA-sequencing was carried out. From this analysis, changes in expression patterns were clearer to see when the embryos were side mounted, rather than flat mounted. Therefore, the numbers quoted for a given phenotype will refer to side mounted embryos.

tubb2b expression does not alter when Eph-ephrin signalling is blocked with expression of soluble ephrinB1a (Figure 29: B, F, J, N). Likewise, *tubb2b* expression does not alter in double Eph receptor mutants (Figure 29: C, G, K, M), nor in double ephrin mutants (Figure 29: D, H, L, N).

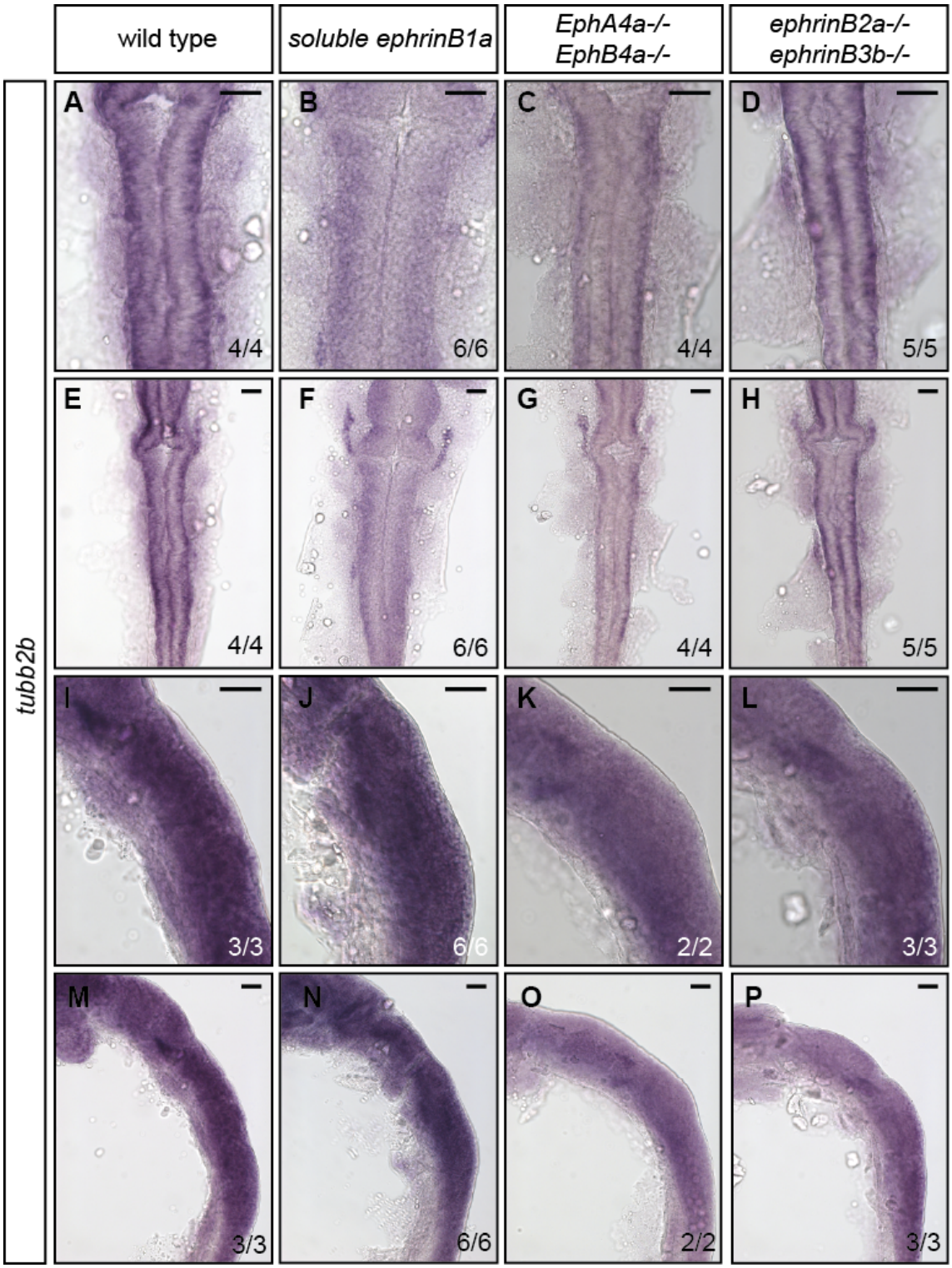

Figure 29 *tubb2b* expression at 20 ss when Eph-ephrin signalling is blocked

Embryos at 20 ss / 19 hpf after *in situ* hybridisation for *tubb2b*. (A-H) Flat mount view and (I-P) and a side mount view with A-D and I-L at a higher magnification than E-H and M-P. A-D and E-H show the same embryo in each column at a different magnification, as well as I-L and M-P. Scale bar represents 100 µm.

hmgb2a expression does not alter when Eph-ephrin signalling is blocked with expression of soluble ephrinB1a (Figure 30: B, F, J, N), nor in double Eph receptor mutants (Figure 30: C, G, K, M), nor in double ephrin mutants (Figure 30: D, H, L, N).

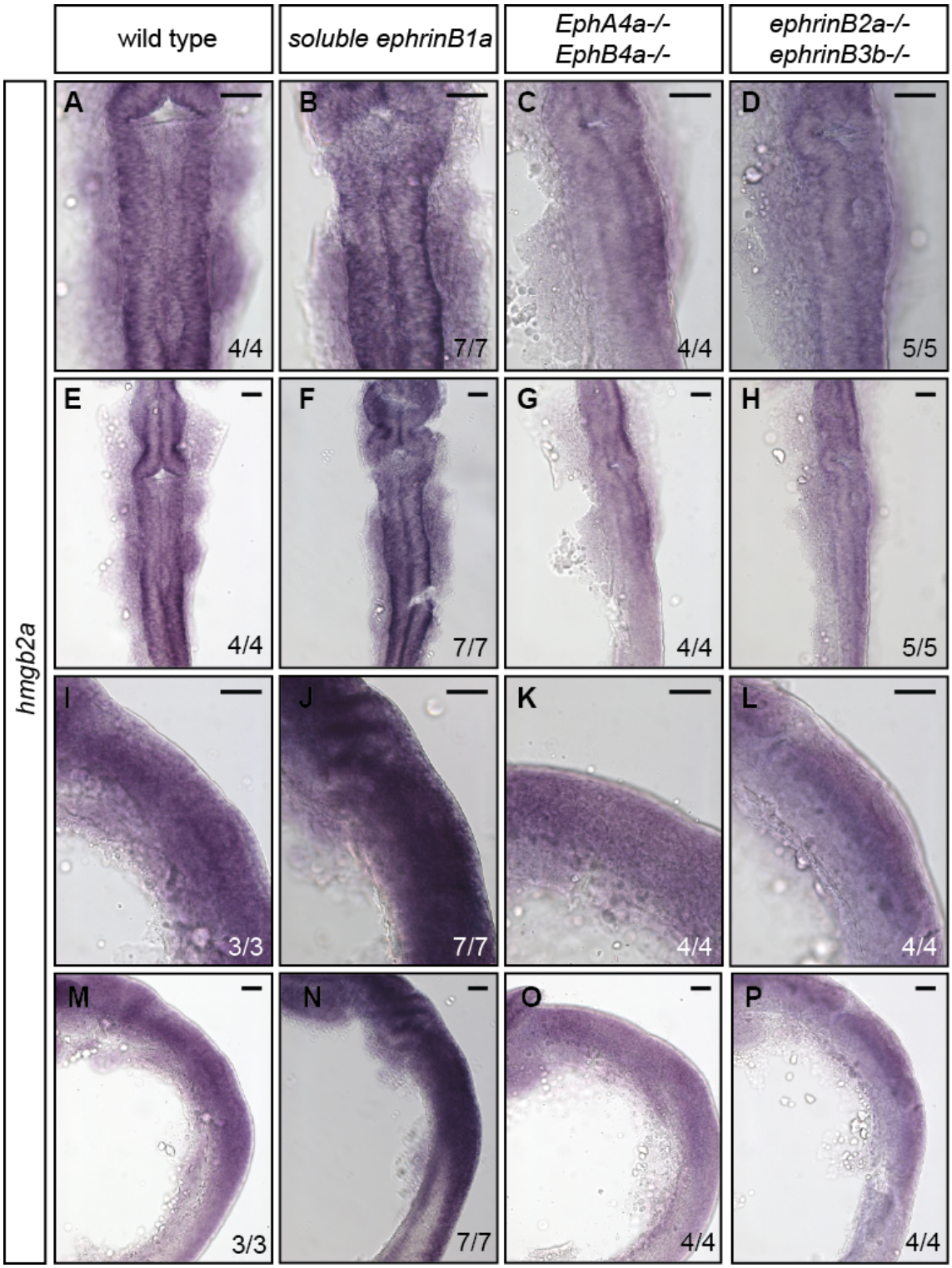

Figure 30 *hmgb2a* expression at 20 ss when Eph-ephrin signalling is blocked

Embryos at 20 ss / 19 hpf after *in situ* hybridisation for *hmgb2a*. (A-H) Flat mount view and (I-P) and a side mount view with A-D and I-L at a higher magnification than E-H and M-P. A-D and E-H show the same embryo in each column at a different magnification, as well as I-L and M-P. Scale bar represents 100 µm.

In wild type embryos *nap1l1* expression is higher in specific regions of the hindbrain (black arrowheads, Figure 31: A, E, I, M), and has a region of lower expression (white arrowheads, Figure 31: A, E, I, M). The expression pattern of *nap1l1* changes when Eph-ephrin signalling is disrupted. When Eph-ephrin signalling is blocked with soluble ephrinB1a the expression of *nap1l1* is uniform (Figure 31: B, F, J, N). This is observed in 62% of embryos, those likely to be the ones over-expressing soluble ephrinB1a. There is also uniform *nap1l1* expression in the Eph receptor double homozygous mutants (Figure 31: C, G, K, O), as well as in the ephrin double mutants (Figure 31: D, H, L, P).

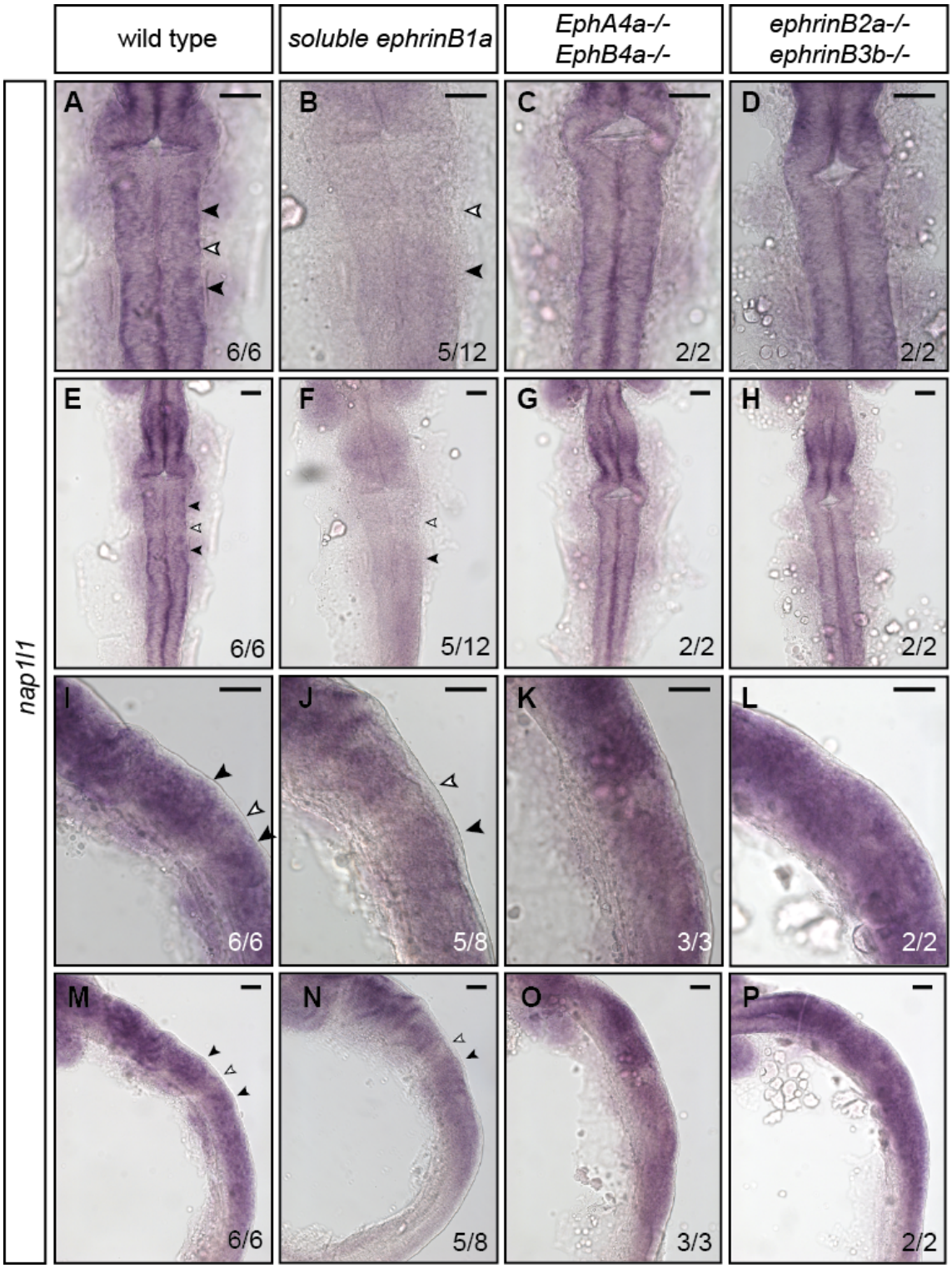

Figure 31 *nap1l1* expression at 20 ss when Eph-ephrin signalling is blocked

Embryos at 20 ss / 19 hpf after *in situ* hybridisation for *nap1l1*. (A-H) Flat mount view and (I-P) and a side mount view with A-D and I-L at a higher magnification than E-H and M-P. A-D and E-H show the same embryo in each column at a different magnification, as well as I-L and M-P. Arrowheads indicate regions of higher *nap1l1* expression. Scale bar represents 100 µm.

In wild type embryos, *mdka* expression is localised and segmented (arrowheads, Figure 32: A, E, I, M). In the Eph receptor double mutants, *mdka* expression is more uniform than in wild type embryos but there is higher expression in certain segments (arrowheads, Figure 32: K, O). When Eph-ephrin signalling is blocked globally with soluble ephrinB1a, 43% of embryos have uniform *mdka* expression throughout the hindbrain (Figure 32: B, F, J, N). The expression of *mdka* in ephrin double mutants is similar to the double Eph receptor mutants, with more uniform expression than in wild type embryos but higher expression in certain segments (arrowheads, Figure 32: L, P).

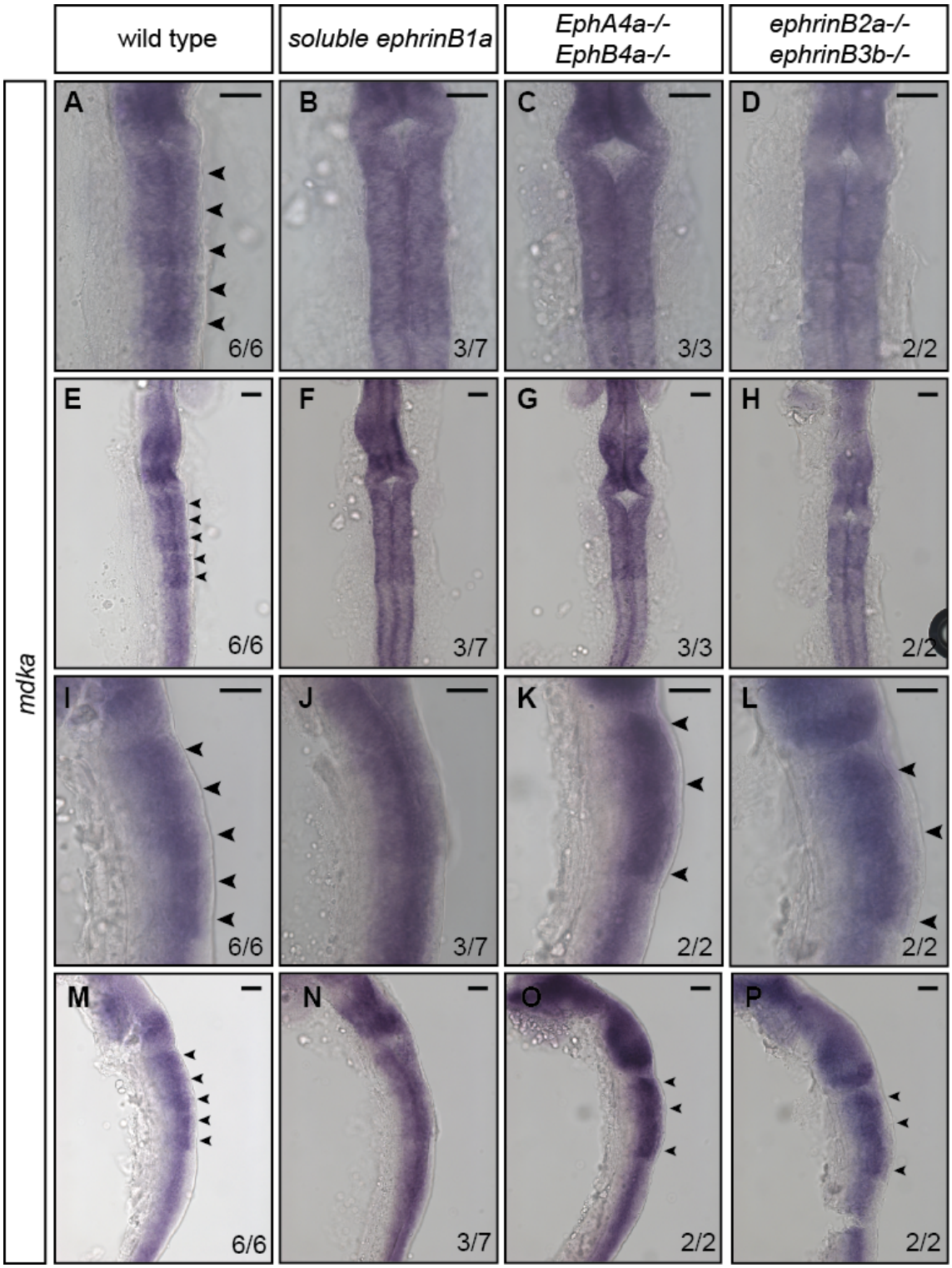

Figure 32 *mdka* expression at 20 ss when Eph-ephrin signalling is blocked

Embryos at 20 ss / 19 hpf after *in situ* hybridisation for mdka. (A-H) Flat mount view and (I-P) and a side mount view with A-D and I-L at a higher magnification than E-H and M-P. A-D and E-H show the same embryo in each column at a different magnification, as well as I-L and M-P. Arrowheads indicate regions of higher *mdka* expression. Scale bar represents 100 µm.

5.4 Expression of target genes in the tail

In situ hybridisation analysis revealed that when Eph-ephrin signalling was disrupted, *nap1l1* and *mdka* had altered expression patterns, whereas changes in expression could not be detected by this technique for *tubb2b* and *hmgb2a*, which had uniform expression in the hindbrain. The four genes selected have been previously implicated in neuronal differentiation and cell proliferation and thus these markers may reflect the pattern of progenitors and neurogenesis. It is known that hindbrain boundary cells have lower neurogenesis than non-boundary regions (Cheng et al., 2004). There were differences observed for some of these genes by whole embryo RT-qPCR and hindbrain RNA-sequencing, which could be the result of Eph-ephrin signalling regulating the progression of neurogenesis. The stage of neurogenesis differs along the A-P axis, with the anterior being earlier than the posterior. Therefore, when observing changes in gene expression in the whole embryo the effects may be different to the hindbrain because it includes tissues that are at different stages of neurogenesis. In addition, this may also be a result of Eph-ephrin signalling regulating the progression of neurogenesis throughout the embryo. In order to test this hypothesis, the expression of the four candidate genes was investigated in the tail as this is at an earlier stage than the hindbrain. At the caudal end of the tail, neural epithelial cells are being generated, as these progress to a more mature stage and undergo neurogenesis. The stage used was 19 hpf, the stage at which RNA-sequencing and RT-qPCR validation was carried out.

The expression of *tubb2b*, *hmgb2a*, *nap1l1* and *mdka* were analysed in tails of embryos where Eph-ephrin signalling had been disrupted (Figure 33). For these genes, the wild type expression patterns were not consistent with them marking the transition in cell differentiation in the tail as they do not have a gradient of expression along the A-P axis or a domain of expression where neural progenitors are situated in the tail (Figure 33: A, F, K, P). These data argue against the hypothesis of Eph-ephrin signalling regulating the progression of neurogenesis throughout the embryo. In addition, no major changes in expression were observed when Eph-ephrin signalling was disrupted (Figure 33: B-E, G-J, L-O, Q-T).

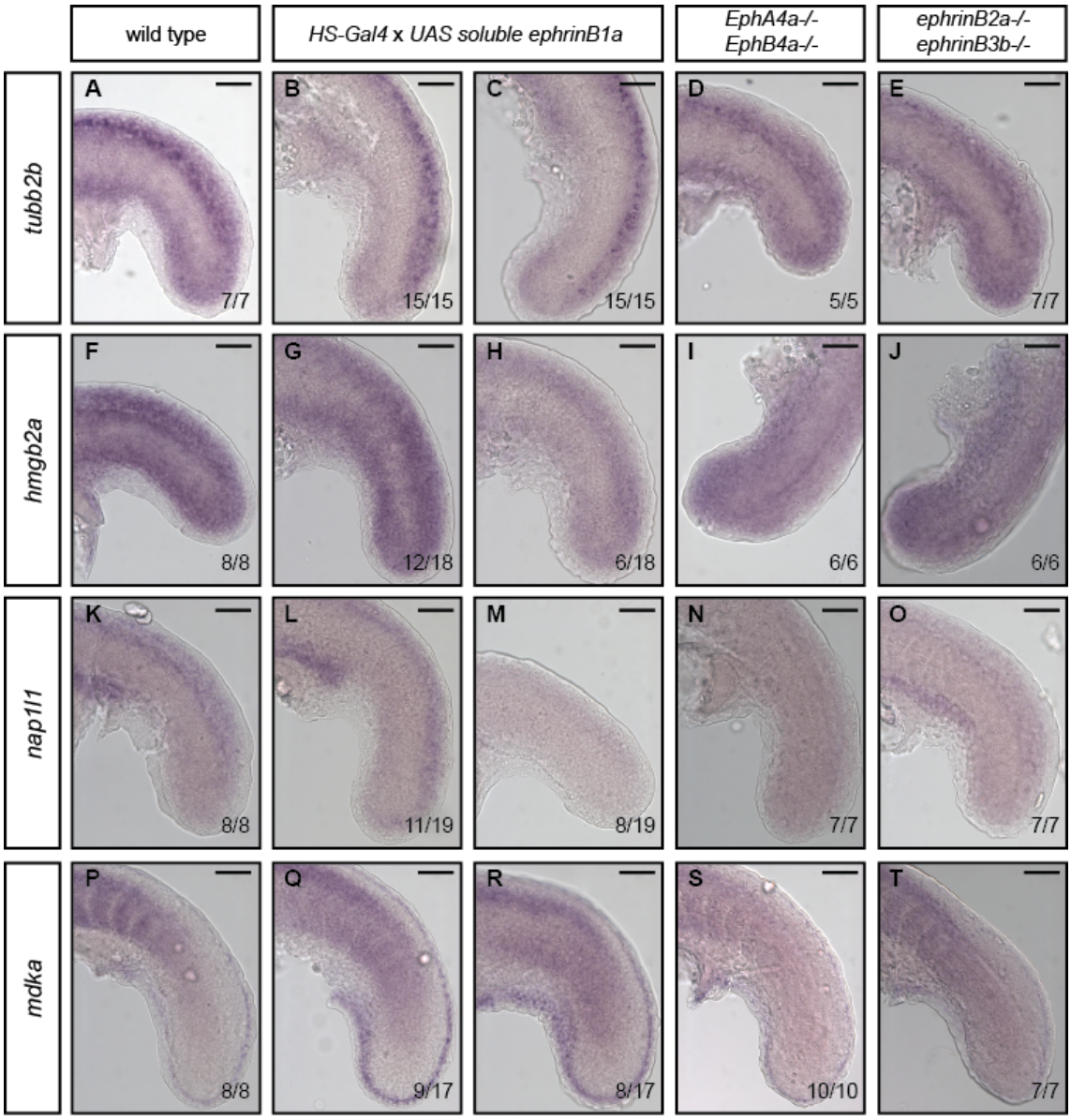

Figure 33 Expression of candidate genes in the tail

(A-T) Embryos at 19 hpf after *in situ* hybridisation for *tubb2b* (A-E), *hmgb2a* (F-J), *nap1l1* (K-O) and *mdka* (P-T). Values indicate the number of embryos with the phenotype. Scale bar represents 100 µm.

5.5 Discussion

In this chapter, candidate transcriptional targets of Eph-ephrin signalling that had been identified by RNA-sequencing were validated using a two-step approach of RT-qPCR and *in situ* hybridisation. The genes chosen for validation were selected by ranking the RNA-sequencing data in four different ways: the most significantly differentially expressed genes, genes with the highest fold change, genes with the

most correlated expression to *ephrinB1a* and genes with the highest number of reads. Individual whole embryos were used in order to screen through multiple potential candidate genes rather than single genes and to eliminate any bias resulting from hindbrain dissection. The outcomes of this validation were interpreted with caution as this was carried out in whole embryos and blocking Eph-ephrin signalling in other regions of the embryo may mask the effects in the hindbrain. For this reason, when genes were selected, the known functions were considered in order to identify the genes that are regulated downstream of Eph-ephrin signalling and potentially involved in hindbrain development.

The four genes selected for further investigation were *tubb2b*, *hmgb2a*, *nap1l1* and *mdka*. These genes have been implicated in neural progenitor maintenance and neural differentiation and are likely markers of the state of neurogenesis. Firstly, the changes in expression were quantified by RT-qPCR in double Eph receptor mutant and double ephrin mutants, which showed that there were opposing changes in gene expression for some of the genes in the two mutants in comparison to wild type embryos. This will reflect where the Eph receptor or ephrins are expressed and signal. Some of the Eph receptors and ephrins are likely to have roles elsewhere in the embryo and bind other partners. The alteration in expression of these genes elsewhere in the embryo will depend on these factors.

There were also differences observed between the changes in gene expression in whole embryos detected by RT-qPCR and hindbrains detected by RNA-sequencing. The expression of *hmgb2a* and *nap1l1* did not alter in whole embryos, but expression increased in the hindbrain when Eph-ephrin signalling was blocked. *mdka* expression decreased in whole embryos but increased in the hindbrain, and *tubb2b* expression increased in both samples but was greater in the hindbrain.

It was hypothesised that the findings may be the result of Eph-ephrin signalling regulating the progression of neurogenesis, based on the candidate genes being markers of neurogenesis. Identifying the expression patterns of these genes in the tail argued against this hypothesis as the expression patterns did not suggest a correlation with neural differentiation. However, this does not rule out the possibility that these genes may be expressed in other tissues and their expression is affected

there when Eph-ephrin signalling is blocked. As the main aim of this project is to identify transcriptional targets in the hindbrain, it was beyond the scope of this study to investigate this further.

I*n situ* hybridisation revealed that the expression patterns of *tubb2b* and *hmgb2a* were uniform along the A-P axis of the hindbrain, whereas *nap1l1* and *hmgb2a* had localised expression. Unfortunately, this technique is not sensitive enough to detect subtle alterations in broad expression, and as a result changes to *tubb2b* and *hmgb2a* expression were not observed. However, the localised expression of *nap1l1* and *mdka* altered when Eph-ephrin signalling was disrupted, and the expression patterns of these two genes became uniform along the A-P axis of the hindbrain. This is similar to what has been observed previously, when boundary cell formation is inhibited leading to a disruption in neuronal patterning in the hindbrain. The consequence is an increase in the number of differentiating neurons (Terriente et al., 2012). It is known that the boundary cells are absent when Eph-ephrin signalling is blocked by soluble ephirnB1a and that *nap1l1* and *mdka* are markers of neurogenesis. Therefore, these data suggest that Eph-ehprin signalling may be altering gene expression indirectly via the loss of the boundary cells. This is supported by the phenotypes observed in double Eph receptor or ephrin mutants, where there is a specific loss of boundaries. The regions of the hindbrain where expression becomes more uniform corresponds to where Eph-ephrin signalling had been disrupted and the hindbrain boundaries are lost. These data argue that Eph-ephrin signalling may be disrupting the expression of neurogenic markers via the loss of hindbrain boundary cells.

5.6 Conclusion

In summary, candidate genes of Eph-ephrin signalling identified by RNA-sequencing were validated by RT-qPCR and subsequent *in situ* hybridisation. This shortlisted four genes to identify their expression patterns when Eph-ephrin signalling was blocked via different methods. The genes selected were: *tubb2b* and *mdka*, markers of neural differentiation, and *hmgb2a* and *nap1l1*, markers of progenitor cells. *nap1l1* and *mdka* have localised expression patterns in the hindbrain which alter when

Eph-ephrin signalling is disrupted. These data suggest that Eph-ephrin signalling may play a role in the balance between progenitor cell maintenance and neural cell differentiation in the hindbrain. However, because little is known about these candidate genes in the context of hindbrain development it is difficult to decipher the sequence of events, as well as how these proteins are interacting to control neurogenesis. Therefore, in order to investigate the regulation of Eph-ephrin signalling on neuronal progenitor maintenance and neuronal cell differentiation in the hindbrain, known molecular markers of neurogenesis will be used. This will be investigated by *in situ* hybridisation and changes in gene expression will be identified in embryos where Eph-ephrin signalling has been disrupted by soluble ephrinB1a or in Eph receptor and ephrin mutants in comparison to wild type embryos.

Chapter 6. Investigating the role of Eph-ephrin signalling during neurogenesis in the hindbrain

6.1 Introduction

In the previous chapter, four genes *tubb2b*, *hmgb2a*, *nap1l1* and *mdka*, were found to be regulated downstream of Eph-ephrin signalling in the hindbrain. These genes have roles in cell differentiation and proliferation, in particular in neuronal cell types. In order to explore the hypothesis that Eph-ephrin signalling may be controlling the balance between neuronal progenitors and neurogenesis, expression of neurogenic markers was investigated. Eph receptor and ephrin double mutants, and over-expression of soluble ephrinB1a were used to disrupt Eph-ephrin signalling in attempt to elucidate if and how signalling regulates neurogenesis.

6.2 Wild type expression of neural markers

The following genes were chosen to explore the potential effects of Eph-ephrin signalling on neurogenesis: *nestin*, *deltaD*, *neurogenin1* (*neurog1*), *neuroD4* and *huC/D (*Figure 34*)*. *nestin* is expressed in neural progenitor cells and is broadly expressed in the zebrafish central nervous system at 24 hpf and is down-regulated as the neural precursors undergo differentiation (Dahlstrand et al., 1995; Yamaguchi et al., 2000; Wiese et al., 2004; Mahler and Driever, 2007). *deltaD* is a marker of neurogenesis and is expressed in neurogenic clusters that are undergoing neuronal differentiation. *deltaD* is important for lateral inhibition to prevent neurogenesis in neighbouring cells and when its function is blocked neurons arise in excess. This gene is expressed in the hindbrain, other regions of the brain, the presomitic mesoderm and in the posterior region of newly formed somites (Haddon et al., 1998). Another early marker of neurogenesis is *neurog1*, which is a bHLH transcription factor and is expressed in cells undergoing neuronal differentiation. It is expressed in Type B proneural clusters, from which the primary neuronal network will be established (Gradwohl et al., 1996; Ma et al., 1996). Proneural genes, such as *neurog1*, up-regulate the expression of Notch ligands, which then activate Notch receptor in adjacent cells leading to the inhibition of proneural gene expression

(Blader et al., 1997). An additional marker of neuronal differentiation is *neuroD4*, which is expressed downstream of proneural genes in post-mitotic neurons that migrate from the neurogenic zones to the mantle layer (Lee et al., 1995; Gonzalez-Quevedo et al., 2010; Wang et al., 2003). *huC/D* is a marker of late neurogenesis as it is expressed in post-mitotic neurons in the mantle zone of the neural epithelium, which have already undergone neuronal differentiation (Marusich et al., 1994). It promotes neuronal differentiation by stabilising neuronal transcripts (Kim et al., 1996; Antic et al., 1999). *huC/D* is expressed in neurons in the mantle zone that occupy the spaces between radial glial fibres (Trevarrow et al., 1990; Terriente et al., 2012).

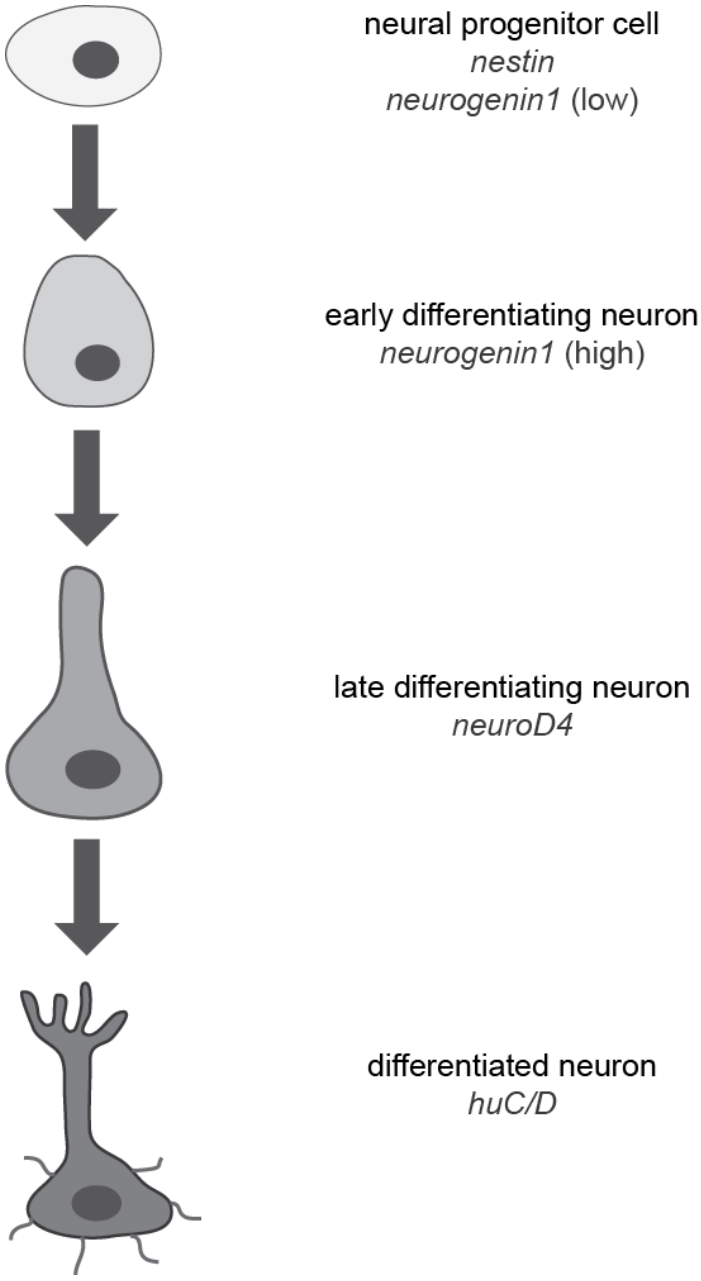

Figure 34 Markers of neurogenesis

Schematic showing the stages of neural differentiation from neural progenitor cell through to differentiated neuron and the gene expression associated with the respective stage in development.

The expression patterns of the five markers of neurogenesis were first determined in wild type embryos. The stages chosen were 24 hpf and 30 hpf. It has been previously shown that at 20 hpf, neurogenesis is widespread and there are small differences in expression across the hindbrain. This then becomes restricted to neurogenic zones that are adjacent to the hindbrain boundaries by 36 hpf (Cheng et al., 2004; Amoyel et al., 2005; Gonzalez-Quevedo et al., 2010). The neurogenic zones are flanked by

non-neurogenic zones in which these markers are absent (Cheng et al., 2004). This is regulated by FGF20a-expressing neurons which are found in the segment centres in the mantle zone and inhibit neurogenesis in the centre of rhombomeres in the adjacent neural epithelium (Gonzalez-Quevedo et al., 2010; Terriente et al., 2012). Notch activation inhibits neurogenesis at hindbrain boundaries (Cheng et al., 2004). Therefore, these time points enable neurogenesis to be observed as it becomes increasingly restricted.

nestin is expressed laterally in segment centres in the hindbrain at 24 hpf and excluded from the boundary cells (Figure 35: A, F), and at 30 hpf expression occurs throughout the hindbrain and up-regulated in the neurogenic zones (Figure 35: K, P). *deltaD* and *neurog1* expression is widespread at 24 hpf (Figure 35: B, G, C, H) and their expression becomes restricted to the neurogenic zones adjacent to the boundaries at 30 hpf (Figure 35: B, G, C, H), as shown previously (Gonzalez-Quevedo et al., 2010). *neuroD4* is expressed in lateral regions of the hindbrain and is widespread along the A-P axis at 24 hpf (Figure 35: D, I), and expression is restricted to the regions adjacent to the boundaries at 30 hpf (Figure 35: N, S). Finally, *huC/D* expression is lateral and segmented at 24 hpf (Figure 35: E, J), and becomes more widespread at 30 hpf but is excluded from the regions underlying the hindbrain boundaries (Figure 35: O, T), as observed previously (Gonzalez-Quevedo et al., 2010; Terriente et al., 2012).

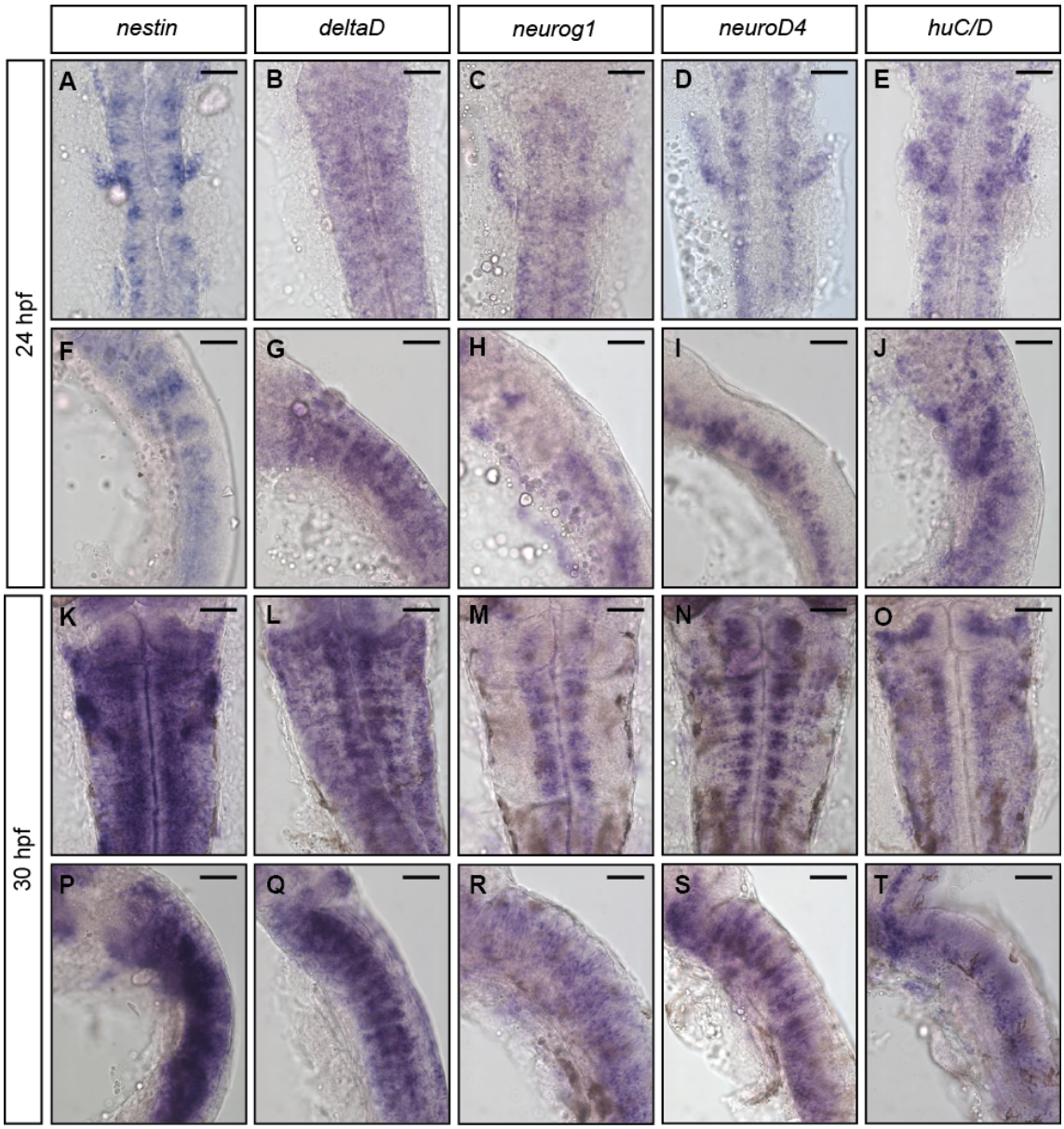

Figure 35 Expression of neuronal markers in wild type embryos

(A-T) Embryos after *in situ* hybridisation for markers of neurogenesis. A-J are at 24 hpf and K-T are at 30 hpf, in flat mount (A-E, P-T) and side mount (F-J, P-T). Scale bar represents 100 µm.

6.3 Expression of neuronal markers when Eph-ephrin signalling is blocked

Once the expression patterns of the neurogenic markers had been identified in wild type embryos (Figure 35), they were observed in embryos where Eph-ephrin signalling had been blocked. In previous experiments, soluble ephrinB1a had been over-expressed by heat shock at bud and 15 hpf / 12 ss, to block Eph-ephrin

signalling from the onset in the hindbrain. In the experiments to follow, soluble ephrinB1a expression was induced at 18 hpf / 18 ss in attempt to separate Eph-ephrin signalling from the role in boundary cell formation to observe more direct effects of blocking signalling. Previous experiments in optimising the conditions for blocking Eph-ephrin signalling to completely remove all hindbrain boundaries found that inducing soluble ephrinB1a expression at 15 hpf / 12 ss did not prevent boundary cell formation (Chapter 3.4.1). For these experiments, expression will be induced at 19 hpf / 20 ss with the intention that the boundaries may not be disrupted. In these experiments, around 50% of embryos will express soluble ephirnB1a because of the inheritance of the *HS-Gal4* and *UAS-soluble ephrinB1a* transgenes. From this analysis, the numbers quoted for a given phenotype will refer to changes in expression patterns observed in side mounted embryos.

6.3.1 The effect on hindbrain boundary cells when disrupting Eph-ephrin signalling at 18 hpf

Firstly, the experiment described above was carried out and embryos were collected at 24 hpf before *rfng* expression was analysed by *in situ* hybridisation to determine the effect on hindbrain boundary cells. This showed that from the experimental cross when Eph-ephrin signalling is blocked at 19 hpf there is a decrease in *rfng* expression at the boundaries in 59% of embryos (Figure 36: E). The remaining 41% of embryos from the experimental cross have the same expression as control embryos (Figure 36: D). This shows that blocking Eph-ephrin signalling at this stage leads to partial disruption of boundary cell formation.

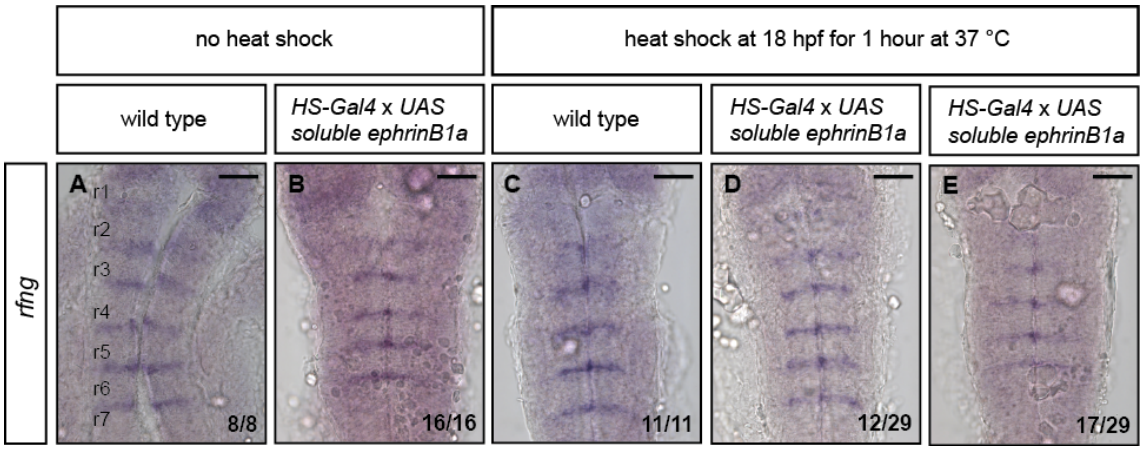

Figure 36 *rfng* expression after blocking Eph-ephrin signalling at 18 hpf

(A-E) Embryos at 24 hpf after *in situ* hybridisation for *rfng* to mark the hindbrain boundary cells. A-C are control embryos, D and E are two different phenotypes from the *HS-Gal4* x *UAS-soluble ephrinB1a* cross. The scale bar represents 50 μm.

6.3.2 *nestin* expression when Eph-ephrin signalling is blocked

At 24 hpf, there is a striking difference in *nestin* expression between the control embryos (Figure 37: A, B) and 56% of embryos of the experimental condition (Figure 37: D, F), which are likely to be the embryos where Eph-ephrin signalling is blocked. When Eph-ephrin signalling is blocked there is more uniform expression of *nestin* along the A-P axis of the hindbrain, showing that there is a more widespread distribution of neural progenitor cells (Figure 37: D, F), in comparison to control embryos (Figure 37: A, B).

There are also changes in the expression pattern of *nestin* in some embryos of the experimental condition at 30 hpf. Control embryos have widespread *nestin* expression in the hindbrain with higher expression in clusters of cells more medial than at 24 hpf (Figure 37: G, H). In the experimental condition, 25% of embryos have more uniform and much weaker *nestin* expression (Figure 37: J, L) than in the control embryos. In the remaining 75% of embryos in the experimental condition, the expression of *nestin* is slightly weaker than in controls, but the expression patterns are the same as control embryos (Figure 37: I, K). These data show that the distribution of neural progenitors is altered at 24 hpf with progenitor cells being present in regions where the boundaries would normally reside. At 30 hpf there are fewer neural progenitors.

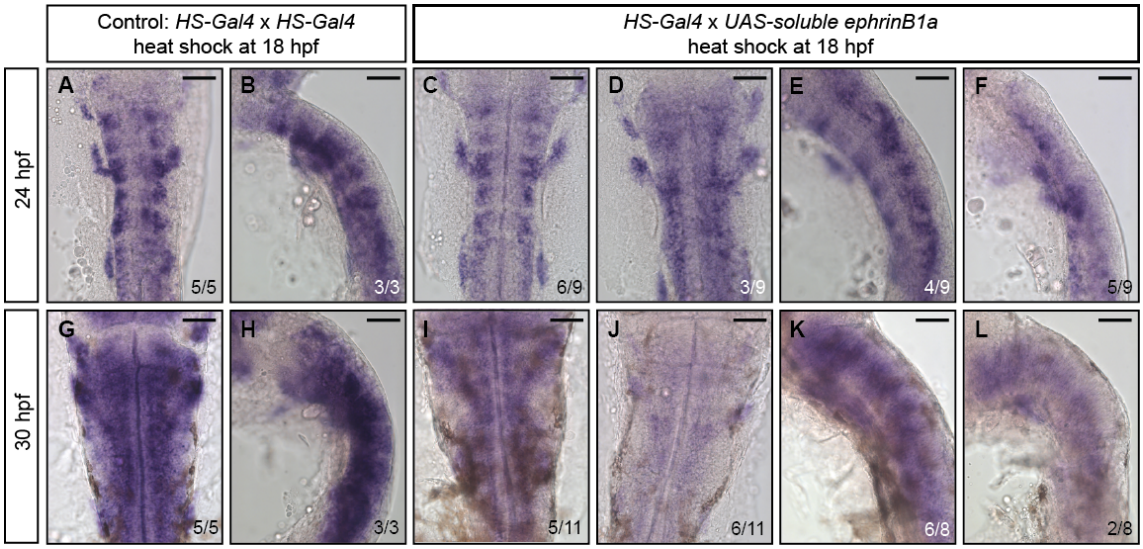

Figure 37 *nestin* expression when Eph-ephrin signalling is blocked

(A-L) Embryos after *in situ* hybridisation to show *nestin* expression. A-J are at 24 hpf and K-T are at 30 hpf, in flat mount (A, C, D, G, I, J) and side mount (F-J, P-T). Control embryos (A-B, G-H) are derived from an in-cross of the transgenic line *HS-Gal4* and the experimental samples (C-F, I-L) are derived from a cross of two transgenic lines: *HS-Gal4* x *UAS-soluble ephrinB1a*, with around 50% of embryos inheriting both transgenes. All embryos have been heat shocked at 18 hpf for 1 hour at 38 °C. Scale bar represents 100 µm.

6.3.3 *deltaD* expression when Eph-ephrin signalling is blocked

The early marker of neurogenesis, *deltaD*, showed a subtle change in expression when Eph-ephrin signalling is blocked. At 24 hpf, control embryos have broad expression in the hindbrain with regions of higher expression (Figure 38: A, B). In embryos from the experimental condition, 56% had the same expression pattern as the control embryos (Figure 38: C, E) and 44% show a more uniform expression pattern (Figure 38: D, F).

At 30 hpf, the difference between embryos is clearer, as there is organisation of neurogenic and non-neurogenic zones in control embryos at this stage (Figure 38: G, H). In contrast, 40% of embryos from the experimental condition have more uniform *deltaD* expression that is weaker than in the controls and the non-neurogenic zones can no longer been seen (Figure 38: K, L).

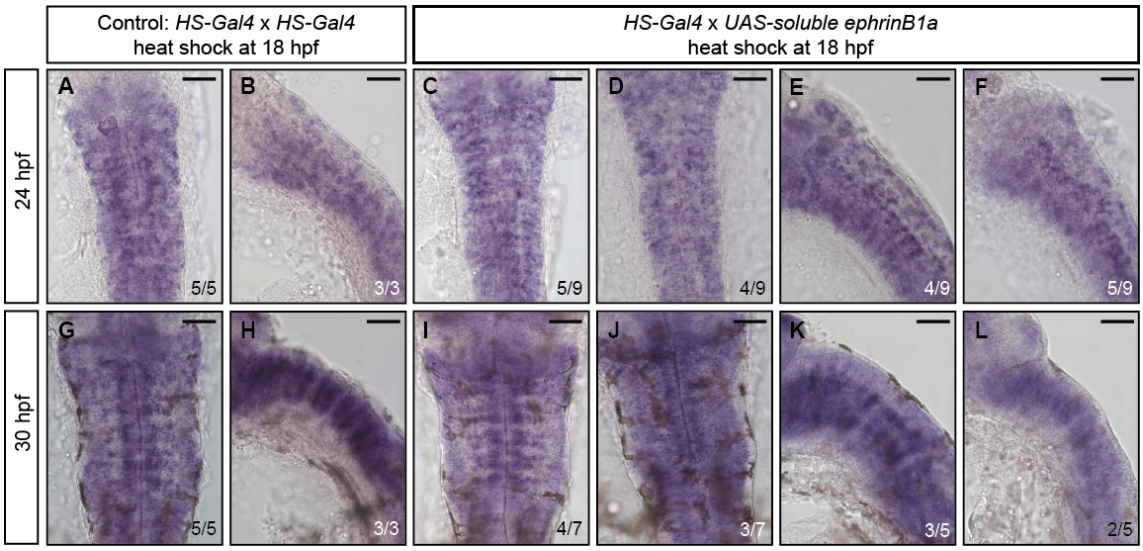

Figure 38 *deltaD* expression when Eph-ephrin signalling is blocked

(A-L) Embryos after *in situ* hybridisation to show *deltaD* expression. A-J are at 24 hpf and K-T are at 30 hpf, in flat mount (A, C, D, G, I, J) and side mount (F-J, P-T). Control embryos (A-B, G-H) are derived from an in-cross of the transgenic line *HS-Gal4* and the experimental samples (C-F, I-L) are derived from a cross of two transgenic lines: *HS-Gal4* x *UAS-soluble ephrinB1a*, with around 50% of embryos inheriting both transgenes. All embryos have been heat shocked at 18 hpf for 1 hour at 38 °C. Scale bar represents 100 μm.

6.3.4 *neurog1* expression when Eph-ephrin signalling is blocked

The second gene investigated to determine the effects Eph-ephrin signalling has on differentiating neurons is *neurog1*. The changes in expression are easier to see at 30 hpf, although there is a mild phenotype at 24 hpf. Control embryos express neurog1 throughout the hindbrain at 24 hpf, with higher expression in stripes adjacent to the boundaries (Figure 39: A, B). In the experimental condition 56% of embryos have more continuous *neurog1* expression along the A-P axis compared to control embryos (Figure 39: D, F). The remaining 44% have similar expression to control embryos (Figure 39: C, E).

Analysis at 30 hpf shows clearer changes to *neurog1* expression that are similar to those seen at 24 hpf. In the experimental condition, 43% of embryos have continuous *neurog1* expression along the A-P axis with no separation between neurogenic and non-neurogenic zones (Figure 39: J, L). The remaining 57% of embryos show striped *neurog1* expression in neurogenic zones, the same as controls (Figure 39: G, H).

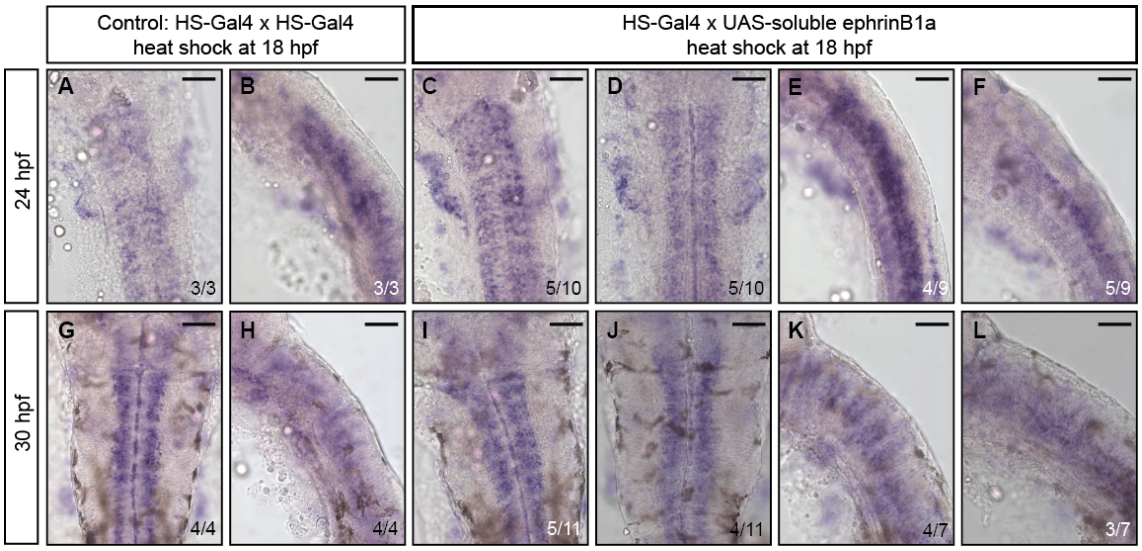

Figure 39 *neurog1* expression when Eph-ephrin signalling is blocked

(A-L) Embryos after *in situ* hybridisation to show *neurog1* expression. A-J are at 24 hpf and K-T are at 30 hpf, in flat mount (A, C, D, G, I, J) and side mount (F-J, P-T). Control embryos (A-B, G-H) are derived from an in-cross of the transgenic line HS-Gal4 and the experimental samples (C-F, I-L) are derived from a cross of two transgenic lines: *HS-Gal4* x *UAS-soluble ephrinB1a*, with around 50% of embryos inheriting both transgenes. All embryos have been heat shocked at 18 hpf for 1 hour at 38 °C. Scale bar represents 100 μm.

6.3.5 *neuroD4* expression when Eph-ephrin signalling is blocked

neuroD4 is a late marker of differentiating neurons and its expression too was found to alter when Eph-ephrin signalling was blocked. At 24 hpf, control embryos express *neuroD4* in lateral clusters in the hindbrain, although at this stage the regions of expression are not clearly defined (Figure 40: A, B). *neuroD4* expression has subtle differences in 60% of embryos in the experimental condition, which have more continuous expression (Figure 40: D, F). The remaining 40% of embryos from the experimental condition have similar expression to control embryos (Figure 40: C, E).

At 30 hpf, defined regions of *neuroD4* expression are seen in control embryos (Figure 40: G, H), which are absent in 43% of embryos from the experimental condition that have more continuous and weaker expression (Figure 40: J, L). The remaining 57% of embryos have the same expression as control embryos (Figure 40: I, K). These data show that the localisation of differentiating neurons is disrupted when Eph-ephrin signalling is blocked, and that there is ectopic expression in the hindbrain.

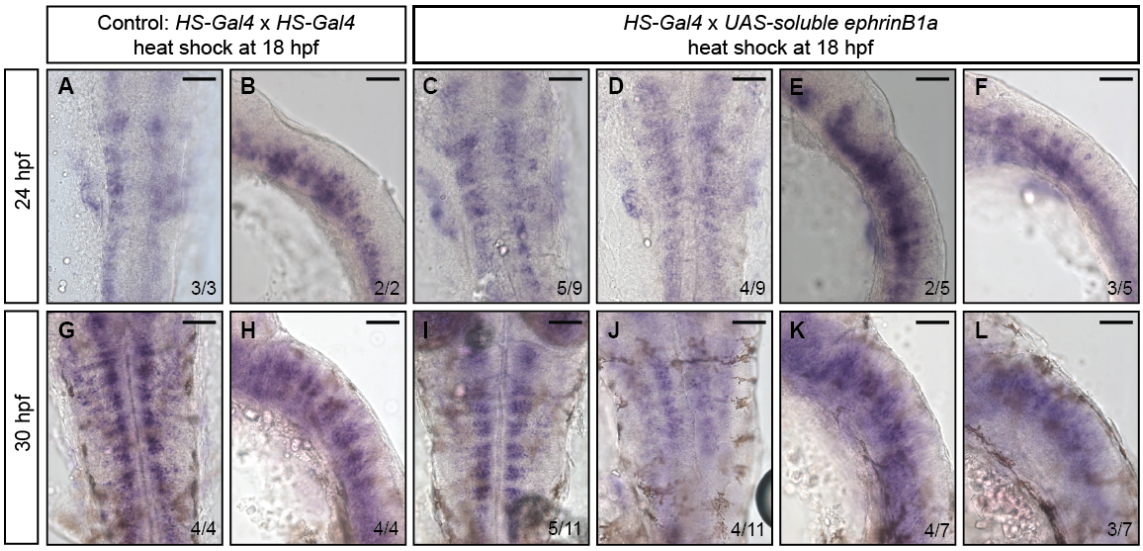

Figure 40 *neuroD4* expression when Eph-ephrin signalling is blocked

(A-L) Embryos after *in situ* hybridisation to show *neuroD4* expression. A-J are at 24 hpf and K-T are at 30 hpf, in flat mount (A, C, D, G, I, J) and side mount (F-J, P-T). Control embryos (A-B, G-H) are derived from an in-cross of the transgenic line *HS-Gal4* and the experimental samples (C-F, I-L) are derived from a cross of two transgenic lines: *HS-Gal4* x *UAS-soluble ephrinB1a*, with around 50% of embryos inheriting both transgenes. All embryos have been heat shocked at 18 hpf for 1 hour at 38 °C. Scale bar represents 100 µm.

6.3.6 *huC/D* expression when Eph-ephrin signalling is blocked

The final marker of neurogenesis investigated is *huC/D*, a marker of differentiated neurons. Similar to the previous neuronal markers investigated, the phenotype is subtle at 24 hpf with more obvious differences at 30 hpf. Control embryos have segmented expression of *huC/D*, marking the differentiated neurons in the mantle zone (Figure 41: A, B). *huC/D* expression is more continuous in 56% of embryos from the experimental condition (Figure 41: D, F). The remaining 44% of embryos have similar expression to the control embryos (Figure 41: C, E).

huC/D expression is more widespread at 30 hpf in control embryos (Figure 41: G, H), as more neurons have differentiated. In 56% of embryos from the experimental condition *huC/D* expression is weaker and more continuous (Figure 41: J, L). The remaining embryos have similar expression to control embryos (Figure 41: I, K). These data show that there is ectopic neurogenesis at 24 hpf and a depletion of neurons at 30 hpf.

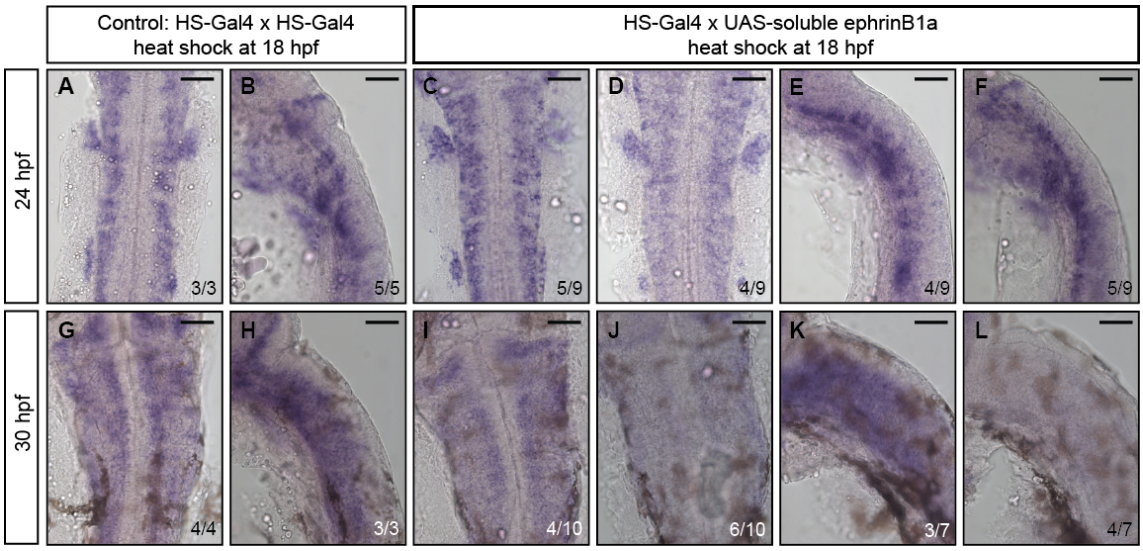

Figure 41 *huC/D* expression when Eph-ephrin signalling is blocked

(A-L) Embryos after *in situ* hybridisation to show *huC/D* expression. A-J are at 24 hpf and K-T are at 30 hpf, in flat mount (A, C, D, G, I, J) and side mount (F-J, P-T). Control embryos (A-B, G-H) are derived from an in-cross of the transgenic line *HS-Gal4* and the experimental samples (C-F, I-L) are derived from a cross of two transgenic lines: *HS-Gal4* x *UAS-soluble ephrinB1a*, with around 50% of embryos inheriting both transgenes. All embryos have been heat shocked at 18 hpf for 1 hour at 38 °C. Scale bar represents 100 µm.

6.4 Expression of neuronal markers in Eph receptor and ephrin mutants

Blocking Eph-ephrin signalling with soluble ephrinB1a showed that the impact on neurogenesis was greater at 30 hpf than 24 hpf, likely due to this being a cumulative effect. To further understand the effects of Eph-ephrin signalling on neurogenesis, expression of the neurogenic markers was observed in Eph receptor and ephrin double mutants at 30 hpf. In the double Eph receptor or ephrin mutants, the hindbrain boundaries are disrupted earlier and only at the boundaries of r2/r3, r3/r4 and r6/r7, whereas with soluble ephrinB1a expression Eph ephrin signalling is blocked later, at 18 hpf, which results in disruption to the boundaries and weaker boundary cell marker expression at 24 hpf.

Firstly, *nestin* expression is uniform along the A-P axis in wild type embryos with regions of segmented higher expression (Figure 42: Ai, Aii). *nestin* is more continuous along the A-P axis in double Eph receptor mutants (Figure 42: Fi, Fii) and double ephrin mutants (Figure 42: Ki, Kii).

deltaD is expressed in stripes along the A-P axis of the hindbrain in wild type embryos, marking the neurogenic zones (arrowheads indicate non-neurogenic zones, Figure 42: Bi, Bii). In double Eph receptor mutants, *deltaD* expression is more continuous along the A-P axis, although there is higher expression in the neurogenic zones (Figure 42: Gi, Gii). In the double ephrin mutants *deltaD* expression is more continuous and the neurogenic and non-neurogenic zones are no longer visible (Figure 42: Li, Lii).

The second marker of differentiating neurons, *neurog1*, is expressed in stripes along the anterior posterior axis, marking the neurogenic zones (arrowheads indicate non-neurogenic zones, Figure 42: Ci, Cii). In the double Eph receptor mutants, *neurog1* expression is more continuous, showing that the non-neurogenic zones are absent (Figure 42: Hi, Hii), which is also observed for the double ephrin mutants (Figure 42: Mi, Mii). Interestingly, in double ephrin mutants there is a gap in the A-P expression of neurog1 (arrowheads, Figure 42: Gi). This could coincide with the r4/r5 boundary at which Eph-ephrin signalling persists (Chapter 3: Figure 10), and may explain why this non-neurogenic zone is still present. However, it would be expected that this phenotype would be the same in the double Eph receptor mutants because they both have the same boundary loss phenotype.

The marker of late neural differentiation, *neuroD4*, is expressed in stripes and is absent in regions that correspond to the hindbrain boundaries and the segment centres (black arrowheads and white arrowheads, respectively, Figure 42: Di, Dii). In the double Eph receptor mutants, *neuroD4* expression is more continuous and weaker in the hindbrain (Figure 42: Ii, Iii), which is also observed in the double ephrin mutants (Figure 42: Ni, Nii).

In wild type embryos, *huC/D* expression is widespread with up-regulated expression in stripes along the A-P axis (Figure 42: Ei, Eii). In double Eph receptor mutants *huC/D*, expression is more continuous and weaker than in wild type embryos (Figure 42: Ji, Jii), and this is also observed in double ephrin mutant embryos (Figure 42: Oi, Oii). This is a surprising observation as there is no evidence to suggest that *huC/D* expression is down-regulated in post-mitotic neurons and should mark the

accumulation of neurons. Previous work has shown that transcripts can still be detected by *in situ* hybridisation at 5 days post fertilisation (Cox et al., 2016). In order to investigate this further, HuC/D protein was detected by immunofluorescence.

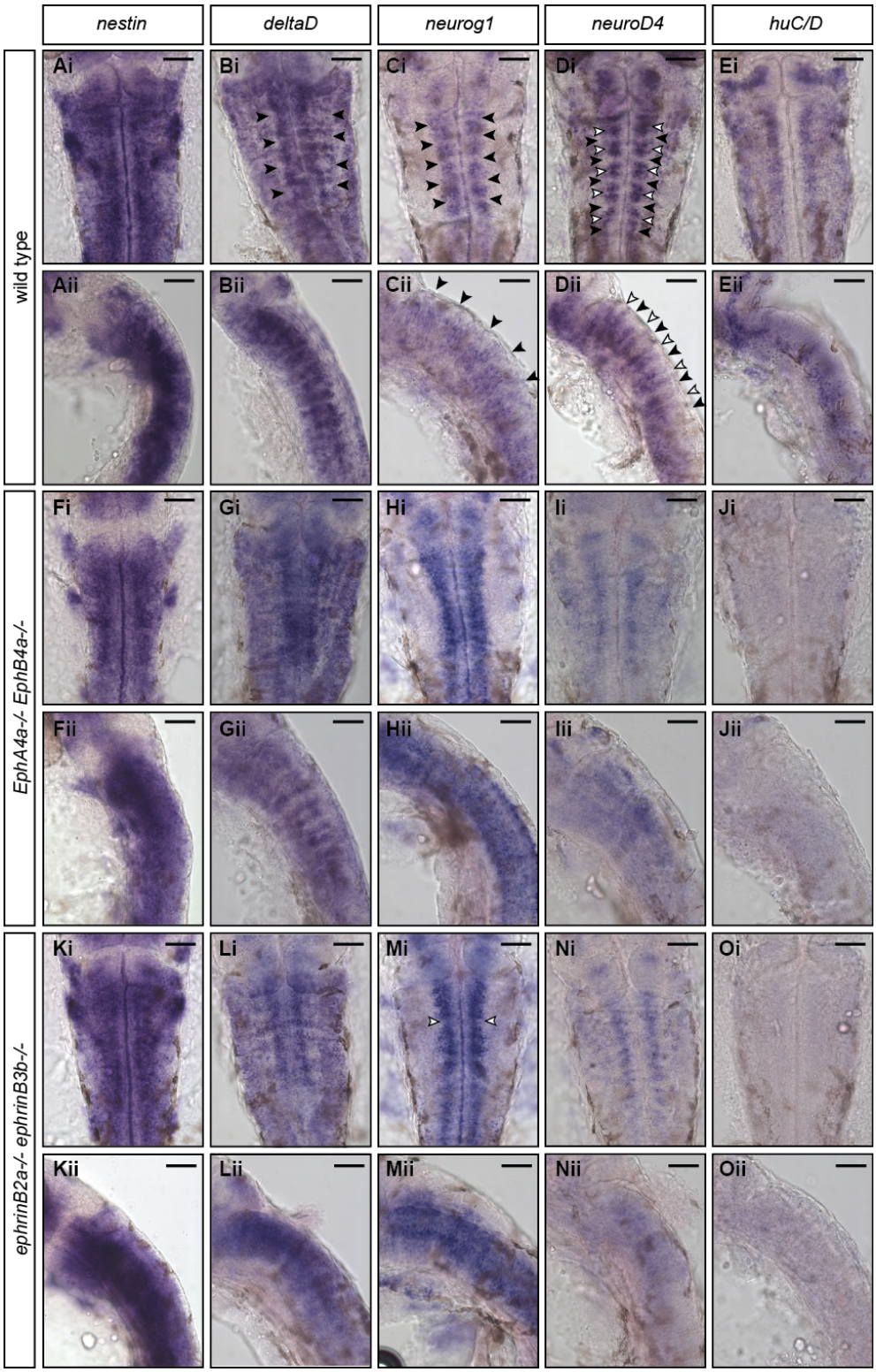

Figure 42 Expression of neuronal markers in wild type, double Eph receptor and double ephrin mutants

(A-O) Embryos at 30 hpf after *in situ* hybridisation for markers of neurogenesis in wild type embryos (A-E), *EphA4a* and *EphB4a* double mutants (F-J) and *ephrinB2a* and *ephrinB3b* double mutants (K-O). Black arrowheads mark non-neurogenic zones in rhombomeres and white arrowheads mark non-neurogenic zones at hindbrain boundaries. Scale bar represents 100 µm.

6.4.1 HuC/D expression in Eph receptor and ephrin mutants

After fewer *huC/D* transcripts were detected when Eph-ephrin signalling was disrupted (Figure 41; Figure 42), protein was detected by immunofluorescence in order to confirm the changes observed (Figure 43). This analysis was carried out in *EphA4a* and *EphB4a* double mutant embryos as well as *ephrinB2a* and *ephrinB3b* double mutant embryos. At 18 hpf there is little difference in HuC/D expression in wild type embryos and double Eph receptor or double ephrin mutants (Figure 43: A-C). At 24 hpf, 30 hpf and 36 hpf, ectopic HuC/D expression is seen in double Eph receptor mutants (Figure 43: E, H, K), and more strikingly in double ephrin mutants (Figure 43: F, I, L), in comparison to wild type embryos (Figure 43: D, G, J). This suggest that there is ectopic neurogenesis when Eph-ephrin signalling is disrupted and agrees with the finding of increased neural differentiation observed by ectopic expression of neural differentiation markers. However, this contradicts the observations by *in situ* hybridisation for *huC/D* where there is a decrease in RNA. This could be regulated by mechanisms that we do not understand well enough to interpret. As there are numerous studies that use HuC/D protein as a marker of differentiated neurons rather than RNA detection by *in situ* hybridisation, the observations made by immunostaining will be used interpret these findings.

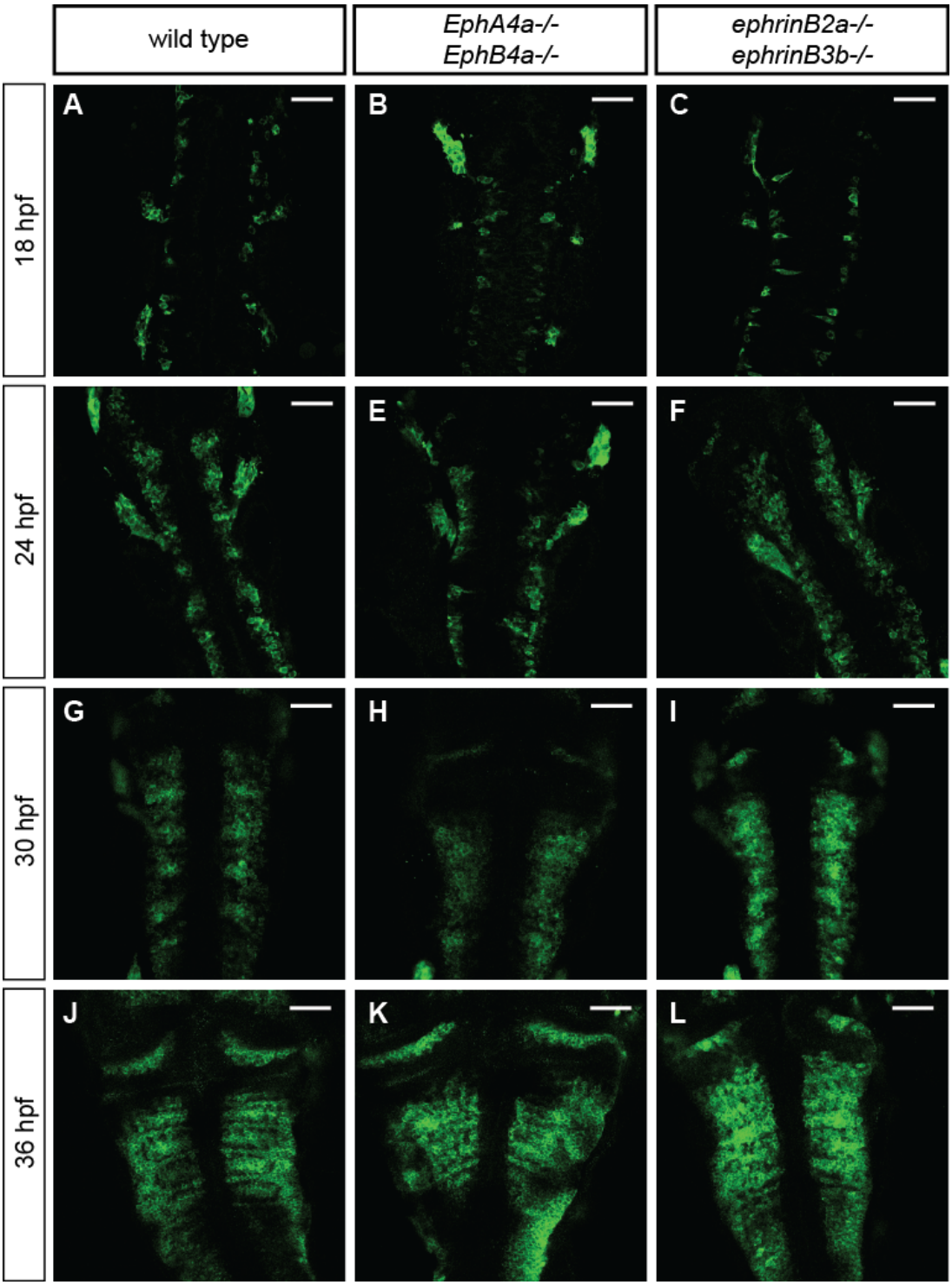

Figure 43 Immunofluorescence of HuC/D

(A-L) Embryos flat mounted after immunofluorescence for HuC/D from 18-36 hpf in wild type embryos (A, E, G, J), double *EphA4a* and *EphB4a* receptor mutants (B, F, H, K) and double *ephrinB2a* and *ephrinB3b* mutants (C, G, I, L). Scale bar represents 100 µm.

6.5 Discussion

In this chapter, markers of different stages of neurogenesis have been utilised to determine the role of Eph-ephrin signalling in the context of neural differentiation. The reason for exploring neurogenesis was that the genes found to be regulated downstream of Eph-ephrin signalling are markers of progenitor cells and neural differentiation. To explore this, embryos were collected at later stages of development which coincided with when neurogenesis is becoming increasingly restricted to the neurogenic zones adjacent to the hindbrain boundaries. Two methods of disrupting Eph-ephrin signalling were used to observe any changes. The first method was to express soluble ephrinB1a at 18 hpf in attempt look specifically at any changes to neurogenesis more directly as signalling has been blocked at a later stage of development. However, this still resulted in disruption to the boundary cells, shown by weaker expression of *rfng*. Secondly, Eph receptor and ephrin double mutants were used to determine the effects on neurogenesis when Eph-ephrin signalling was disrupted earlier in development and embryos have partial hindbrain boundary loss (remaining boundaries r1/r2, r4/r5 and r6/r7). Despite attempts to separate Eph-ephrin signalling from the role in boundary cell formation to find more direct effects of blocking signalling, from the phenotypes observed it appears that the effects on neurogenesis are an indirect consequence of boundary cell loss. This suggests that the decreased expression of *rfng* at the boundaries at 24 hpf is not sufficient to enable the normal function of boundary cells.

When Eph-ephrin signalling is blocked at 18 hpf by expression of soluble ephrinB1a, at 24 hpf there is ectopic neurogenesis in the hindbrain. This is observed by neuronal progenitor cells, differentiating cells and neurons being more widespread throughout the hindbrain than in control embryos. The phenotypes observed are similar to what has been found previously when boundary cells are lost or FGF20 signalling is disrupted (Gonzalez-Quevedo et al., 2010; Terriente et al., 2012). This suggests that the effects on neurogenesis are a result of boundary cell loss and that the weaker *rfng* expression observed at 24 hpf when Eph-ephrin signalling is blocked at 18 hpf, is not sufficient for the inhibition of neurogenesis in boundary cells (Cheng et al., 2004). Instead the boundaries are now neurogenic progenitors and are differentiating to form neurons (shown by the expression of *nestin* and *deltaD*). At 30 hpf, blocking

Eph-ephrin signalling then results in fewer neural progenitor cells and ectopic neurogenesis in segment centres and an increase in differentiated neurons. This suggests that blocking Eph-ephrin signalling results in neurogenesis in regions of the hindbrain where it is normally absent, which leads to a depletion of progenitor cells at the later stage of 30 hpf.

The double Eph receptor and double ephrin mutants disrupt signalling via either EphA4a and EphB4a, or ephrinB2a and ephrinB3b, respectively, and have a loss of boundaries at r2/r3, r3/r4 and r5/r6. In both mutants, at 30 hpf, there was ectopic neurogenesis in the hindbrain and an increase in differentiated neurons. However, in contrast, the neural progenitor cells did not decrease in the double Eph receptor and double ephrin mutants, but instead were more continuous. The effect on neurogenesis would be expected to greater in the double ephrin mutant embryos because in the hindbrain there are three ephrinBs present and signalling via two has been disrupted, whereas in the double Eph receptor mutant embryos there are more Eph receptors that are able to signal redundantly. There was more ectopic neurogenesis in the double ephrin mutant than the double Eph receptor mutant, shown by *deltaD* expression, but, this was not clearly observed for any of the other neurogenic markers. The phenotypes observed are likely to be secondary to the loss of boundaries as there is ectopic neurogenesis which is a known consequence of the loss of boundaries. In addition, direct phenotypes would show a correlation between Eph receptor or ephrin expression, in the respective mutants, which is not observed for *nestin*, *deltaD* and *neurog1*. *neuroD4* and *huC/D* are altered in double Eph receptor and double ephrin mutants in regions that are not specific to the boundaries and thus would argue that Eph-ephrin signalling is regulating neurogenesis indirectly.

6.6 Conclusion

In this chapter, known markers of neuronal progenitors, neuronal differentiation and differentiated neurons were used to decipher the role in which Eph-ephrin signalling may play in neurogenesis during hindbrain development. It was found that at 24 hpf blocking of Eph-ephrin signalling leads to increased ectopic neurogenesis which results in the depletion of neural progenitors at 30 hpf. In double *EphA4a* and

EphB4a mutant embryos, or double *ephrinB2a* and *ephrinB3b* mutant embryos, there is also ectopic neurogenesis and an increase in differentiated neurons at 30 hpf, but a decrease in neural progenitors is not observed. The effects observed are likely to be secondary to the loss of boundary cells as this has been previously shown to result in ectopic neurogenesis.

Chapter 7. Discussion

7.1 Identification of genes regulated downstream of Eph-ephrin signalling in the hindbrain

The aim of this project was to identify transcriptional targets of Eph receptor and ephrin signalling in the zebrafish hindbrain in order to further understand the role of this signalling. Among the genes identified are markers of neural progenitor cells and neural differentiation. *hmgb2a* and *nap1l1* are expressed in neural stem cells, whilst *tubb2b* is a marker of differentiating neurons and mdka a marker of differentiation and proliferation. The expression of these four genes was quantified by RT-qPCR in whole embryos and the expression patterns determined by *in situ* hybridisation. This identified two types of expression patterns in the hindbrain: expression localised to specific regions, and uniform expression. The localised expression of *mdka* and *nap1l1* in the hindbrain becomes more uniform when Eph-ephrin signalling was blocked and the gaps in expression at the boundary cells are no longer seen for *mdka*. In addition, the change in expression of *mdka* is the same in both *EphA4a* and *EphB4a* double mutants and *ephrinB2a* and *ephrinB3b* double mutants, and there is the same boundary loss in both mutants. The effect of Eph-ephrin signalling on neurogenesis was investigated further by looking at known markers of neurogenesis and it was found that disrupting Eph-ephrin signalling results in ectopic neurogenesis and at later stages and this causes a depletion of neural progenitor cells. These findings suggested that Eph-ephrin signalling is involved in regulating the progression of neurogenesis in the hindbrain and that this is occurring indirectly via the loss of boundary cells.

7.2 Direct versus indirect consequences of blocking Eph-ephrin signalling

Due to the complementary segmental expression of Eph receptors and ephrin that have high binding affinity, activation occurs at segment borders. However, what is observed is that the effects on neurogenesis are found within the hindbrain segments in Eph receptor and ephrin double mutants and when signalling is blocked with

soluble ephrinB1a. Previous work has down that Eph-ephrin signalling is required for formation of boundary cells and it was anticipated that boundary markers would be found in the RNA-sequencing analysis (which will be discussed in Chapter 7.3). This raises the question of why blocking Eph-ephrin signalling alters progenitor cells and neural differentiation, which are not located at the site of Eph-ephrin signalling.

The boundary cells are essential for the positioning of FGF20a-expressing neurons by acting as a source of chemorepellent, which localises these neurons to the segment centres in the mantle zone (Terriente et al., 2012). The FGF20a-expressing neurons then inhibit neurogenesis at the segment centres of the neural epithelium (Gonzalez-Quevedo et al., 2010). When boundary cell formation is prevented, the FGF20a-expressing neurons are no longer positioned in the segment centres to provide a concentrated source of FGF to inhibit neurogenesis and establish the non-neurogenic zones. Consequently, boundary cell disruption results in ectopic neurogenesis (Terriente et al., 2012). In the experiments in the current study, blocking Eph-ephrin signalling results in weaker expression of the boundary cell marker *rfng*, and ectopic neurogenesis at boundaries is observed (shown by *nestin* and *deltaD* expression). This suggests that weaker *rfng* expression is not sufficient for the inhibition of neurogenesis at the boundaries (Cheng et al., 2004). Another possibility is Eph-ephrin signalling acts in parallel to *rfng* to inhibit neurogenesis at boundaries.

In addition to the effect on neurogenesis as a result of disrupted boundaries, there is a depletion of *nestin*-expressing neural progenitors, which is a novel finding. Previous work has shown that *nestin* is expressed in some radial glial progenitor cells and that when radial glial cells are ablated *nestin*-expressing neural progenitor cells are lost in the neural tube (Johnson et al., 2016). The observations made during this project have shown that HuC/D expressing cells are increased in the hindbrain from 24 hpf to 36 hpf in embryos where Eph-ephrin signalling is disrupted (shown by immunofluorescence). HuC/D is expressed in neurons and excluded from radial glial cells (Trevarrow et al., 1990; Terriente et al., 2012), and the change in expression is complementary to the loss of *nestin*-expressing neural progenitor cells. The decrease in *nestin*-expressing neural progenitors suggests that ectopic neurogenesis leads to a lack of radial glial cells.

Based on previous work, it is possible that the non-neurogenic zones are a source of neural progenitors for the neurogenic zones. Consequently, the ectopic neurogenesis observed in the non-neurogenic zones results in a depletion of neural progenitor cells at later stages. This is observed in other parts of the nervous system where FGF signalling maintains progenitor cells by promoting proliferation and inhibiting neural differentiation (Fu et al., 2017). Cells that are further away from the source of FGF are able to differentiate, which is similar to the hindbrain where the neurogenic regions are furthest from the segment centres where the FGF20a-expressing neurons are clustered (Gonzalez-Quevedo et al., 2010). The hindbrain boundary cells in chick have been suggested to be a source of neural progenitor cells (Peretz et al., 2016), although unlike in zebrafish the boundary cells are not separate from the neurogenic populations. The boundary cells in the zebrafish hindbrain could also be a source of progenitor cells and when Eph-ephrin signalling is blocked these are no longer maintained, due to ectopic neurogenesis.

It would be interesting to test further whether blocking Eph-ephrin signalling is regulating neurogenesis directly or indirectly. One way to do this would be to disrupt the boundary cells via another mechanism and study how this alters the expression of neurogenic markers. This could be done by knocking down genes that are expressed in the boundaries, such as *rfng*. By comparing the phenotypes to those observed in my study, this would determine if signalling is acting indirectly as a result of boundary cell loss.

7.3 Is soluble ephrinB1a blocking or activating signalling?

It was initially expected that carrying out RNA-sequencing on hindbrains with and without blocking of Eph-ephrin signalling would identify genes that are boundary cell markers. However, no boundary cell markers were identified. *rfng* expression was used to confirm whether Eph-ephrin signalling had been blocked in the hindbrain when soluble ephrinB1a was over-expressed and was found by *in situ* hybridisation to no longer be expressed. However, RNA-sequencing showed that there was no overall change in the level of *rfng* expression in the hindbrain. One potential

explanation for this is that soluble ephrinB1a is in fact weakly activating, rather than blocking Eph receptor activation.

It was observed that when soluble ephrinB1a is over-expressed there is a decrease in the level of EphB4a protein in the hindbrain, but not for EphA4a protein. This result implies that soluble ephrinB1a is activating some Eph-ephrin signalling rather than blocking, as internalisation and degradation of Eph receptor is a hallmark of activation (Marston et al., 2003; Zimmer et al., 2003; Mann et al., 2003; Lauterbach and Klein, 2006; Goh and Sorkin, 2013). However, this contradicts the observation that *rfng* expression is absent when soluble ephrinB1a is over-expressed, implying that signalling is blocked.

In the majority of cases, soluble ephrins block signalling as they are not membrane bound, and are unable to form higher order clusters needed for signal activation (Davis et al., 1994). However, some studies have reported that soluble ephrin ligands are able to activate signalling. Firstly, the addition of soluble ephrinA1 in rat cortical neurons results in EphA2 receptor internalisation and induces the cellular response of growth cone collapse. The same response is found when EphA2 is activated with dimeric ephrinA1 (Wykosky et al., 2008). Another study showed that adding soluble ephrinA1 to cells that over-express EphA2 causes EphA2 internalisation and changes in cell morphology, which are known responses of EphA2 activation by ephrinA1 (Beauchamp et al., 2012). Previous work has also shown that forward signalling can be activated by soluble ephrins through cross-linking by transglutaminase action, which results in increased Eph receptor phosphorylation and a change in cell behaviour (Alford et al., 2007). It has also been suggested that the formation of tetramers for signal activation, which is comprised of two Eph receptors and two ephrins, is initially formed by one ephrin and two Eph receptors and one ephrin. In addition, soluble ephrins could activate Eph receptors but at a lower affinity than dimeric ephrins (Pabbisetty et al., 2007).

The examples discussed of soluble ephrins activating signalling are less common than for blocking and have not been shown for ephrinB ligands. Based on this evidence that soluble ephrinB1 may be a weak activator, I propose that where Eph-ephrin signalling is normally strongly activated at the boundaries, there is weak

activation of *rfng* expression. However, within the segments where Eph-ephrin signalling is not normally active soluble ephrinB1a is able to weakly activate signalling and low level *rfng* expression. Thus, boundary cell marker expression is decreased at the region where the boundary cells normally arise and increased within the segments, resulting in no overall change in RNA levels (Figure 44).

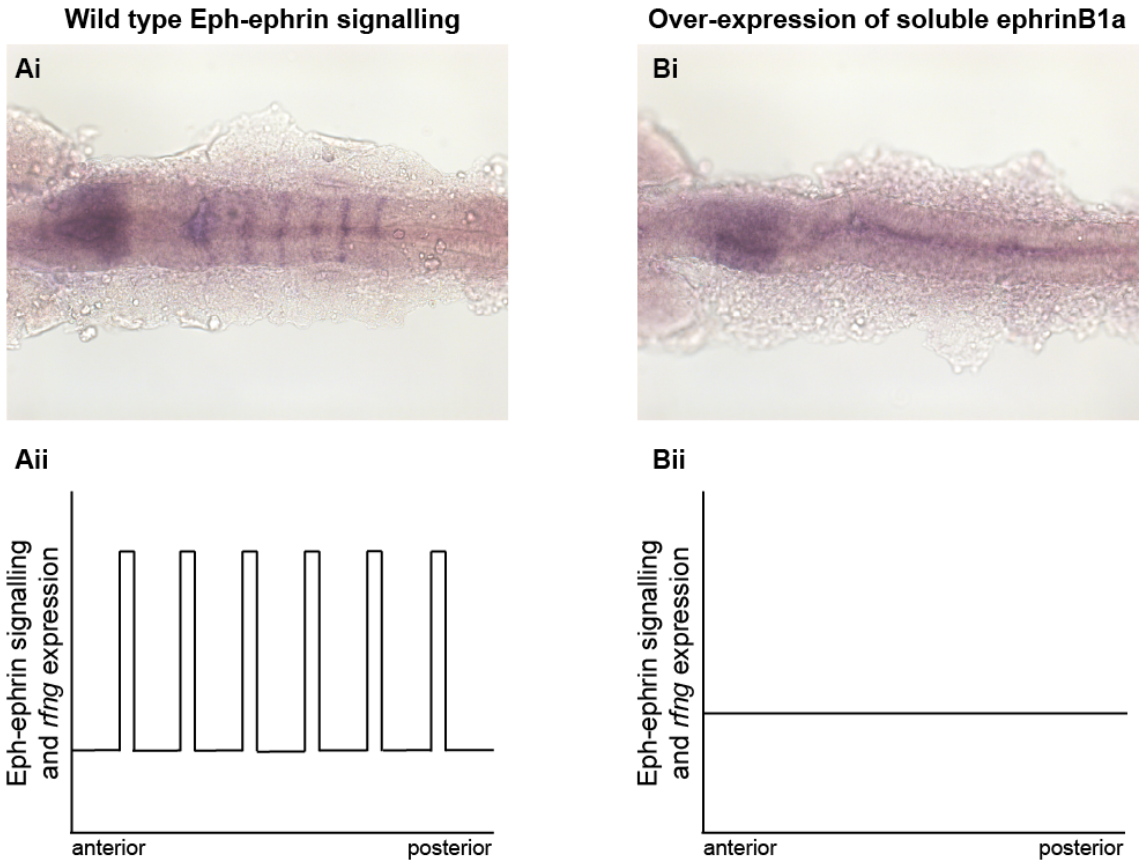

Figure 44 Hypothesis of soluble ephrinB1a effect on Eph receptor activity in the hindbrain

Schematic showing hypothesis of the effect of soluble ephrinB1a on Eph-ephrin signalling in the hindbrain. (A) Wild type Eph-ephrin signalling results in the formation six boundaries, shown by *in situ* hybridisation for *rfng* (Ai). Eph-ephrin signalling is highest at the boundaries (Aii). (B) Over-expression of soluble ephrinB1a results in decreased Eph-ephrin activation and *rfng* expression at boundaries. However, weak activation now occurs throughout the segments which may induce weak *rfng* expression.

In order to investigate whether soluble ephrinB1a is activating or blocking signalling, experiments were carried out to try to identify if the Eph receptors present in the hindbrain were phosphorylated upon soluble ephrinB1a over-expression. The approach taken was to pull down phosphorylated proteins in whole embryo lysates after soluble ephrinB1a over-expression. Despite attempts to optimise

immunoprecipitation and carrying out western blots, the results are currently unclear and leave open the question as to how this reagent is acting.

7.4 Future work to identify direct targets of Eph-ephrin signalling in the hindbrain

To further this study, it would be interesting to identify the direct targets of Eph-ephrin signalling. In order to identify direct targets one approach would be to look earlier in development before the boundary cells have formed and thus eliminates any changes that are downstream of boundary cell formation.

A more direct approach would be to find a cleaner way to disrupt Eph-ephrin signalling. This may be possible in the future when more Eph-ephrin binding pairs are identified that account for the boundaries that remain when EphA4a-ephrinB3b and EphB4a-ephrinB2a signalling is blocked. During this project, a quadruple mutant was generated for *EphA4a-EphB4a-ephrinB2a-ephrinB3b*, but due to the complexity of crosses only one quadruple homozygous mutant fish was identified. If more of these were to be generated in the future, these or other Eph receptor and ephrin mutants may generate embryos with complete hindbrain boundary loss.

A further approach is to find pathways downstream of Eph-ephrin signalling that are required for boundary marker expression. There is evidence for a role of the Jak-Stat signalling pathway which is known to be activated by Eph receptors and ephrins (Angela Cheung, Wilkinson Lab). Another approach being currently undertaken is to use single cell RNA-sequencing of hindbrain cells (Monica Tambalo, Wilkinson Lab). This will reveal the transcription of boundary cells, and genes that are specifically expressed by boundary cells can then be analysed to determine if they are targets of Eph-ephrin signalling.

One approach to further investigate the differentially expressed genes identified by RNA-sequencing could be to use Gene Ontology (GO) terms. This could identify known functions of validated genes and to see what other genes also known to have the same function. These could be of interest to investigate further. In addition, it

would be interesting to see which differentially expressed genes are known to have a role in neural progenitors and neural differentiation and validate and investigate these.

Reference List

AARONSON, D. S. & HORVATH, C. M. 2002. A road map for those who don't know JAK-STAT. *Science,* 296**,** 1653-5.

ABRAHAM, A. B., BRONSTEIN, R., REDDY, A. S., MALETIC-SAVATIC, M., AGUIRRE, A. & TSIRKA, S. E. 2013. Aberrant neural stem cell proliferation and increased adult neurogenesis in mice lacking chromatin protein HMGB2. *PLoS One,* 8**,** e84838.

ALFORD, S. C., BAZOWSKI, J., LORIMER, H., ELOWE, S. & HOWARD, P. L. 2007. Tissue transglutaminase clusters soluble A-type ephrins into functionally active high molecular weight oligomers. *Exp Cell Res,* 313**,** 4170-9.

AMOYEL, M., CHENG, Y. C., JIANG, Y. J. & WILKINSON, D. G. 2005. Wnt1 regulates neurogenesis and mediates lateral inhibition of boundary cell specification in the zebrafish hindbrain. *Development,* 132**,** 775-85.

ANTIC, D., LU, N. & KEENE, J. D. 1999. ELAV tumor antigen, Hel-N1, increases translation of neurofilament M mRNA and induces formation of neurites in human teratocarcinoma cells. *Genes Dev,* 13**,** 449-61.

AOKI, M., YAMASHITA, T. & TOHYAMA, M. 2004. EphA receptors direct the differentiation of mammalian neural precursor cells through a mitogen-activated protein kinase-dependent pathway. *J Biol Chem,* 279**,** 32643-50.

ARVANITIS, D. & DAVY, A. 2008. Eph/ephrin signaling: networks. *Genes Dev,* 22**,** 416-29.

ASHTON, R. S., CONWAY, A., PANGARKAR, C., BERGEN, J., LIM, K. I., SHAH, P., BISSELL, M. & SCHAFFER, D. V. 2012. Astrocytes regulate adult hippocampal neurogenesis through ephrin-B signaling. *Nat Neurosci,* 15**,** 1399-406.

BATLLE, E., HENDERSON, J. T., BEGHTEL, H., VAN DEN BORN, M. M., SANCHO, E., HULS, G., MEELDIJK, J., ROBERTSON, J., VAN DE WETERING, M., PAWSON, T. & CLEVERS, H. 2002. Beta-catenin and TCF mediate cell positioning in the intestinal epithelium by controlling the expression of EphB/ephrinB. *Cell,* 111**,** 251-63.

BEAUCHAMP, A., LIVELY, M. O., MINTZ, A., GIBO, D., WYKOSKY, J. & DEBINSKI, W. 2012. EphrinA1 is released in three forms from cancer cells by matrix metalloproteases. *Mol Cell Biol,* 32**,** 3253-64.

BELL, E., WINGATE, R. J. & LUMSDEN, A. 1999. Homeotic transformation of rhombomere identity after localized Hoxb1 misexpression. *Science,* 284**,** 2168-71.

BLADER, P., FISCHER, N., GRADWOHL, G., GUILLEMOT, F. & STRAHLE, U. 1997. The activity of neurogenin1 is controlled by local cues in the zebrafish embryo. *Development,* 124**,** 4557-69.

BOISSIER, P., CHEN, J. & HUYNH-DO, U. 2013. EphA2 signaling following endocytosis: role of Tiam1. *Traffic,* 14**,** 1255-71.

BONANOMI, D., CHIVATAKARN, O., BAI, G., ABDESSELEM, H., LETTIERI, K., MARQUARDT, T., PIERCHALA, B. A. & PFAFF, S. L. 2012. Ret is a multifunctional coreceptor that integrates diffusible- and contact-axon guidance signals. *Cell,* 148**,** 568-82.

BOSSING, T. & BRAND, A. H. 2002. Dephrin, a transmembrane ephrin with a unique structure, prevents interneuronal axons from exiting the Drosophila embryonic CNS. *Development,* 129**,** 4205-18.

BRETAUD, S., PAGNON-MINOT, A., GUILLON, E., RUGGIERO, F. & LE GUELLEC, D. 2011. Characterization of spatial and temporal expression pattern of Col15a1b during zebrafish development. *Gene Expr Patterns,* 11**,** 129-34.

BREUSS, M., MORANDELL, J., NIMPF, S., GSTREIN, T., LAUWERS, M., HOCHSTOEGER, T., BRAUN, A., CHAN, K., SANCHEZ GUAJARDO, E. R., ZHANG, L., SUPLATA, M., HEINZE, K. G., ELSAYAD, K. & KEAYS, D. A. 2015. The Expression of Tubb2b Undergoes a Developmental Transition in Murine Cortical Neurons. *J Comp Neurol,* 523**,** 2161-86.

BRONSTEIN, R., KYLE, J., ABRAHAM, A. B. & TSIRKA, S. E. 2017. Neurogenic to Gliogenic Fate Transition Perturbed by Loss of HMGB2. *Front Mol Neurosci,* 10**,** 153.

BRUCKNER, K., PASQUALE, E. B. & KLEIN, R. 1997. Tyrosine phosphorylation of transmembrane ligands for Eph receptors. *Science,* 275**,** 1640-3.

BUSH, J. O. & SORIANO, P. 2009. Ephrin-B1 regulates axon guidance by reverse signaling through a PDZ-dependent mechanism. *Genes Dev,* 23**,** 1586-99.

BUSH, J. O. & SORIANO, P. 2010. Ephrin-B1 forward signaling regulates craniofacial morphogenesis by controlling cell proliferation across Eph-ephrin boundaries. *Genes Dev,* 24**,** 2068-80.

CALZOLARI, S., TERRIENTE, J. & PUJADES, C. 2014. Cell segregation in the vertebrate hindbrain relies on actomyosin cables located at the interhombomeric boundaries. *EMBO J,* 33**,** 686-701.

CHENG, H. J., NAKAMOTO, M., BERGEMANN, A. D. & FLANAGAN, J. G. 1995. Complementary gradients in expression and binding of ELF-1 and Mek4 in development of the topographic retinotectal projection map. *Cell,* 82**,** 371-81.

CHENG, N., BRANTLEY, D. M. & CHEN, J. 2002. The ephrins and Eph receptors in angiogenesis. *Cytokine Growth Factor Rev,* 13**,** 75-85.

CHENG, Y. C., AMOYEL, M., QIU, X., JIANG, Y. J., XU, Q. & WILKINSON, D. G. 2004. Notch activation regulates the segregation and differentiation of rhombomere boundary cells in the zebrafish hindbrain. *Dev Cell,* 6**,** 539-50.

CHIN-SANG, I. D., GEORGE, S. E., DING, M., MOSELEY, S. L., LYNCH, A. S. & CHISHOLM, A. D. 1999. The ephrin VAB-2/EFN-1 functions in neuronal signaling to regulate epidermal morphogenesis in C. elegans. *Cell,* 99**,** 781-90.

CHOW, R. K. K., TSZ-KWAN SIN, S., LIU, M., LI, Y., MAN CHAN, T. H., SONG, Y., CHEN, L., LAI-WAN KWONG, D. & GUAN, X. Y. 2017. AKR7A3 suppresses tumorigenicity and chemoresistance in hepatocellular carcinoma through attenuation of ERK, c-Jun and NF-kappaB signaling pathways. *Oncotarget,* 8**,** 83469-83479.

CHUMLEY, M. J., CATCHPOLE, T., SILVANY, R. E., KERNIE, S. G. & HENKEMEYER, M. 2007. EphB receptors regulate stem/progenitor cell proliferation, migration, and polarity during hippocampal neurogenesis. *J Neurosci,* 27**,** 13481-90.

CLARKE, J. 2009. Role of polarized cell divisions in zebrafish neural tube formation. *Curr Opin Neurobiol,* 19**,** 134-8.

COOKE, J., MOENS, C., ROTH, L., DURBIN, L., SHIOMI, K., BRENNAN, C., KIMMEL, C., WILSON, S. & HOLDER, N. 2001. Eph signalling functions downstream of Val to regulate cell sorting and boundary formation in the caudal hindbrain. *Development,* 128**,** 571-80.

COOKE, J. E., KEMP, H. A. & MOENS, C. B. 2005. EphA4 is required for cell adhesion and rhombomere-boundary formation in the zebrafish. *Curr Biol,* 15**,** 536-42.

COWAN, C. A. & HENKEMEYER, M. 2001. The SH2/SH3 adaptor Grb4 transduces B-ephrin reverse signals. *Nature,* 413**,** 174-9.

COX, A. G., TSOMIDES, A., KIM, A. J., SAUNDERS, D., HWANG, K. L., EVASON, K. J., HEIDEL, J., BROWN, K. K., YUAN, M., LIEN, E. C., LEE, B. C., NISSIM, S., DICKINSON, B., CHHANGAWALA, S., CHANG, C. J., ASARA, J. M., HOUVRAS, Y., GLADYSHEV, V. N. & GOESSLING, W. 2016. Selenoprotein H is an essential regulator of redox homeostasis that cooperates with p53 in development and tumorigenesis. *Proc Natl Acad Sci U S A,* 113**,** E5562-71.

CRAMER, K. S. & MIKO, I. J. 2016. Eph-ephrin signaling in nervous system development. *F1000Res,* 5.

DAAR, I. O. 2012. Non-SH2/PDZ reverse signaling by ephrins. *Semin Cell Dev Biol,* 23**,** 65-74.

DAHLSTRAND, J., LARDELLI, M. & LENDAHL, U. 1995. Nestin mRNA expression correlates with the central nervous system progenitor cell state in many, but not all, regions of developing central nervous system. *Brain Res Dev Brain Res,* 84**,** 109-29.

DALVA, M. B., TAKASU, M. A., LIN, M. Z., SHAMAH, S. M., HU, L., GALE, N. W. & GREENBERG, M. E. 2000. EphB receptors interact with NMDA receptors and regulate excitatory synapse formation. *Cell,* 103**,** 945-56.

DAVIS, S., GALE, N. W., ALDRICH, T. H., MAISONPIERRE, P. C., LHOTAK, V., PAWSON, T., GOLDFARB, M. & YANCOPOULOS, G. D. 1994. Ligands for EPH-related receptor tyrosine kinases that require membrane attachment or clustering for activity. *Science,* 266**,** 816-9.

DAVY, A. & SORIANO, P. 2007. Ephrin-B2 forward signaling regulates somite patterning and neural crest cell development. *Dev Biol,* 304**,** 182-93.

DEL VALLE, K., THEUS, M. H., BETHEA, J. R., LIEBL, D. J. & RICARD, J. 2011. Neural progenitors proliferation is inhibited by EphB3 in the developing subventricular zone. *Int J Dev Neurosci,* 29**,** 9-14.

DEPAEPE, V., SUAREZ-GONZALEZ, N., DUFOUR, A., PASSANTE, L., GORSKI, J. A., JONES, K. R., LEDENT, C. & VANDERHAEGHEN, P. 2005. Ephrin signalling controls brain size by regulating apoptosis of neural progenitors. *Nature,* 435**,** 1244-50.

DOBIN, A., DAVIS, C. A., SCHLESINGER, F., DRENKOW, J., ZALESKI, C., JHA, S., BATUT, P., CHAISSON, M. & GINGERAS, T. R. 2013. STAR: ultrafast universal RNA-seq aligner. *Bioinformatics,* 29**,** 15-21.

DUDANOVA, I. & KLEIN, R. 2011. The axon's balancing act: cis- and trans-interactions between Ephs and ephrins. *Neuron,* 71**,** 1-3.

DURBIN, L., BRENNAN, C., SHIOMI, K., COOKE, J., BARRIOS, A., SHANMUGALINGAM, S., GUTHRIE, B., LINDBERG, R. & HOLDER, N. 1998. Eph signaling is required for segmentation and differentiation of the somites. *Genes Dev,* 12**,** 3096-109.

EGEA, J. & KLEIN, R. 2007. Bidirectional Eph-ephrin signaling during axon guidance. *Trends Cell Biol,* 17**,** 230-8.

ELOWE, S., HOLLAND, S. J., KULKARNI, S. & PAWSON, T. 2001. Downregulation of the Ras-mitogen-activated protein kinase pathway by the EphB2 receptor tyrosine kinase is required for ephrin-induced neurite retraction. *Mol Cell Biol,* 21**,** 7429-41.

FAGOTTO, F., WINKLBAUER, R. & ROHANI, N. 2014. Ephrin-Eph signaling in embryonic tissue separation. *Cell Adh Migr,* 8**,** 308-26.

FALIVELLI, G., LISABETH, E. M., RUBIO DE LA TORRE, E., PEREZ-TENORIO, G., TOSATO, G., SALVUCCI, O. & PASQUALE, E. B. 2013. Attenuation of eph receptor kinase activation in cancer cells by coexpressed ephrin ligands. *PLoS One,* 8**,** e81445.

FASEN, K., CERRETTI, D. P. & HUYNH-DO, U. 2008. Ligand binding induces Cbl-dependent EphB1 receptor degradation through the lysosomal pathway. *Traffic,* 9**,** 251-66.

FELDHEIM, D. A., KIM, Y. I., BERGEMANN, A. D., FRISEN, J., BARBACID, M. & FLANAGAN, J. G. 2000. Genetic analysis of ephrin-A2 and ephrin-A5 shows their requirement in multiple aspects of retinocollicular mapping. *Neuron,* 25**,** 563-74.

FRASER, S., KEYNES, R. & LUMSDEN, A. 1990. Segmentation in the chick embryo hindbrain is defined by cell lineage restrictions. *Nature,* 344**,** 431-5.

FU, T., TOWERS, M. & PLACZEK, M. A. 2017. Fgf10(+) progenitors give rise to the chick hypothalamus by rostral and caudal growth and differentiation. *Development,* 144**,** 3278-3288.

GALE, N. W., HOLLAND, S. J., VALENZUELA, D. M., FLENNIKEN, A., PAN, L., RYAN, T. E., HENKEMEYER, M., STREBHARDT, K., HIRAI, H., WILKINSON, D. G., PAWSON, T., DAVIS, S. & YANCOPOULOS, G. D. 1996. Eph receptors and ligands comprise two major specificity subclasses and are reciprocally compartmentalized during embryogenesis. *Neuron,* 17**,** 9-19.

GENANDER, M., HALFORD, M. M., XU, N. J., ERIKSSON, M., YU, Z., QIU, Z., MARTLING, A., GREICIUS, G., THAKAR, S., CATCHPOLE, T., CHUMLEY, M. J., ZDUNEK, S., WANG, C., HOLM, T., GOFF, S. P., PETTERSSON, S., PESTELL, R. G., HENKEMEYER, M. & FRISEN, J. 2009. Dissociation of EphB2 signaling pathways mediating progenitor cell proliferation and tumor suppression. *Cell,* 139**,** 679-92.

GENANDER, M., HOLMBERG, J. & FRISEN, J. 2010. Ephrins negatively regulate cell proliferation in the epidermis and hair follicle. *Stem Cells,* 28**,** 1196-205.

GEORGE, S. E., SIMOKAT, K., HARDIN, J. & CHISHOLM, A. D. 1998. The VAB-1 Eph receptor tyrosine kinase functions in neural and epithelial morphogenesis in C. elegans. *Cell,* 92**,** 633-43.

GERETY, S. S. & ANDERSON, D. J. 2002. Cardiovascular ephrinB2 function is essential for embryonic angiogenesis. *Development,* 129**,** 1397-410.

GERETY, S. S., WANG, H. U., CHEN, Z. F. & ANDERSON, D. J. 1999. Symmetrical mutant phenotypes of the receptor EphB4 and its specific transmembrane ligand ephrin-B2 in cardiovascular development. *Mol Cell,* 4**,** 403-14.

GERETY, S. S. & WILKINSON, D. G. 2011. Morpholino artifacts provide pitfalls and reveal a novel role for pro-apoptotic genes in hindbrain boundary development. *Dev Biol,* 350**,** 279-89.

GETSIOS, S., HUEN, A. C. & GREEN, K. J. 2004. Working out the strength and flexibility of desmosomes. *Nat Rev Mol Cell Biol,* 5**,** 271-81.

GIBBS, E. M., DAVIDSON, A. E., TRICKEY-GLASSMAN, A., BACKUS, C., HONG, Y., SAKOWSKI, S. A., DOWLING, J. J. & FELDMAN, E. L. 2013. Two dynamin-2 genes are required for normal zebrafish development. *PLoS One,* 8**,** e55888.

GOH, L. K. & SORKIN, A. 2013. Endocytosis of receptor tyrosine kinases. *Cold Spring Harb Perspect Biol,* 5**,** a017459.

GONZALEZ-QUEVEDO, R., LEE, Y., POSS, K. D. & WILKINSON, D. G. 2010. Neuronal regulation of the spatial patterning of neurogenesis. *Dev Cell,* 18**,** 136-47.

GRADWOHL, G., FODE, C. & GUILLEMOT, F. 1996. Restricted expression of a novel murine atonal-related bHLH protein in undifferentiated neural precursors. *Dev Biol,* 180**,** 227-41.

GROSSMAN, E. N., GIURUMESCU, C. A. & CHISHOLM, A. D. 2013. Mechanisms of ephrin receptor protein kinase-independent signaling in amphid axon guidance in Caenorhabditis elegans. *Genetics,* 195**,** 899-913.

GU, X., ZHAO, F., ZHENG, M., FEI, X., CHEN, X., HUANG, S., XIE, Y. & MAO, Y. 2007. Cloning and characterization of a gene encoding the human putative ubiquitin conjugating enzyme E2Z (UBE2Z). *Mol Biol Rep,* 34**,** 183-8.

GUTHRIE, S. & LUMSDEN, A. 1991. Formation and regeneration of rhombomere boundaries in the developing chick hindbrain. *Development,* 112**,** 221-9.

GUTZMAN, J. H. & SIVE, H. 2010. Epithelial relaxation mediated by the myosin phosphatase regulator Mypt1 is required for brain ventricle lumen expansion and hindbrain morphogenesis. *Development,* 137**,** 795-804.

HADDON, C., JIANG, Y. J., SMITHERS, L. & LEWIS, J. 1998. Delta-Notch signalling and the patterning of sensory cell differentiation in the zebrafish ear: evidence from the mind bomb mutant. *Development,* 125**,** 4637-44.

HATTORI, M., OSTERFIELD, M. & FLANAGAN, J. G. 2000. Regulated cleavage of a contact-mediated axon repellent. *Science,* 289**,** 1360-5.

HAUPAIX, N., STOLFI, A., SIROUR, C., PICCO, V., LEVINE, M., CHRISTIAEN, L. & YASUO, H. 2013. p120RasGAP mediates ephrin/Eph-dependent attenuation of FGF/ERK signals during cell fate specification in ascidian embryos. *Development,* 140**,** 4347-52.

HELMBACHER, F., PUJADES, C., DESMARQUET, C., FRAIN, M., RIJLI, F. M., CHAMBON, P. & CHARNAY, P. 1998. Hoxa1 and Krox-20 synergize to control the development of rhombomere 3. *Development,* 125**,** 4739-48.

HERNANDEZ, R. E., PUTZKE, A. P., MYERS, J. P., MARGARETHA, L. & MOENS, C. B. 2007. Cyp26 enzymes generate the retinoic acid response pattern necessary for hindbrain development. *Development,* 134**,** 177-87.

HERNANDEZ, R. E., RIKHOF, H. A., BACHMANN, R. & MOENS, C. B. 2004. vhnf1 integrates global RA patterning and local FGF signals to direct posterior hindbrain development in zebrafish. *Development,* 131**,** 4511-20.

HEYMAN, I., FAISSNER, A. & LUMSDEN, A. 1995. Cell and matrix specialisations of rhombomere boundaries. *Dev Dyn,* 204**,** 301-15.

HEYMAN, I., KENT, A. & LUMSDEN, A. 1993. Cellular morphology and extracellular space at rhombomere boundaries in the chick embryo hindbrain. *Dev Dyn,* 198**,** 241-53.

HIMANEN, J. P., CHUMLEY, M. J., LACKMANN, M., LI, C., BARTON, W. A., JEFFREY, P. D., VEARING, C., GELEICK, D., FELDHEIM, D. A., BOYD, A. W., HENKEMEYER, M. & NIKOLOV, D. B. 2004. Repelling class discrimination: ephrin-A5 binds to and activates EphB2 receptor signaling. *Nat Neurosci,* 7**,** 501-9.

HIMANEN, J. P., RAJASHANKAR, K. R., LACKMANN, M., COWAN, C. A., HENKEMEYER, M. & NIKOLOV, D. B. 2001. Crystal structure of an Eph receptor-ephrin complex. *Nature,* 414**,** 933-8.

HIRAI, H., MARU, Y., HAGIWARA, K., NISHIDA, J. & TAKAKU, F. 1987. A novel putative tyrosine kinase receptor encoded by the eph gene. *Science,* 238**,** 1717-20.

HOLLAND, S. J., GALE, N. W., MBAMALU, G., YANCOPOULOS, G. D., HENKEMEYER, M. & PAWSON, T. 1996. Bidirectional signalling through the EPH-family receptor Nuk and its transmembrane ligands. *Nature,* 383**,** 722-5.

HOLMBERG, J., GENANDER, M., HALFORD, M. M., ANNEREN, C., SONDELL, M., CHUMLEY, M. J., SILVANY, R. E., HENKEMEYER, M. & FRISEN, J. 2006. EphB receptors coordinate migration and proliferation in the intestinal stem cell niche. *Cell,* 125**,** 1151-63.

HOWE, D. G., BRADFORD, Y. M., CONLIN, T., EAGLE, A. E., FASHENA, D., FRAZER, K., KNIGHT, J., MANI, P., MARTIN, R., MOXON, S. A., PADDOCK, H., PICH, C., RAMACHANDRAN, S., RUEF, B. J., RUZICKA, L., SCHAPER, K., SHAO, X., SINGER, A., SPRUNGER, B., VAN SLYKE, C. E. & WESTERFIELD, M. 2013. ZFIN, the Zebrafish Model Organism Database: increased support for mutants and transgenics. *Nucleic Acids Res,* 41**,** D854-60.

HUNT, P., WHITING, J., MUCHAMORE, I., MARSHALL, H. & KRUMLAUF, R. 1991. Homeobox genes and models for patterning the hindbrain and branchial arches. *Dev Suppl,* 1**,** 187-96.

IRIE, F. & YAMAGUCHI, Y. 2002. EphB receptors regulate dendritic spine development via intersectin, Cdc42 and N-WASP. *Nat Neurosci,* 5**,** 1117-8.

IRIE, N., TAKADA, Y., WATANABE, Y., MATSUZAKI, Y., NARUSE, C., ASANO, M., IWAKURA, Y., SUDA, T. & MATSUO, K. 2009. Bidirectional signaling through ephrinA2-EphA2 enhances osteoclastogenesis and suppresses osteoblastogenesis. *J Biol Chem,* 284**,** 14637-44.

IRVING, C., NIETO, M. A., DASGUPTA, R., CHARNAY, P. & WILKINSON, D. G. 1996. Progressive spatial restriction of Sek-1 and Krox-20 gene expression during hindbrain segmentation. *Dev Biol,* 173**,** 26-38.

JAGLIN, X. H. & CHELLY, J. 2009. Tubulin-related cortical dysgeneses: microtubule dysfunction underlying neuronal migration defects. *Trends Genet,* 25**,** 555-66.

JOHNSON, K., BARRAGAN, J., BASHIRUDDIN, S., SMITH, C. J., TYRRELL, C., PARSONS, M. J., DORIS, R., KUCENAS, S., DOWNES, G. B., VELEZ, C. M., SCHNEIDER, C., SAKAI, C., PATHAK, N., ANDERSON, K., STEIN, R., DEVOTO, S. H., MUMM, J. S. & BARRESI, M. J. 2016. Gfap-positive radial glial cells are an essential progenitor population for later-born neurons and glia in the zebrafish spinal cord. *Glia,* 64**,** 1170-89.

JORGENSEN, C., SHERMAN, A., CHEN, G. I., PASCULESCU, A., POLIAKOV, A., HSIUNG, M., LARSEN, B., WILKINSON, D. G., LINDING, R. & PAWSON, T. 2009. Cell-specific information processing in segregating populations of Eph receptor ephrin-expressing cells. *Science,* 326**,** 1502-9.

JUREK, A., GENANDER, M., KUNDU, P., CATCHPOLE, T., HE, X., STRAAT, K., SABELSTROM, H., XU, N. J., PETTERSSON, S., HENKEMEYER, M. & FRISEN, J. 2016. Eph receptor interclass cooperation is required for the regulation of cell proliferation. *Exp Cell Res,* 348**,** 10-22.

KALO, M. S. & PASQUALE, E. B. 1999. Multiple in vivo tyrosine phosphorylation sites in EphB receptors. *Biochemistry,* 38**,** 14396-408.

KAO, T. J., LAW, C. & KANIA, A. 2012. Eph and ephrin signaling: lessons learned from spinal motor neurons. *Semin Cell Dev Biol,* 23**,** 83-91.

KENNEDY, M. J., DAVISON, I. G., ROBINSON, C. G. & EHLERS, M. D. 2010. Syntaxin-4 defines a domain for activity-dependent exocytosis in dendritic spines. *Cell,* 141**,** 524-35.

KETTLEBOROUGH, R. N., BUSCH-NENTWICH, E. M., HARVEY, S. A., DOOLEY, C. M., DE BRUIJN, E., VAN EEDEN, F., SEALY, I., WHITE, R. J., HERD, C., NIJMAN, I. J., FENYES, F., MEHROKE, S., SCAHILL, C., GIBBONS, R., WALI, N., CARRUTHERS, S., HALL, A., YEN, J., CUPPEN, E. & STEMPLE, D. L. 2013. A systematic genome-wide analysis of zebrafish protein-coding gene function. *Nature,* 496**,** 494-7.

KIECKER, C. & LUMSDEN, A. 2012. The role of organizers in patterning the nervous system. *Annu Rev Neurosci,* 35**,** 347-67.

KIM, C. H., UESHIMA, E., MURAOKA, O., TANAKA, H., YEO, S. Y., HUH, T. L. & MIKI, N. 1996. Zebrafish elav/HuC homologue as a very early neuronal marker. *Neurosci Lett,* 216**,** 109-12.

KIMMEL, C. B., BALLARD, W. W., KIMMEL, S. R., ULLMANN, B. & SCHILLING, T. F. 1995. Stages of embryonic development of the zebrafish. *Dev Dyn,* 203**,** 253-310.

KOZMA, R., SARNER, S., AHMED, S. & LIM, L. 1997. Rho family GTPases and neuronal growth cone remodelling: relationship between increased complexity induced by Cdc42Hs, Rac1, and acetylcholine and collapse induced by RhoA and lysophosphatidic acid. *Mol Cell Biol,* 17**,** 1201-11.

KRUMLAUF, R. 2016. Hox Genes and the Hindbrain: A Study in Segments. *Curr Top Dev Biol,* 116**,** 581-96.

KUDOH, T., WILSON, S. W. & DAWID, I. B. 2002. Distinct roles for Fgf, Wnt and retinoic acid in posteriorizing the neural ectoderm. *Development,* 129**,** 4335-46.

KULLANDER, K. & KLEIN, R. 2002. Mechanisms and functions of Eph and ephrin signalling. *Nat Rev Mol Cell Biol,* 3**,** 475-86.

KULLANDER, K., MATHER, N. K., DIELLA, F., DOTTORI, M., BOYD, A. W. & KLEIN, R. 2001. Kinase-dependent and kinase-independent functions of EphA4 receptors in major axon tract formation in vivo. *Neuron,* 29**,** 73-84.

KUMARI, P., GILLIGAN, P. C., LIM, S., TRAN, L. D., WINKLER, S., PHILP, R. & SAMPATH, K. 2013. An essential role for maternal control of Nodal signaling. *Elife,* 2**,** e00683.

LAI, K. O., CHEN, Y., PO, H. M., LOK, K. C., GONG, K. & IP, N. Y. 2004. Identification of the Jak/Stat proteins as novel downstream targets of EphA4 signaling in muscle: implications in the regulation of acetylcholinesterase expression. *J Biol Chem,* 279**,** 13383-92.

LAN, C. C., TANG, R., UN SAN LEONG, I. & LOVE, D. R. 2009. Quantitative real-time RT-PCR (qRT-PCR) of zebrafish transcripts: optimization of RNA extraction, quality control considerations, and data analysis. *Cold Spring Harb Protoc,* 2009**,** pdb prot5314.

LAUTERBACH, J. & KLEIN, R. 2006. Release of full-length EphB2 receptors from hippocampal neurons to cocultured glial cells. *J Neurosci,* 26**,** 11575-81.

LEE, H. S., BONG, Y. S., MOORE, K. B., SORIA, K., MOODY, S. A. & DAAR, I. O. 2006. Dishevelled mediates ephrinB1 signalling in the eye field through the planar cell polarity pathway. *Nat Cell Biol,* 8**,** 55-63.

LEE, H. S., NISHANIAN, T. G., MOOD, K., BONG, Y. S. & DAAR, I. O. 2008. EphrinB1 controls cell-cell junctions through the Par polarity complex. *Nat Cell Biol,* 10**,** 979-86.

LEE, J. E., HOLLENBERG, S. M., SNIDER, L., TURNER, D. L., LIPNICK, N. & WEINTRAUB, H. 1995. Conversion of Xenopus ectoderm into neurons by NeuroD, a basic helix-loop-helix protein. *Science,* 268**,** 836-44.

LI, J., ZHANG, D. S., YE, J. C., LI, C. M., QI, M., LIANG, D. D., XU, X. R., XU, L., LIU, Y., ZHANG, H., ZHANG, Y. Y., DENG, F. F., FENG, J., SHI, D., CHEN, J. J., LI, L., CHEN, G., SUN, Y. F., PENG, L. Y. & CHEN, Y. H. 2013. Dynamin-2 mediates heart failure by modulating Ca2+ -dependent cardiomyocyte apoptosis. *Int J Cardiol,* 168**,** 2109-19.

LI, R., SUN, Y., JIANG, A., WU, Y., LI, C., JIN, M., YAN, H. & JIN, H. 2016. Knockdown of ephrin receptor A7 suppresses the proliferation and metastasis of A549 human lung cancer cells. *Mol Med Rep,* 13**,** 3190-6.

LIM, Y. S., MCLAUGHLIN, T., SUNG, T. C., SANTIAGO, A., LEE, K. F. & O'LEARY, D. D. 2008. p75(NTR) mediates ephrin-A reverse signaling required for axon repulsion and mapping. *Neuron,* 59**,** 746-58.

LIN, S., GORDON, K., KAPLAN, N. & GETSIOS, S. 2010. Ligand targeting of EphA2 enhances keratinocyte adhesion and differentiation via desmoglein 1. *Mol Biol Cell,* 21**,** 3902-14.

LISABETH, E. M., FALIVELLI, G. & PASQUALE, E. B. 2013. Eph receptor signaling and ephrins. *Cold Spring Harb Perspect Biol,* 5.

LOVE, M. I., HUBER, W. & ANDERS, S. 2014. Moderated estimation of fold change and dispersion for RNA-seq data with DESeq2. *Genome Biol,* 15**,** 550.

LU, Q., SUN, E. E., KLEIN, R. S. & FLANAGAN, J. G. 2001. Ephrin-B reverse signaling is mediated by a novel PDZ-RGS protein and selectively inhibits G protein-coupled chemoattraction. *Cell,* 105**,** 69-79.

LUMSDEN, A. & KEYNES, R. 1989. Segmental patterns of neuronal development in the chick hindbrain. *Nature,* 337**,** 424-8.

LUMSDEN, A. & KRUMLAUF, R. 1996. Patterning the vertebrate neuraxis. *Science,* 274**,** 1109-15.

MA, Q., KINTNER, C. & ANDERSON, D. J. 1996. Identification of neurogenin, a vertebrate neuronal determination gene. *Cell,* 87**,** 43-52.

MACONOCHIE, M., NONCHEV, S., MORRISON, A. & KRUMLAUF, R. 1996. Paralogous Hox genes: function and regulation. *Annu Rev Genet,* 30**,** 529-56.

MAGAL, E., HOLASH, J. A., TOSO, R. J., CHANG, D., LINDBERG, R. A. & PASQUALE, E. B. 1996. B61, a ligand for the Eck receptor protein-tyrosine kinase, exhibits

neurotrophic activity in cultures of rat spinal cord neurons. *J Neurosci Res,* 43**,** 735-44.

MAHLER, J. & DRIEVER, W. 2007. Expression of the zebrafish intermediate neurofilament Nestin in the developing nervous system and in neural proliferation zones at postembryonic stages. *BMC Dev Biol,* 7**,** 89.

MANN, F., MIRANDA, E., WEINL, C., HARMER, E. & HOLT, C. E. 2003. B-type Eph receptors and ephrins induce growth cone collapse through distinct intracellular pathways. *J Neurobiol,* 57**,** 323-36.

MARLER, K. J., BECKER-BARROSO, E., MARTINEZ, A., LLOVERA, M., WENTZEL, C., POOPALASUNDARAM, S., HINDGES, R., SORIANO, E., COMELLA, J. & DRESCHER, U. 2008. A TrkB/EphrinA interaction controls retinal axon branching and synaptogenesis. *J Neurosci,* 28**,** 12700-12.

MARQUARDT, T., SHIRASAKI, R., GHOSH, S., ANDREWS, S. E., CARTER, N., HUNTER, T. & PFAFF, S. L. 2005. Coexpressed EphA receptors and ephrin-A ligands mediate opposing actions on growth cone navigation from distinct membrane domains. *Cell,* 121**,** 127-39.

MARSTON, D. J., DICKINSON, S. & NOBES, C. D. 2003. Rac-dependent trans-endocytosis of ephrinBs regulates Eph-ephrin contact repulsion. *Nat Cell Biol,* 5**,** 879-88.

MARUSICH, M. F., FURNEAUX, H. M., HENION, P. D. & WESTON, J. A. 1994. Hu neuronal proteins are expressed in proliferating neurogenic cells. *J Neurobiol,* 25**,** 143-55.

MCCAFFREY, L. M. & MACARA, I. G. 2012. Signaling pathways in cell polarity. *Cold Spring Harb Perspect Biol,* 4.

MEIMA, L., KLJAVIN, I. J., MORAN, P., SHIH, A., WINSLOW, J. W. & CARAS, I. W. 1997. AL-1-induced growth cone collapse of rat cortical neurons is correlated with REK7 expression and rearrangement of the actin cytoskeleton. *Eur J Neurosci,* 9**,** 177-88.

MOELLER, M. L., SHI, Y., REICHARDT, L. F. & ETHELL, I. M. 2006. EphB receptors regulate dendritic spine morphogenesis through the recruitment/phosphorylation of focal adhesion kinase and RhoA activation. *J Biol Chem,* 281**,** 1587-98.

MOENS, C. B. & PRINCE, V. E. 2002. Constructing the hindbrain: insights from the zebrafish. *Dev Dyn,* 224**,** 1-17.

MOENS, C. B., YAN, Y. L., APPEL, B., FORCE, A. G. & KIMMEL, C. B. 1996. valentino: a zebrafish gene required for normal hindbrain segmentation. *Development,* 122**,** 3981-90.

MOHAMED, A. M., BOUDREAU, J. R., YU, F. P., LIU, J. & CHIN-SANG, I. D. 2012. The Caenorhabditis elegans Eph receptor activates NCK and N-WASP, and inhibits Ena/VASP to regulate growth cone dynamics during axon guidance. *PLoS Genet,* 8**,** e1002513.

MOLERI, S., CAPPELLANO, G., GAUDENZI, G., CERMENATI, S., COTELLI, F., HORNER, D. S. & BELTRAME, M. 2011. The HMGB protein gene family in zebrafish: Evolution and embryonic expression patterns. *Gene Expr Patterns,* 11**,** 3-11.

NEKRASOVA, O. & GREEN, K. J. 2013. Desmosome assembly and dynamics. *Trends Cell Biol,* 23**,** 537-46.

NOBERINI, R., RUBIO DE LA TORRE, E. & PASQUALE, E. B. 2012. Profiling Eph receptor expression in cells and tissues: a targeted mass spectrometry approach. *Cell Adh Migr,* 6**,** 102-12.

NONCHEV, S., VESQUE, C., MACONOCHIE, M., SEITANIDOU, T., ARIZA-MCNAUGHTON, L., FRAIN, M., MARSHALL, H., SHAM, M. H., KRUMLAUF, R. & CHARNAY, P. 1996. Segmental expression of Hoxa-2 in the hindbrain is directly regulated by Krox-20. *Development,* 122**,** 543-54.

OIKE, Y., ITO, Y., HAMADA, K., ZHANG, X. Q., MIYATA, K., ARAI, F., INADA, T., ARAKI, K., NAKAGATA, N., TAKEYA, M., KISANUKI, Y. Y., YANAGISAWA, M., GALE, N. W. & SUDA, T. 2002. Regulation of vasculogenesis and angiogenesis by EphB/ephrin-B2 signaling between endothelial cells and surrounding mesenchymal cells. *Blood,* 100**,** 1326-33.

PABBISETTY, K. B., YUE, X., LI, C., HIMANEN, J. P., ZHOU, R., NIKOLOV, D. B. & HU, L. 2007. Kinetic analysis of the binding of monomeric and dimeric ephrins to Eph receptors: correlation to function in a growth cone collapse assay. *Protein Sci,* 16**,** 355-61.

PALMER, A., ZIMMER, M., ERDMANN, K. S., EULENBURG, V., PORTHIN, A., HEUMANN, R., DEUTSCH, U. & KLEIN, R. 2002. EphrinB phosphorylation and reverse signaling: regulation by Src kinases and PTP-BL phosphatase. *Mol Cell,* 9**,** 725-37.

PANDEY, A., SHAO, H., MARKS, R. M., POLVERINI, P. J. & DIXIT, V. M. 1995. Role of B61, the ligand for the Eck receptor tyrosine kinase, in TNF-alpha-induced angiogenesis. *Science,* 268**,** 567-9.

PARK, E., KIM, Y., NOH, H., LEE, H., YOO, S. & PARK, S. 2013. EphA/ephrin-A signaling is critically involved in region-specific apoptosis during early brain development. *Cell Death Differ,* 20**,** 169-80.

PARK, I. & LEE, H. S. 2015. EphB/ephrinB signaling in cell adhesion and migration. *Mol Cells,* 38**,** 14-9.

PARK, S. 2013. Brain-Region Specific Apoptosis Triggered by Eph/ephrin Signaling. *Exp Neurobiol,* 22**,** 143-8.

PASQUALE, E. B. 2008. Eph-ephrin bidirectional signaling in physiology and disease. *Cell,* 133**,** 38-52.

PATAN, S. 2004. Vasculogenesis and angiogenesis. *Cancer Treat Res,* 117**,** 3-32.

PERETZ, Y., EREN, N., KOHL, A., HEN, G., YANIV, K., WEISINGER, K., CINNAMON, Y. & SELA-DONENFELD, D. 2016. A new role of hindbrain boundaries as pools of neural stem/progenitor cells regulated by Sox2. *BMC Biol,* 14**,** 57.

PICCO, V., HUDSON, C. & YASUO, H. 2007. Ephrin-Eph signalling drives the asymmetric division of notochord/neural precursors in Ciona embryos. *Development,* 134**,** 1491-7.

POLIAKOV, A., COTRINA, M. L., PASINI, A. & WILKINSON, D. G. 2008. Regulation of EphB2 activation and cell repulsion by feedback control of the MAPK pathway. *J Cell Biol,* 183**,** 933-47.

PROVOST, E., WEIER, C. A. & LEACH, S. D. 2013. Multiple ribosomal proteins are expressed at high levels in developing zebrafish endoderm and are required for normal exocrine pancreas development. *Zebrafish,* 10**,** 161-9.

QIU, R., WANG, X., DAVY, A., WU, C., MURAI, K., ZHANG, H., FLANAGAN, J. G., SORIANO, P. & LU, Q. 2008. Regulation of neural progenitor cell state by ephrin-B. *J Cell Biol,* 181**,** 973-83.

QIU, X., LIM, C. H., HO, S. H., LEE, K. H. & JIANG, Y. J. 2009. Temporal Notch activation through Notch1a and Notch3 is required for maintaining zebrafish rhombomere boundaries. *Dev Genes Evol,* 219**,** 339-51.

QIU, X., XU, H., HADDON, C., LEWIS, J. & JIANG, Y. J. 2004. Sequence and embryonic expression of three zebrafish fringe genes: lunatic fringe, radical fringe, and manic fringe. *Dev Dyn,* 231**,** 621-30.

RILEY, B. B., CHIANG, M. Y., STORCH, E. M., HECK, R., BUCKLES, G. R. & LEKVEN, A. C. 2004. Rhombomere boundaries are Wnt signaling centers that regulate metameric patterning in the zebrafish hindbrain. *Dev Dyn,* 231**,** 278-91.

ROBINSON, D. R., WU, Y. M. & LIN, S. F. 2000. The protein tyrosine kinase family of the human genome. *Oncogene,* 19**,** 5548-57.

ROBU, M. E., LARSON, J. D., NASEVICIUS, A., BEIRAGHI, S., BRENNER, C., FARBER, S. A. & EKKER, S. C. 2007. p53 activation by knockdown technologies. *PLoS Genet,* 3**,** e78.

ROSSI, A., KONTARAKIS, Z., GERRI, C., NOLTE, H., HOLPER, S., KRUGER, M. & STAINIER, D. Y. 2015. Genetic compensation induced by deleterious mutations but not gene knockdowns. *Nature,* 524**,** 230-3.

SCHAFER, M., REMBOLD, M., WITTBRODT, J., SCHARTL, M. & WINKLER, C. 2005. Medial floor plate formation in zebrafish consists of two phases and requires trunk-derived Midkine-a. *Genes Dev,* 19**,** 897-902.

SCHAUPP, A., SABET, O., DUDANOVA, I., PONSERRE, M., BASTIAENS, P. & KLEIN, R. 2014. The composition of EphB2 clusters determines the strength in the cellular repulsion response. *J Cell Biol,* 204**,** 409-22.

SCHEER, N. & CAMPOS-ORTEGA, J. A. 1999. Use of the Gal4-UAS technique for targeted gene expression in the zebrafish. *Mech Dev,* 80**,** 153-8.

SCULLY, A. L., MCKEOWN, M. & THOMAS, J. B. 1999. Isolation and characterization of Dek, a Drosophila eph receptor protein tyrosine kinase. *Mol Cell Neurosci,* 13**,** 337-47.

SEGURA, I., ESSMANN, C. L., WEINGES, S. & ACKER-PALMER, A. 2007. Grb4 and GIT1 transduce ephrinB reverse signals modulating spine morphogenesis and synapse formation. *Nat Neurosci,* 10**,** 301-10.

SELA-DONENFELD, D., KAYAM, G. & WILKINSON, D. G. 2009. Boundary cells regulate a switch in the expression of FGF3 in hindbrain rhombomeres. *BMC Dev Biol,* 9**,** 16.

SHAMAH, S. M., LIN, M. Z., GOLDBERG, J. L., ESTRACH, S., SAHIN, M., HU, L., BAZALAKOVA, M., NEVE, R. L., CORFAS, G., DEBANT, A. & GREENBERG, M. E. 2001. EphA receptors regulate growth cone dynamics through the novel guanine nucleotide exchange factor ephexin. *Cell,* 105**,** 233-44.

SHI, W. & LEVINE, M. 2008. Ephrin signaling establishes asymmetric cell fates in an endomesoderm lineage of the Ciona embryo. *Development,* 135**,** 931-40.

SHI, Y., PONTRELLO, C. G., DEFEA, K. A., REICHARDT, L. F. & ETHELL, I. M. 2009. Focal adhesion kinase acts downstream of EphB receptors to maintain mature dendritic spines by regulating cofilin activity. *J Neurosci,* 29**,** 8129-42.

SIMS, N. A. & MARTIN, T. J. 2014. Coupling the activities of bone formation and resorption: a multitude of signals within the basic multicellular unit. *Bonekey Rep,* 3**,** 481.

SMITH, A., ROBINSON, V., PATEL, K. & WILKINSON, D. G. 1997. The EphA4 and EphB1 receptor tyrosine kinases and ephrin-B2 ligand regulate targeted migration of branchial neural crest cells. *Curr Biol,* 7**,** 561-70.

STEIN, E., HUYNH-DO, U., LANE, A. A., CERRETTI, D. P. & DANIEL, T. O. 1998. Nck recruitment to Eph receptor, EphB1/ELK, couples ligand activation to c-Jun kinase. *J Biol Chem,* 273**,** 1303-8.

STOLFI, A., WAGNER, E., TALIAFERRO, J. M., CHOU, S. & LEVINE, M. 2011. Neural tube patterning by Ephrin, FGF and Notch signaling relays. *Development,* 138**,** 5429-39.

TAKASU, M. A., DALVA, M. B., ZIGMOND, R. E. & GREENBERG, M. E. 2002. Modulation of NMDA receptor-dependent calcium influx and gene expression through EphB receptors. *Science,* 295**,** 491-5.

TANAKA, M., KAMO, T., OTA, S. & SUGIMURA, H. 2003. Association of Dishevelled with Eph tyrosine kinase receptor and ephrin mediates cell repulsion. *EMBO J,* 22**,** 847-58.

TANAKA, M., OHASHI, R., NAKAMURA, R., SHINMURA, K., KAMO, T., SAKAI, R. & SUGIMURA, H. 2004. Tiam1 mediates neurite outgrowth induced by ephrin-B1 and EphA2. *EMBO J,* 23**,** 1075-88.

TERRIENTE, J., GERETY, S. S., WATANABE-ASAKA, T., GONZALEZ-QUEVEDO, R. & WILKINSON, D. G. 2012. Signalling from hindbrain boundaries regulates neuronal clustering that patterns neurogenesis. *Development,* 139**,** 2978-87.

THEIL, T., FRAIN, M., GILARDI-HEBENSTREIT, P., FLENNIKEN, A., CHARNAY, P. & WILKINSON, D. G. 1998. Segmental expression of the EphA4 (Sek-1) receptor tyrosine kinase in the hindbrain is under direct transcriptional control of Krox-20. *Development,* 125**,** 443-52.

THISSE, B. & THISSE, C. 2014. In situ hybridization on whole-mount zebrafish embryos and young larvae. *Methods Mol Biol,* 1211**,** 53-67.

TOLIAS, K. F., BIKOFF, J. B., KANE, C. G., TOLIAS, C. S., HU, L. & GREENBERG, M. E. 2007. The Rac1 guanine nucleotide exchange factor Tiam1 mediates EphB receptor-dependent dendritic spine development. *Proc Natl Acad Sci U S A,* 104**,** 7265-70.

TREVARROW, B., MARKS, D. L. & KIMMEL, C. B. 1990. Organization of hindbrain segments in the zebrafish embryo. *Neuron,* 4**,** 669-79.

TUMPEL, S., WIEDEMANN, L. M. & KRUMLAUF, R. 2009. Hox genes and segmentation of the vertebrate hindbrain. *Curr Top Dev Biol,* 88**,** 103-37.

WALKER-DANIELS, J., RIESE, D. J., 2ND & KINCH, M. S. 2002. c-Cbl-dependent EphA2 protein degradation is induced by ligand binding. *Mol Cancer Res,* 1**,** 79-87.

WALSH, R. & BLUMENBERG, M. 2011. Specific and shared targets of ephrin A signaling in epidermal keratinocytes. *J Biol Chem,* 286**,** 9419-28.

WALSH, R. & BLUMENBERG, M. 2012. Eph-2B, acting as an extracellular ligand, induces differentiation markers in epidermal keratinocytes. *J Cell Physiol,* 227**,** 2330-40.

WALSHE, J., MAROON, H., MCGONNELL, I. M., DICKSON, C. & MASON, I. 2002. Establishment of hindbrain segmental identity requires signaling by FGF3 and FGF8. *Curr Biol,* 12**,** 1117-23.

WANG, H. U. & ANDERSON, D. J. 1997. Eph family transmembrane ligands can mediate repulsive guidance of trunk neural crest migration and motor axon outgrowth. *Neuron,* 18**,** 383-96.

WANG, H. U., CHEN, Z. F. & ANDERSON, D. J. 1998. Molecular distinction and angiogenic interaction between embryonic arteries and veins revealed by ephrin-B2 and its receptor Eph-B4. *Cell,* 93**,** 741-53.

WANG, X., EMELYANOV, A., KORZH, V. & GONG, Z. 2003. Zebrafish atonal homologue zath3 is expressed during neurogenesis in embryonic development. *Dev Dyn,* 227**,** 587-92.

WANG, X., ROY, P. J., HOLLAND, S. J., ZHANG, L. W., CULOTTI, J. G. & PAWSON, T. 1999. Multiple ephrins control cell organization in C. elegans using kinase-dependent and -independent functions of the VAB-1 Eph receptor. *Mol Cell,* 4**,** 903-13.

WANG, Y. W., WEI, C. Y., DAI, H. P., ZHU, Z. Y. & SUN, Y. H. 2013. Subtractive phage display technology identifies zebrafish marcksb that is required for gastrulation. *Gene,* 521**,** 69-77.

WASKIEWICZ, A. J., RIKHOF, H. A. & MOENS, C. B. 2002. Eliminating zebrafish pbx proteins reveals a hindbrain ground state. *Dev Cell,* 3**,** 723-33.

WESELY, J., STEINER, M., SCHNUTGEN, F., KAULICH, M., RIEGER, M. A. & ZORNIG, M. 2017. Delayed Mesoderm and Erythroid Differentiation of Murine Embryonic Stem Cells in the Absence of the Transcriptional Regulator FUBP1. *Stem Cells Int,* 2017**,** 5762301.

WESTERFIELD, M. 2000. *The zebafish book. A guide for the laboratory use of zebrafish (Danio rerio). ,* Eugene, University of Oregon Press.

WHITE, R. J., NIE, Q., LANDER, A. D. & SCHILLING, T. F. 2007. Complex regulation of cyp26a1 creates a robust retinoic acid gradient in the zebrafish embryo. *PLoS Biol,* 5**,** e304.

WIESE, C., ROLLETSCHEK, A., KANIA, G., BLYSZCZUK, P., TARASOV, K. V., TARASOVA, Y., WERSTO, R. P., BOHELER, K. R. & WOBUS, A. M. 2004. Nestin expression--a property of multi-lineage progenitor cells? *Cell Mol Life Sci,* 61**,** 2510-22.

WILKINSON, D. G. 2014. Regulation of cell differentiation by Eph receptor and ephrin signaling. *Cell Adh Migr,* 8**,** 339-48.

WILKINSON, D. G., BHATT, S., CHAVRIER, P., BRAVO, R. & CHARNAY, P. 1989a. Segment-specific expression of a zinc-finger gene in the developing nervous system of the mouse. *Nature,* 337**,** 461-4.

WILKINSON, D. G., BHATT, S., COOK, M., BONCINELLI, E. & KRUMLAUF, R. 1989b. Segmental expression of Hox-2 homoeobox-containing genes in the developing mouse hindbrain. *Nature,* 341**,** 405-9.

WINKLER, C., SCHAFER, M., DUSCHL, J., SCHARTL, M. & VOLFF, J. N. 2003. Functional divergence of two zebrafish midkine growth factors following fish-specific gene duplication. *Genome Res,* 13**,** 1067-81.

WYKOSKY, J., PALMA, E., GIBO, D. M., RINGLER, S., TURNER, C. P. & DEBINSKI, W. 2008. Soluble monomeric EphrinA1 is released from tumor cells and is a functional ligand for the EphA2 receptor. *Oncogene,* 27**,** 7260-73.

XU, N. J. & HENKEMEYER, M. 2009. Ephrin-B3 reverse signaling through Grb4 and cytoskeletal regulators mediates axon pruning. *Nat Neurosci,* 12**,** 268-76.

XU, Q., ALLDUS, G., HOLDER, N. & WILKINSON, D. G. 1995. Expression of truncated Sek-1 receptor tyrosine kinase disrupts the segmental restriction of gene expression in the Xenopus and zebrafish hindbrain. *Development,* 121**,** 4005-16.

XU, Q., MELLITZER, G., ROBINSON, V. & WILKINSON, D. G. 1999. In vivo cell sorting in complementary segmental domains mediated by Eph receptors and ephrins. *Nature,* 399**,** 267-71.

XU, Q. & WILKINSON, D. G. 2013. Boundary formation in the development of the vertebrate hindbrain. *Wiley Interdiscip Rev Dev Biol,* 2**,** 735-45.

YAMAGUCHI, M., SAITO, H., SUZUKI, M. & MORI, K. 2000. Visualization of neurogenesis in the central nervous system using nestin promoter-GFP transgenic mice. *Neuroreport,* 11**,** 1991-6.

YAMANAKA, T., HORIKOSHI, Y., SUZUKI, A., SUGIYAMA, Y., KITAMURA, K., MANIWA, R., NAGAI, Y., YAMASHITA, A., HIROSE, T., ISHIKAWA, H. & OHNO, S. 2001. PAR-6 regulates aPKC activity in a novel way and mediates cell-cell contact-induced formation of the epithelial junctional complex. *Genes Cells,* 6**,** 721-31.

YAN, Y., YIN, P., GONG, H., XUE, Y., ZHANG, G., FANG, B., CHEN, Z., LI, Y., YANG, C., HUANG, Z., YANG, X., GE, J. & ZOU, Y. 2016. Nucleosome Assembly Protein 1-Like 1 (Nap1l1) Regulates the Proliferation of Murine Induced Pluripotent Stem Cells. *Cell Physiol Biochem,* 38**,** 340-50.

YEN, T. H. & WRIGHT, N. A. 2006. The gastrointestinal tract stem cell niche. *Stem Cell Rev,* 2**,** 203-12.

YIN, Y., YAMASHITA, Y., NODA, H., OKAFUJI, T., GO, M. J. & TANAKA, H. 2004. EphA receptor tyrosine kinases interact with co-expressed ephrin-A ligands in cis. *Neurosci Res,* 48**,** 285-96.

YU, Y., LIU, M., NG, T. T., HUANG, F., NIE, Y., WANG, R., YAO, Z. P., LI, Z. & XIA, J. 2016. PDZ-Reactive Peptide Activates Ephrin-B Reverse Signaling and Inhibits Neuronal Chemotaxis. *ACS Chem Biol,* 11**,** 149-58.

ZAUCKER, A., NAGORSKA, A., KUMARI, P., HECKER, N., WANG, Y., HUANG, S., COOPER, L., SIVASHANMUGAM, L., VIJAYKUMAR, S., BROSENS, J.,

GORODKIN, J. & SAMPATH, K. 2017. Translational co-regulation of a ligand and inhibitor by a conserved RNA element. *Nucleic Acids Res*.

ZERBINO, D. R., ACHUTHAN, P., AKANNI, W., AMODE, M. R., BARRELL, D., BHAI, J., BILLIS, K., CUMMINS, C., GALL, A., GIRON, C. G., GIL, L., GORDON, L., HAGGERTY, L., HASKELL, E., HOURLIER, T., IZUOGU, O. G., JANACEK, S. H., JUETTEMANN, T., TO, J. K., LAIRD, M. R., LAVIDAS, I., LIU, Z., LOVELAND, J. E., MAUREL, T., MCLAREN, W., MOORE, B., MUDGE, J., MURPHY, D. N., NEWMAN, V., NUHN, M., OGEH, D., ONG, C. K., PARKER, A., PATRICIO, M., RIAT, H. S., SCHUILENBURG, H., SHEPPARD, D., SPARROW, H., TAYLOR, K., THORMANN, A., VULLO, A., WALTS, B., ZADISSA, A., FRANKISH, A., HUNT, S. E., KOSTADIMA, M., LANGRIDGE, N., MARTIN, F. J., MUFFATO, M., PERRY, E., RUFFIER, M., STAINES, D. M., TREVANION, S. J., AKEN, B. L., CUNNINGHAM, F., YATES, A. & FLICEK, P. 2018. Ensembl 2018. *Nucleic Acids Res,* 46**,** D754-D761.

ZHAO, C., IRIE, N., TAKADA, Y., SHIMODA, K., MIYAMOTO, T., NISHIWAKI, T., SUDA, T. & MATSUO, K. 2006. Bidirectional ephrinB2-EphB4 signaling controls bone homeostasis. *Cell Metab,* 4**,** 111-21.

ZHOU, Z. J., DAI, Z., ZHOU, S. L., HU, Z. Q., CHEN, Q., ZHAO, Y. M., SHI, Y. H., GAO, Q., WU, W. Z., QIU, S. J., ZHOU, J. & FAN, J. 2014. HNRNPAB induces epithelial-mesenchymal transition and promotes metastasis of hepatocellular carcinoma by transcriptionally activating SNAIL. *Cancer Res,* 74**,** 2750-62.

ZIMMER, M., PALMER, A., KOHLER, J. & KLEIN, R. 2003. EphB-ephrinB bi-directional endocytosis terminates adhesion allowing contact mediated repulsion. *Nat Cell Biol,* 5**,** 869-78.

ZISCH, A. H., PAZZAGLI, C., FREEMAN, A. L., SCHNELLER, M., HADMAN, M., SMITH, J. W., RUOSLAHTI, E. & PASQUALE, E. B. 2000. Replacing two conserved tyrosines of the EphB2 receptor with glutamic acid prevents binding of SH2 domains without abrogating kinase activity and biological responses. *Oncogene,* 19**,** 177-87.